Winter 2008

# MALDI Mass Spectrometry Imaging for the Discovery of Prostate Carcinoma Biomarkers

Lisa Harris Cazares
*Old Dominion University*

# MALDI MASS SPECTROMETRY IMAGING FOR THE DISCOVERY OF

# PROSTATE CARCINOMA BIOMARKERS

by

Lisa Harris Cazares
B.S. May 1986, University of South Florida

A Thesis Submitted to the Faculty of
Eastern Virginia Medical School and
Old Dominion University in Partial Fulfillment of the
Requirement for the Degree of

DOCTOR OF PHILOSOPHY

BIOMEDICAL SCIENCES

EASTERN VIRGINIA MEDICAL SCHOOL
AND OLD DOMINION UNIVERSITY
December 2008

Approved by:

_____
O. John Semmes (Director)

_____
Richard R. Drake (Member)

_____
Julie A. Kerry (Member)

_____
Ann E. Campell (Member)

[Type text]

# ABSTRACT

## MALDI MASS SPECTROMETRY IMAGING FOR THE DISCOVERY OF PROSTATE CARCINOMA BIOMARKERS

Lisa Harris Cazares
Eastern Virginia Medical School and Old Dominion University, 2008
Director: Dr. O. John Semmes

The elucidation of new biological markers of prostate cancer (PCa) should aid in the detection, and prognosis of this disease. Diagnostic decision making by pathologists in prostate cancer is highly dependent on tissue morphology. The ability to localize disease-specific molecular changes in tissue would help improve this critical pathology decision making process. Direct profiling of proteins in tissue sections using MALDI imaging mass spectrometry (MALDI-IMS) has the power to link molecular detail to morphological and pathological changes, enhancing the ability to identify candidates for new specific biomarkers. However, critical questions remain regarding the integration of this technique with clinical decision making. To address these questions, and to investigate the potential of MALDI-IMS for the diagnosis of prostate cancer, we have used this approach to analyze prostate tissue for the determination of the cellular origins of different protein signals to improve cancer detection and to identify specific protein markers of PCa. We found that specific protein/ peptide expression changes correlated with the presence or absence of prostate cancer as well as the presence of micro-metastatic disease. Additionally, the over-expression of a single peptide ($m/z$ = 4355) was able to accurately define primary cancer tissue from adjacent normal tissue. Tandem mass spectrometry analysis identified this peptide as a fragment of MEKK2, a member of the MAP kinase signaling pathway. Validation of MEKK2 overexpression in moderately differentiated PCa and prostate cancer cell lines was performed using

immunohistochemistry and Western Blot analysis. Classification algorithms using specific ions differentially expressed in PCa tissue and a ROC cut-off value for the normalized intensity of the MEKK2 fragment at *m/z* 4355 were used to classify a blinded validation set. Finally, the optimization of sample processing in a new fixative which preserves macromolecules has led to improved through-put of samples making MALDI-IMS more compatible with current histological applications, facilitating its implementation in a clinical setting. This study highlights the potential of MALDI-IMS to define the molecular events involved in prostate tumorigenesis and demonstrates the applicability of this approach to clinical diagnostics as an aid to pathological decision making in prostate cancer.

*I am among those who think that science has great beauty. A scientist in his laboratory is not only a technician: he is also a child placed before natural phenomena which impress him like a fairy tale.*
Marie Curie
French (Polish-born) chemist & physicist (1867 – 1934)

*If I have ever made any valuable discoveries, it has been owing more to patient attention, than to any other talent.*
Isaac Newton
English mathematician & physicist (1642 - 1727)


This Dissertation is dedicated to my loving family.

To my husband, Michael Ward who is my scientific sounding board,
and ever-supportive partner.

To my children A.J and Julia who provide me with love, support
and understanding beyond their years.

To my Mother Erline and my Father Michael who raised me with the knowledge that
anything is possible if you work hard enough.

# ACKNOWLEDGEMENTS

First and foremost, I would like to express my sincere gratitude to my Mentor, Dr O. John Semmes who offered me the opportunity to study for my Ph.D. at EVMS. Many thanks for the professional and financial support during my years of study. Your encouragement and constructive criticism throughout the course of my project provided me with an atmosphere conducive to scientific success.

I am also indebted to my co-Mentor, Dr Richard Drake, who provided invaluable insight and enthusiasm for my project. Thanks for your support and confidence in me as a "non-traditional" Ph.D. student.

I would like to express my gratitude to the other members of my thesis committee, Dr. Julie Kerry and Dr. Ann Campell. I admire you both as professional and accomplished role models for women in science. Thank you for your guidance.

And my acknowledgments could never be complete without thanking my first supervisor and scientific mentor at EVMS, Dr. George L. Wright Jr. Dr. Wright's insight and influence was indispensible to both my interest and success in the field of proteomic research.

# TABLE OF CONTENTS

# LIST OF TABLES

# LIST OF FIGURES

# CHAPTER 1

# INTRODUCTION

## 1.1 Molecular Pathology of Cancer

Tumors are classified by their site of origin and their appearance under a microscope. The hallmarks of cancer diagnosis are variations in cell architecture and nuclear structure, but no single histological feature is absolutely diagnostic of cancer. Considerable effort has been invested over the years by pathologists in the standardization of the morphological analysis and classification of tumors for the facilitation of scientific research and more importantly, for patient diagnoses and prognoses. Molecular pathology studies the origins of disease based on the characterization of acquired genetic mutations and alterations of gene products. Defining the molecular mechanisms that give rise to the cancer phenotype is believed to represent a critical step in developing methods of early detection and effective therapeutic regimens for cancer patients. Over the last 20 years, morphological analysis has benefitted from the biochemical, immunohistochemical, and nucleic acid examination of tissue samples [1]. Pathology reports containing molecular data of clinical relevance are now being generated in many tumor types. For example, the reporting of breast carcinomas includes, in most instances, estrogen receptor status, and Her2/Neu expression and amplification [2, 3]. Molecular techniques are slowly but surely transitioning into the clinical arena making molecular diagnostics an integral part of clinical practice.

A major challenge in cancer diagnosis and treatment is related to the fact that the pathological features of a tumor and the protein expression of existing markers do not

This manuscript is modeled after *Cancer Research*

provide complete guidance and accuracy in patient risk assessment and treatment

response [4]. Additionally, histopathology, which guides treatment in many cancers,

often subcategorizes aggressiveness insufficiently in early stage tumors [5]. These

differences in outcome may relate, in part, to stochastic events, such as the time at which

a single cancer cell happens to undergo all of the steps necessary for successful

metastasis, or they may relate to factors that can be reasonably well understood at a

deterministic level such as a field affect.


**The Cancer Field Effect**

The field affect or the idea of field cancerization was first conceived by Slaughter

in a 1953 publication [6]. It is defined as an area surrounding transformed cells which

contains daughter cells exhibiting early genetic changes without changes in

histopathology. Field cancerization is now a well known and well documented process of

malignant transformation. Several studies have confirmed the importance of this

phenomenon in tumor development. In one such study, by measuring loss of

heterozygosity [7], Larson et al showed that at least one-third of biopsy samples from

head and neck squamous cell carcinoma have tumor-associated genetic alterations in the

macroscopically normal mucosa adjacent to the tumor [8]. Histopathological analysis had

failed to detect tumor cells in these margins. Thus the high recurrence rate of some

cancers may be explained by field cancerization. The molecular/genetic abnormalities in

the histopathology negative tumor margins may represent tumor cells invading and

metastasizing from the original primary tumor. The genetic defects that comprise the

genotypic features of cancerous growths may coexist in benign appearing cells adjacent

to the primary tumor and therefore cannot be assessed by conventional histopathological techniques. The implication is that cancerization fields may remain after surgery of the primary tumor and may subsequently develop into loco-regionally recurrent cancers. Determining that histologically normal biopsy specimens possess molecular signatures of cancer fields suggest either the tumor was missed by the biopsy procedure or that some cells in the tissue are progressing towards malignancy. This would help to classify these individual as high risk for recurrence, necessitating closer surveillance. Thus, the ability to detect field cancerization by examining existing and new molecular markers would greatly aid clinicians in the assessment of surgical margins as well as the evaluation of pre-neoplastic processes.

**Tumor Stroma Interactions**

Homeostasis of normal organs such as the prostate or breast is maintained through reciprocal interactions between epithelial cells and their surrounding stroma with minimal proliferation of either cell type [9]. It is possible that, following genetic alteration to the prostatic epithelium, signaling from the epithelium to the surrounding stromal compartment becomes altered. This can cause the reacting stroma cells to receive an "inductive cue" from tumor epithelium to undergo trans-differentiation, whereby stromal fibroblasts adjacent to tumor epithelium convert both morphologically and phenotypically to myofibroblasts [10, 11]. A consequence of such a transformation may be a change in the local microenvironment from promoting epithelial homeostasis to promoting epithelial mitogenesis. Fibroblasts are primarily responsible for the synthesis, deposition, and remodeling of the extracellular matrix (ECM) as well as for the

production of many soluble factors that regulate cell proliferation, morphology, survival, and apoptosis [12] . In the past fibroblasts have been thought to be passive participants in the neoplastic transformation of tissues; however, recent data indicates that they play an active role [13] and, in combination with inflammatory cells, can promote the neoplastic programming of tissues by increasing epithelial proliferation and migration, potentially enhancing the invasive potential of the genetically altered epithelial cell [14, 15].

**Summary**

The current "gene-centric" paradigm of cancer theorizes that once we understand all the genetic aberrations associated with cancer we will be able to target them individually and reverse their effects to treat and cure the disease [16]. This view has many misconceptions and overlooks the importance of protein alterations in disease. First, due to the dynamic nature of cancer, both the number and type of genetic alterations may change over time. Furthermore, the number of genes is far fewer than the number of proteins and there is only a moderate correlation between mRNA transcript levels and protein abundance in most cells and tissues [17]. Many genes can be alternatively spliced and mRNA editing is also quite common [18, 19]. Finally, post translational modifications (PTMs) often change protein function and behavior significantly and the diverse realm of these modifications encompasses many of the critical signaling events which occur during neoplastic transformation [20].

As an important biological indicator of cancer status and physiological state of the cell at a specific time, protein biomarkers represent powerful tools for monitoring the course of cancer [21]. They can have tremendous therapeutic impact in clinical oncology,

especially if the biomarker is detected before clinical symptoms [22]. Unfortunately, despite enormous efforts, in only a few tumor types have relevant markers been established that can be used for early diagnosis or improved therapy in cancer [23, 24]. The lack of a sensitive robust technology to detect the signatures of cancer cells from minute quantities of available tissues or serum has significantly slowed the identification of reliable biomarkers to accurately diagnose and predict the course of most types of cancers [25, 26]. Thus, enhancements in the molecular profiling of early lesions using appropriate control tissue will enable important pathways that predict disease progression to be deciphered.

### 1.1.1   Prostate Cancer Development and Epidemiology

Prostate cancer (PCa) is one of the most common malignancies in the US and over 98% of all prostate cancers are adenocarcinomas that arise from epithelial cells in the acini or ducts of the prostate gland [27]. Microscopically PCa can be well, moderate or poorly differentiated [28]. Despite the common occurrence, little is known about the etiology of prostate cancer, and the natural history of the disease has not been fully established. PCa is slow growing in many cases with a long phase in which it remains undiscovered. In fact many tumors may never become clinically important [29]. The relatively benign course of many tumors means that treatment might not be beneficial and may actually do more harm than good.

Ageing is still the most significant risk factor in the development of prostate cancer. More than 70% of all PCa cases are diagnosed in men over 65 [30]. Other important factors are race and steroid hormones. According to a multiethnic cohort study,

PCa incidence is highest in African American men with more than double the risk compared to Caucasians [31]. However, some studies have suggested that black men who receive active therapy for newly diagnosed prostate cancer are probably not at any greater risk for disease recurrence than are white men with tumors of similar pathologic grade and clinical stage who receive the same treatment [32]. Clinical studies show a similarity in prostate cancer outcome when pathological stage is organ confined but a worse outcome when disease is locally advanced or metastatic in African-American versus European-American men [33]. Additionally, there is increasing genetic evidence that suggests prostate cancer in African-American men may be more aggressive, especially when it occurs in younger men [34].

Less than 10% of all prostate cancers are inherited, and most cases appear to be sporadic [35]. Dietary, lifestyle-related and environmental factors such as chronic or recurrent inflammation [36] have also been implicated in the initiation and promotion of prostate cancer. The Western lifestyle diet consisting of higher intake of fat, meat and dairy products may be responsible for an increase in PCa risk [37-40]. Most likely, the pathogenesis of prostate cancer involves interplay between environmental and genetic factors.

The growth and development of the prostate is dependent on androgens [41]. Ablation of androgens by surgical or medical castration is an effective strategy in the treatment of advanced prostate cancer [42]. Moreover, men with congenital abnormalities in androgen metabolism and those who undergo castration before puberty do not develop prostate cancer [43]. The normal prostate contains three zones and a fibromuscular

stromal compartment. Approximately 70% of all PCa cases arise in the peripheral zone, 10-20% in the transition zone, and 5-10% in the central zone [44].

The histopathological changes encompassing prostatic intraepithelial neoplasia (PIN) are the most likely precursor to PCa [45]. PIN is defined as a non-invasive pre-neoplastic growth of the cells lining prostatic ducts and acini. Disruption of the basal cell layer increases with increasing grades of PIN (in PCa there is complete loss of the basal cell layer) [46] . PIN has been shown to co-exist with PCa in approximately 85% of all prostate surgery specimens and it has been suggested that most patients with PIN detected in a biopsy sample will develop prostate carcinoma within ten years [47, 48]. The prostate lesion described as proliferative inflammatory atrophy (PIA) has been proposed as a precursor to PIN, a possible earlier step in prostate carcinogenesis [49]. Several studies have found frequent association of PIA with inflammatory processes [36], suggesting that chronic inflammation may result in damage to epithelial cells and produce proliferative lesions [50]. The chronic inflammatory microenvironment, characterized by the accumulation of macrophages and lymphocytes, is extremely common in the tissue stroma and epithelium of the prostate and may support both the initiation and progression of prostate cancer. [51]. This inflammatory environment has also been associated with benign lesions of the prostate known as cystic atrophy.

### 1.1.2 Prostate Cancer Detection and Morphology

Standard methods for diagnosis and the assessment of prognosis in PCa include digital rectal exam (DRE), serum prostate specific antigen (PSA), and ultrasound directed biopsies [42]. The discovery and widespread utilization of serum PSA monitoring for

early detection has greatly changed the way prostate cancer is diagnosed and treated [52]. However, PSA lacks specificity as a screening tool for prostate cancer, and there is really no lower limit of PSA that entirely excludes cancer [53]. Unfortunately, PSA and DRE results alone cannot diagnose prostate cancer, but can only indicate further testing is necessary. Thus clinical decision making in PCa places a significant burden on biopsy results. Ultrasound guided needle biopsy is the standard for diagnosis however a negative result does not exclude the presence of cancer [54]. Multiple biopsy cores (8-12) are most often taken, but sampling and analytical variables account for many false negative results [55]. In clinical practice, false negative results promote a need for repeat biopsies which can delay diagnosis and treatment or unnecessarily subject cancer-free men to repeat biopsies.

The Gleason grading system which has been widely adopted for PCa is a strong predictor of outcome [56]. This grading system separates the architectural features of the cancerous glands into 5 histological patterns of decreasing differentiation, pattern 1 being the most differentiated and pattern 5 being the least differentiated (see Figure 1 for details). The Gleason sum score is obtained by adding the dominating primary grade and the next most common secondary grade. A major limitation of this grading system, and a result of aggressive screening procedures, is that a majority of newly diagnosed prostate cancer cases are Gleason grade 6 or 7 tumors. These moderately differentiated tumors can either be indolent or aggressive [57] and there are no reliable molecular markers for the determination of these subclasses. New methods and molecular markers to assist pathologists in both diagnostic and prognostic decision making are needed to aid in the detection and treatment of prostate cancer.

Recent advances in molecular research enable us to understand the functions of many of the protein products of oncogenes and tumor suppressor genes in great detail. However, a set of characteristic alterations have not been identified in the development and progression of PCa. This is partly due to the marked heterogeneity and multifocal nature of prostate tumors [58].

A candidate tumor suppressor gene for prostate cancer is PTEN. This gene is among the most commonly mutated tumor suppressor genes in human cancer and encodes for a lipid phosphatase that cleaves 3-phosphorylated phosphoinositides and functions as a negative regulator of phosphoinositol-3-kinase signaling [59]. Like many other tumor suppressors, PTEN targets proteins in signaling pathways that regulate cell growth and apoptosis in healthy tissue and contributes to cancer when dysfunctional. The frequency of PTEN inactivation appears to increase during the progression of prostatic cancer [60]. ETS factors (named for the oncogene: v-ets) represent one of the largest families of transcriptional regulators and have known functional roles in many biological processes [61]. ETS factors have oncogenic activity and their aberrant expression is associated with many of the processes that lead to prostate cancer progression. Essentially, the upregulation of ETS gene expression in prostate cancers appears to be driven by chromosomal rearrangements leading to oncogenic gene fusion products. Fusion transcripts have been observed to result from fusion of a prostate-specific transmembrane protease serine 2 (TMPRSS2) gene with the oncogenic ETS transcription factors [62, 63]. The TMPRSS2 gene encodes for a transmembrane-bound serine protease that is highly localized to the prostate gland, and is overexpressed in neoplastic epithelium and androgen regulated [64]. The most prevalent gene fusion in PCa is
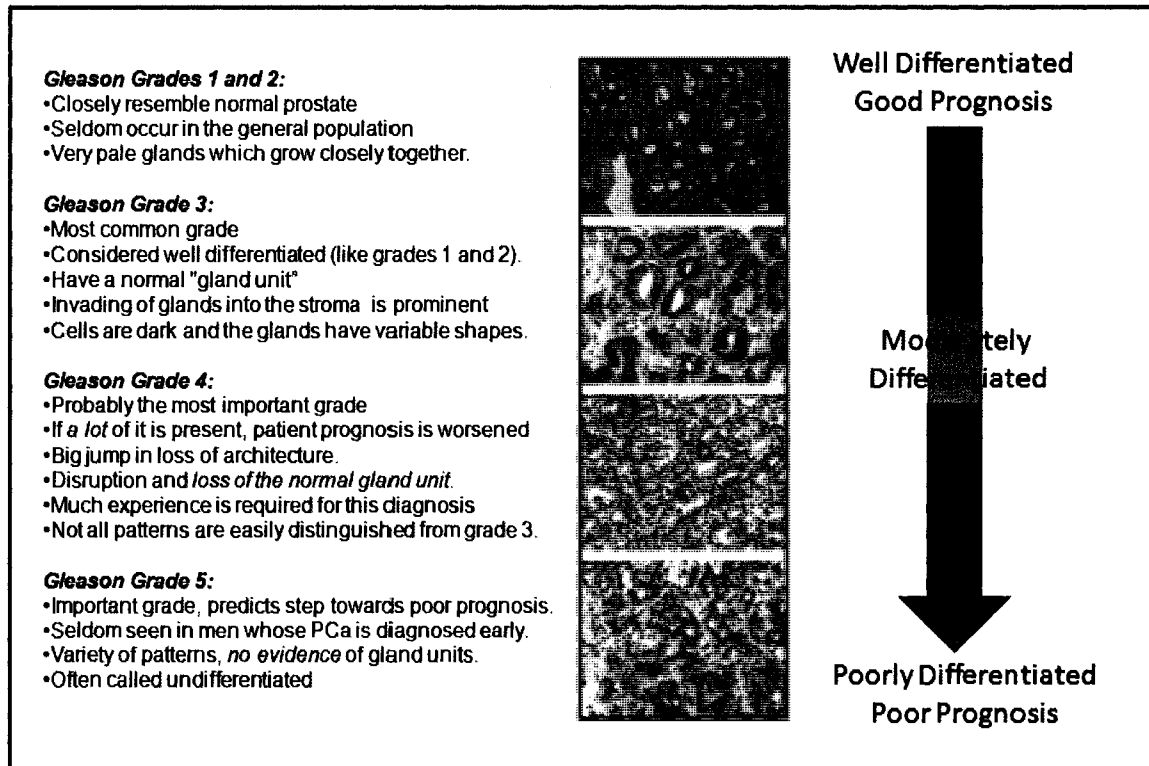
**Figure 1.** Description of the Gleason Scoring Paradigm.

TMPRSS2 with the ETS transcription family member ERG [65]. The TMPRSS2-ERG

fusion occurs in 50% of clinically localized PCa, making it one of the most common

somatic genomic alterations identified in a human malignancy [66, 67]. A recent study

found that the TMPRSS2-ERG fusion status has the biological effect of promoting

common morphological features found in prostate cancer [68]. This study was the first to

show a connection between molecular alterations and distinct phenotypic features in PCa.

Precedence for this finding can be found in several other tumor types. Breast cancer

associated with BRCA1 germline mutations often has a higher mitotic rates and larger

areas of tumor with continuous pushing margins [69]. Additionally, microsatellite

unstable colon cancer is characterized by poorly differentiated tumor cells with an

expanding growth pattern and pronounced increase in lymphocyte infiltration [70]. The

histological identification of a tumor phenotype associated with a specific genotype

establishes an important bridge between pathology and molecular analysis. If these

observations hold clinical significance, they will become relevant for patient care.

### 1.1.3 Prostate Cancer Prognosis and Treatment

Many of the clinically important predictive factors in prostate cancer are still

derived from a pathologist's examination of tissue specimens using light microscopy.

Morphology based prognostic markers in use today for PCa patient management include

tumor type, tumor grade, tumor stage, tumor volume and surgical margins [58]. The most

important clinical prognostic indicators of disease outcome in prostate cancer are pre-

therapy PSA level and Gleason score. Patients with localized PCa who have pre-

treatment PSA levels of less than 4ng/ml and Gleason scores of less than 4 have greater

than 90% chance of disease free survival [71]. In contrast, patients with PSA levels of greater than 20ng/ml and Gleason scores of more than 8 have a poor prognosis (less than 50% disease-free survival) [71]. For the patients with intermediate values of PSA and Gleason scores, additional prognostic strategies are required to give an accurate prediction of disease outcome. DNA ploidy in PCa has been studied extensively and provides prognostic information independent of histological grade and tumor stage [72]. Recent studies have shown that angiogenic potential is a potent prognostic indicator for patients with PCa and that the evaluation of endothelial growth factors is useful in assessing the angiogenic phenotype in prostate tumors [73]. Moreover, the choice of therapeutic interventions for PCa at the time of diagnosis is almost solely dependent on clinical and pathologic staging based on morphology and the prediction of degree of aggressiveness of the disease [74]. Clinically applicable prognostic markers are urgently needed therefore to assist in prognosis and the selection of optimal therapy.

Treatment for PCa depends on the stage of the disease, the age of the patient, and the presence of other medical conditions. To date, there are four major treatment options for patients with localized PCa: radical prostatectomy, radiotherapy, hormone therapy and watchful waiting [75]. If the cancer has spread outside the prostate, with lymph nodes and bone being the most common sites for metastasis, the most common treatment is surgical or chemical castration, to lower androgen levels, causing a reduction in tumor growth and symptomatic relief [76]. In men older than 70 diagnosed with well or moderately differentiated tumors and low PSA levels, the physician may elect to follow a course of "watchful waiting," in which the patient returns frequently for check-ups. Treatment occurs only if the man's condition worsens (i.e. PSA levels rise). In patients

undergoing radical prostatectomy, post surgical detection of PSA is consistent with recurrent or persistent disease [71]. It is important to remember that PSA is not only elevated in prostate cancer, but in benign prostatic hyperplasia (BPH) and inflammatory conditions of the prostate such as prostatitis [77]. New biomarkers to determine the aggressiveness of tumors and metastatic potential should aid in the treatment decision process for localized PCa.

### 1.1.4  Prostate Cancer Biomarkers

PSA is a glycoprotein and a serine protease produced by prostatic epithelial cells. Normally, PSA is secreted into seminal fluid where it functions to digest the gel formed by seminogelins and fibronectin after ejaculation [52]. Small amounts of PSA naturally leak into the bloodstream, but when cancer is present there is increased leakage due to the destruction of the basement membrane of the organ, setting up a "leaky prostate"[77]. PSA isolated from seminal plasma, was first described in 1971 [78, 79] and the first assay for PSA in serum was developed in 1981 [80]. By 1999 PSA was adapted by urologists as a marker for PCa detection. Today, PSA is the most widely used tumor marker in urology [52]. Despite this acceptance, the PSA serum test, as mentioned above, lacks specificity and sensitivity. About 70% of men with an elevated PSA will not have detectable PCa at biopsy [54] and 20% of all men with a normal serum PSA levels have clinically significant PCa [81].

Numerous new biomarkers for PCa have been reported, but only a few have been used in a clinical setting [82]. For example, the gene PCA3, also known as DD3, expresses a non-coding messenger RNA, and is markedly upregulated in cancerous

prostate cells, being overexpressed in >95% clinical specimens [7]. No discreet

cytoplasmic protein results from PCA3 transcription, and the function of this gene is not

clearly defined at present [83]. The T-cell coregulatory ligand B7-H3 protein is over-

expressed in prostate tumor cells, and is significantly associated with multiple adverse

prognostic features of PCa, including larger tumor volume, extra-prostatic spread, higher

Gleason score, seminal vesicle involvement, and positive surgical margins [84]. Another

tissue marker over-expressed in prostate cancer cells is alpha-methylacyl CoA racemase

(P504S). This enzyme catalyzes the conversion of (2R) alpha-methyl branched chain

fatty acyl CoAs to their (S) stereoisomers. Positive staining for alpha-methylacyl CoA

racemase can be used to support a diagnosis of cancer on prostate needle core biopsies

when the tumor focus in question is greater than 1mm in dimension [85]. Thus far,

racemase is the only new tissue biomarker of prostate cancer that has gained clinical

acceptance.

## 1.2 Proteomics and Mass Spectrometry

Although DNA is the information archive, proteins do all of the work of the cell.

Proteins closely reflect the ongoing local pathophysiology of diseased tissue and thereby

become candidates for diagnostic and prognostic biomarkers and add to the archive of

molecular changes of cancer found through genomic studies. Proteomics encompasses

the comprehensive identification and quantification of proteins specific to the

physiological state of a cell, tissue or organism. Instead of focusing on one particular

protein, most proteomic studies seek to investigate hundreds or even thousands of

proteins simultaneously in a single experiment by coupling newly developed proteomic

strategies with modern mass spectrometry techniques. Proteome investigations are focused on either expression proteomics, which analyses up- and downregulation of protein levels, or on functional proteomics, aimed at identifying interacting proteins and multiprotein complexes in order to unravel molecular functions and signaling pathways [86]. A detailed understanding of proteins found to be differentially expressed in a disease-specific fashion should offer great insight into the understanding of specific pathogenic mechanisms.

The cancer proteome is an exceptionally complex biological sample containing information on perhaps every biological process that takes place in cancer cells, cancer tissue microenvironment, and cancer cell-host interaction. Cancer cells release protein biomarkers into the extracellular fluid through secretion of intact or cleaved peptides or presumably due to dying/apoptotic tumor cells. In addition, cancer-associated circulating markers can be contributed by the tumor microenvironment of surrounding host cells such as fibroblasts and macrophages [87]. Some of these products can end up in the bloodstream and hence serve as potential serum biomarkers. Therefore, studying the cancer proteome is the logical starting point for identifying diagnostic biomarkers and therapeutic targets for cancer.

The main goal of the emerging field of clinical proteomics is the development of robust, sensitive and specific methodologies for the detection of protein biomarkers or biomarker patterns which will enable scientists and physicians to make reliable early diagnosis and predication of tumor progression. Understanding the molecular basis of tumor characteristics offers great promise for unraveling the complex molecular events of tumorigenesis, as well as those that control clinically important tumor behaviors such as

metastases. Oncoproteomic analysis therefore represents a more direct way of investigating malignancy at the individual cancer patient level opening up a new era of individualized therapy. Although proteomics has proven its promise for biomarker discovery [26, 88, 89], further work is still required to enhance the performance and reproducibility of established proteomic tools before they can be routinely used in clinical laboratory.

As a technology-driven science, proteomics has benefited by the simultaneous advancement of many related research areas. For example, the completion of the genomic sequences of human and other species have provided the amino acid sequence of all the potentially encoded proteins for those species [90]. The resulting genomic sequence databases encompass a library of amino acid sequence information that is required for proteomic study. The development of modern mass spectrometry (MS), especially matrix-assisted laser desorption/ionization (MALDI) and electrospray ionization (ESI) [91, 92], has made it possible to ionize and examine the resulting spectra of large analytes such as proteins without significant fragmentation.

MS instruments consist of at least two basic components: an ionization module and a mass analyzer. The ionization component confers electrical charges to the molecules to be analyzed, typically by adding protons, thus generating ions that can move in the electromagnetic fields of the mass analyzer. Ion movement is dependent on the mass and charge of the ion, and can be measured as mass over charge ($m/z$) ratio. Ions are detected by a device which is able to count the number of ions which strike it for every $m/z$ ratio. Many improvements in MALDI and ESI mass spectrometers have allowed these instruments to emerge as vital tools for protein identification, posttranslational

modification characterization, examination of protein expression patterns, elucidation of protein-protein interactions and the determination of protein structure [93-96]. These improvements offer levels of sensitivity and mass accuracy never before achieved. The recent progress of proteomics has opened new avenues for cancer-related biomarker discovery.

### 1.2.1 MALDI Mass Spectrometry

MALDI-MS was introduced in 1987-1988 by Karas et al. [97] and Tanaka et al [98] and is an ideal tool to investigate complex protein mixtures. A schematic of MALDI instrumentation is shown in Figure 2. MALDI utilizes a matrix, a small acidic aromatic molecule that absorbs energy at the wavelength of the irradiating laser. The analyte molecule is mixed with the matrix, deposited and allowed to dry on a support. During the drying process, matrix-analyte co-crystals form. These crystals are then subjected to an ultraviolet laser which is fired to induce desorption and simultaneous ionization of the analyte. In the MALDI-Time-of-Flight (TOF) [99] platform, irradiation by laser pulses produces short bursts of ions that are then accelerated through a flight tube by an electrostatic field to a common kinetic energy [99]. If all the ions have the same kinetic energy, the ions with low mass to charge ratio ($m/z$) travel faster than those with higher $m/z$ values, and are separated in the flight tube. The number of ions reaching the detector at the end of the flight tube is recorded as relative intensity. The TOF mass spectrum is a recording of the detector signal as a function of time. The time of flight for a molecule of mass (m) and charge (z) to travel this distance is proportional to the square root of its $m/z$ value. Calibration is achieved by analyzing standards of known molecular weight.

MALDI is considered a "soft" ionization method which does not cause fragmentation of

the sample ions. This soft ionization results predominantly in the generation of singly

charged ions regardless of the molecular mass, hence the spectra are relatively easy to
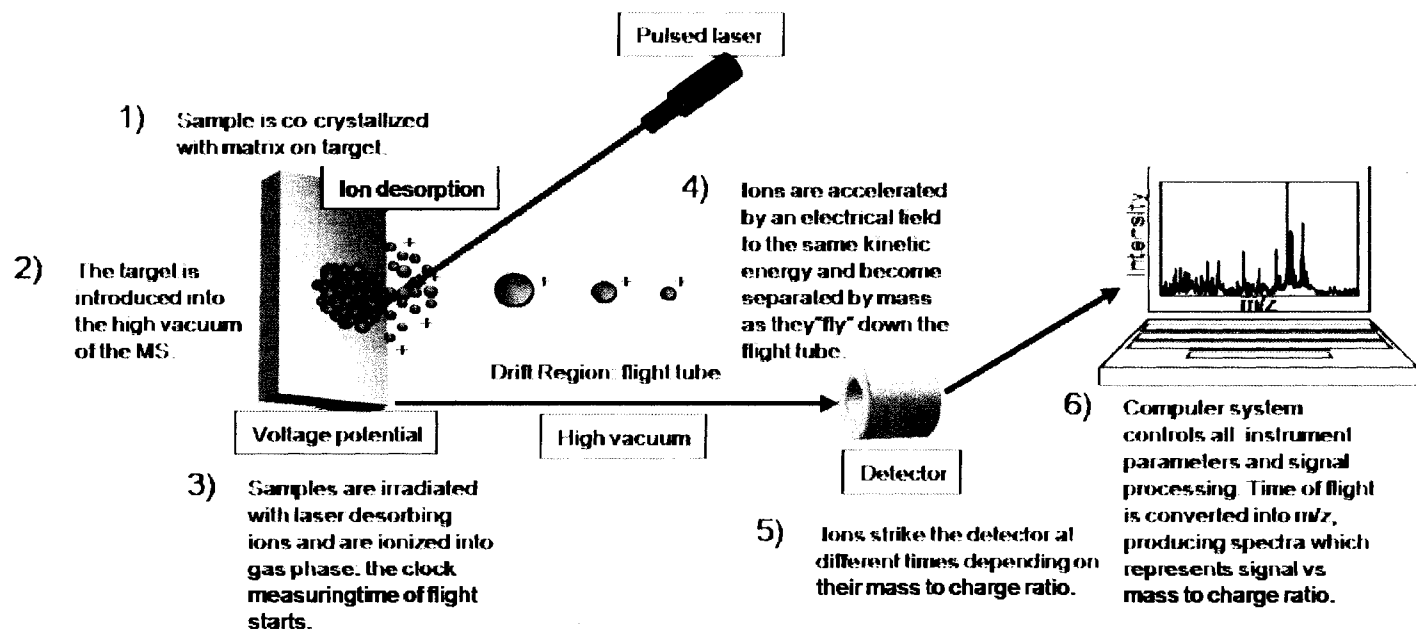
**Figure 2.** Schematic of the components of a MALDI-TOF mass spectrometer.

interpret. If the TOF measurement is performed in the positive ion mode, a general mass shift of +1 Da is observed for all ions. The mono-isotopic form of this ion type is denoted [M+H]$^+$ due to the ionization process in which a proton is exchanged from matrix to analyte. MALDI-TOF-MS is used for detection and characterization of biomolecules, such as proteins, peptides, oligosaccharides and oligonucleotides, with molecular masses between 400 and 350,000 Da [100]. Use of reflectron technology enables much higher resolution and mass accuracy for analyses of peptides in a narrower *m/z* range [101, 102].

The ideal sample preparation for MALDI would be a homogenous layer of small matrix crystals containing a solid solution of the analyte. The matrix should not modify or react with the analyte before laser irradiation. Further, it must be possible to dissolve the matrix in the same solvent as the analyte in order to obtain proper mixing. Matrices must also have low sublimation rates because the sample is introduced into a vacuum for mass spectrometric analysis. Another necessary characteristic is a strong absorption coefficient at the wavelength of the laser. The multiple roles played by the matrix in the desorption and ionization of large analytes has lead to the optimum choice of matrices for different molecular classes being empirically determined [103]. It has been reported that sinapinic acid provides the best signals for higher molecular weight proteins, whereas α-cyano-4-hydroxycinnamic acid is more suitable for lower molecular weight peptides [104].

The protein peaks in a MALDI mass spectrum constitute a pattern that can be interrogated for differences arising from the presence of disease. To move beyond expression patterns and obtain the identities of the components in these highly complex mixtures, it is necessary to use different mass spectrometry techniques for protein

identification. A protein can often be unambiguously identified by the accurate mass

analysis of its constituent peptides (produced by either chemical or enzymatic treatment

of the sample). Tandem mass spectrometry experiments (MS/MS), previously allowed

only with quadrupole and ion trap mass spectrometers are now attainable with MALDI

sources [105]. In MALDI-MS/MS experiments, protein identification is facilitated by

analysis of peptide fragment ions generated inside the MALDI mass spectrometer. In a

process known as collision-induced dissociation (CID), ions desorbed from the MALDI

support or target are accelerated through the first TOF region and precursor ion selection

is performed by a timed gate prior to CID in a gas (usually helium) filled collision cell

[106]. When the gas is introduced into the collision cell, the collision of the peptide

molecules with the gas molecules causes the formation of cleavage products. As seen in

Figure 3, product ions resulting from backbone cleavage of the $\alpha$C-C, the C-N amide

linkage, or the N-$\alpha$C bond are called a-, b-, and c-type ions respectively if the charge is

retained on the amino terminal fragment, or x-, y-, and z-type ions respectively if the

charge is retained on the carboxy-terminal fragment [107]. The most common ions types

formed by MALDI-TOF MS/MS analysis are a-, b- and y- ions. The product ions are

numbered according to their position from their respective terminal end. Therefore the

amino acid sequence and subsequent identification of a parent ion can be determined by

the deconvolution of the fragments present in the MS/MS spectra ("de-novo

sequencing"). Computer algorithms such as SEQUEST or MASCOT can then be used to

determine the "best fit" between the MS/MS sequence information and protein databases.

Another method for protein fragmentation in a MALDI-TOF-MS, termed "LIFT",
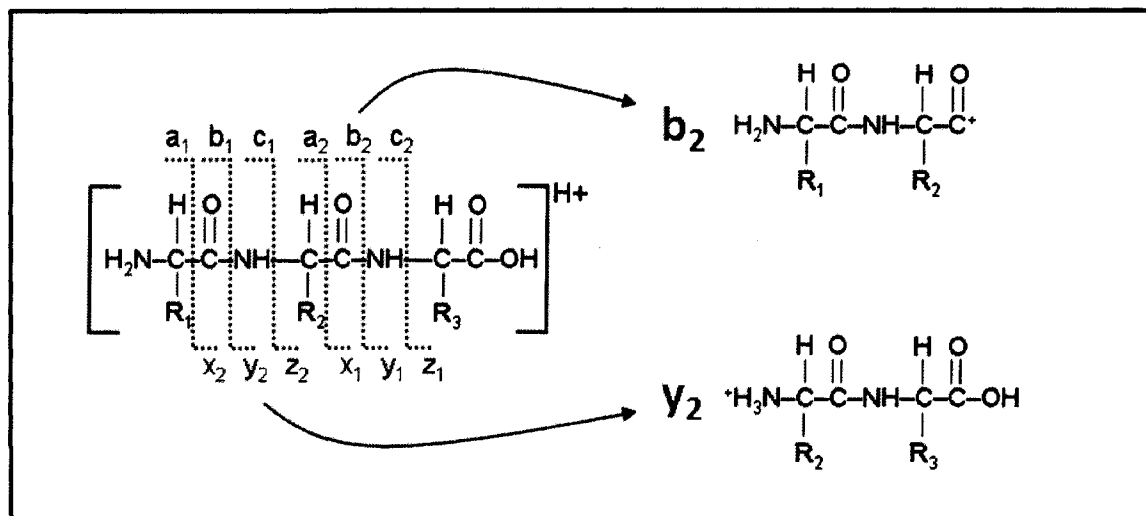
**Figure 3.** The formation of fragment ions during the MS/MS fragmentation of an example peptide with three residue peptide chain. The most commonly observed ions are a, b, and y.

allows for metastable fragmentation induced by a nitrogen laser without the use of collision gas [108]. Selection of the target or parent species is first performed by a precursor ion selector that works as a mass filter for the parent ion and fragments. A relatively low voltage is applied initially for ion acceleration. Fragments are then generated from laser-induced dissociation and subsequently *LIFTed* to a higher potential energy in the LIFT cell. This enables the rapid (seconds) detection of all fragments simultaneously. LIFT is particularly advantageous for the detection of low mass ions of low abundance.

## 1.2.2  Electrospray Mass Spectrometry

Electrospray Ionization mass spectrometry (ESI-MS) was developed by Fenn et al., in the early 1980's but was largely ignored until 1989 when Fenn showed spectra of ionized proteins as large as 40,000 Da [91]. In 2002, Fenn was a Nobel Prize recipient for his contributions to the analysis of biological macromolecules. ESI-MS allows for large, non-volatile molecules to be analyzed directly from the liquid phase, whereas MALDI analyzes samples from a solid state. ESI uses electrical energy to assist the transfer of ions from solution into the gaseous phase before they are subjected to mass spectrometric analysis. Within an ESI source, a continuous stream of sample solution is passed through a stainless steel or quartz silica capillary, maintained at a high voltage. A mist of highly charged droplets with the same polarity as the capillary voltage is generated. The solvent surrounding individual droplets evaporates rapidly in the vacuum chamber of the instrument, leaving unfragmented protein molecules which carry multiple positive charges. These charged molecules are accelerated by an electric field and then deflected

by a magnetic field. They are then separated according to their *m/z*, commonly with an

ion-trap or quadrupole analyzer. A single protein or peptide will show its characteristic

cluster peaks containing multiple-charged ions. The number of charges on the molecules

will depend on the molecular weight of the protein or peptide and the number of

accessible basic sites (e.g. arginine, histidine, and lysine) [109]. Spectrum deconvolution

takes all the multiply charged ions and converts them into a spectrum on a mass (Da)

scale, working out what the molecular weight of the singly charged molecule is most

likely to be. To obtain structural and sequencing information, the precursor ions of

interest can be mass selected and further fragmented in a collision cell. The fragment ions

can then be mass analyzed by a second mass analyzer of a tandem mass spectrometer

system [110]. Since ESI mass spectra depends on the generation of ions in an aerosol, ion

formation is a competitive process. Therefore, salts, phosphate and sulfate buffers,

detergents and polyethylene glycols all compete for the charges. The presence of such

contaminants will result in poor quality spectra. In contrast, MALDI-TOF-MS is much

[107]more tolerant to the presence of salts and detergents [111].

## 1.3 Proteomic Methods for Cancer Biomarker Discovery using Tissue

From work already published, it is clear that the integration of MS into disease

diagnosis as well as outcome prediction will soon take place [112]. For example, recently

discovered protein markers in serum and other body fluids derived from MALDI-MS

proteomic studies have potential for diagnostic and prognostic applications in many

different disease types including cancer [113-118]. Most of these studies employ a

strategy of mining serum for biomarkers. This poses many challenges since abundant

serum proteins make it necessary to fractionate and/or deplete the serum in order to see

proteins which may in fact be seeping into the blood from tumor sites. Using tissue as a starting material for the discovery of biomarkers is attractive because that is where the proteins originate. Unfortunately, tissue proteomics poses great challenges for traditional proteomic approaches because of the heterogeneous nature of most tissues. Tissues are complicated three-dimensional structures composed of multiple subpopulations of cells interacting with each other and with the extracellular matrix. The situation becomes even more complicated as pre-neoplastic and neoplastic lesions develop. For example, histological inspection of prostate cancer tissue typically reveals a juxtaposition of benign glands, preneoplastic (PIN) foci, and neoplastic foci of varying severity [119]. Overcoming these challenges is of the utmost importance since examining the protein distributions in specific tissues is crucial to unraveling biochemical pathways and for the diagnosis of many diseases.

There are two common approaches for proteome analysis in tissue samples: intact protein separation and peptide separation. Protein separation methods include one- and two-dimensional gel electrophoresis (1-DE and 2-DE), one- and two-dimensional liquid chromatography (1D LC and 2D LC), and affinity chromatography for selective isolation of a target protein [93]. Peptide separation is more limited and includes multidimensional liquid chromatography and selective enrichment of a subset of peptides which is highly representative of the parent proteins [120].

### 1.3.1 2D Electrophoresis

Traditionally, proteomic techniques aimed at biomarker discovery have centered on the identification of differentially expressed proteins from cell or tissue samples

following gel or liquid chromatographic separation. Two-dimensional polyacrylamide gel electrophoresis (2D-PAGE) is one of the most widely used techniques for proteomic studies and can resolve thousands of different protein species [24]. Protein mixtures derived from tissue lysates are first separated according to their isoelectric point by isoelectric focusing and then separated according to their size by sodium dodecyl sulfate (SDS-PAGE). The separated proteins are visualized with different staining techniques, such as coomassie blue or silver. For expression proteomic studies, differentially expressed proteins are identified by comparing spot intensities between samples. The gel spots of interested can then be excised and digested with a protease for identification using MS methods such as peptide map fingerprinting, and/or tandem MS [121]. The quantification of proteins has now become more accurate with the introduction of highly sensitive fluorescent stains or dyes with a wide dynamic range. These dyes have been effectively employed in differential gel electrophoresis or DiGE [122]. In DiGE, the protein samples to be compared are covalently labeled with a green or red fluorescent dye. A mixture of both the samples is also labeled with a blue dye and serves as an internal standard. All three samples are then mixed together and separated by 2D-PAGE. The excitation and emission wavelengths of each respective dye are different, enabling the visualization of different images of the protein spots attributed to each sample when the gel is scanned .

Advances in 2D-PAGE technology coupled with robotics and software programs for identifying potential protein alterations have improved this proteomic methodology. Nevertheless, 2D-PAGE is still cumbersome, labor intensive, and suffers reproducibility problems. Additionally 2D-PAGE requires large amounts of starting material (40–100 μg

of total protein to generate ~500 spots/gel) to visualize adequate number of silver-stained

proteins in the gel [123], making it a poor choice for small clinical tissue samples or

biopsies. Furthermore, very acidic or basic proteins, very large or small proteins, and

membrane proteins are all underrepresented in 2D PAGE analysis [124].

Methods such as laser capture microdissection (LCM) have been used with great

success to select homogeneous cell populations [125]. LCM entails placing a transparent

film over a tissue section or a cytological sample, visualizing the cells microscopically,

and selectively adhering the cells of interest to the film with a focused pulse from an

infrared laser [126]. LCM combined with 2D-PAGE and more recently MALDI-MS, has

great applications in a wide range of biological systems. LCM's unique ability to quickly

and accurately generate protein profiles from small numbers of pure cells from a

heterogeneous tissue has extraordinary utility in finding disease markers, elucidating

mechanisms of tumor development, and classifying tissue subtypes by protein expression

levels [127-129]. However, the LCM technique cannot be easily applied to traditional

proteomic analysis because 50,000 to 100,000 cells are required for one 2D-PAGE

experiment [130]. Obtaining this large amount of cells manually is very labor-intensive,

and cannot be done routinely which limits any high throughput analysis. Taken together

the use of LCM followed by 2D-PAGE for any clinical proteomics study is difficult at

best and generally not feasible.

### 1.3.2 Chromotography Techniques

Alternative strategies to 2D-PAGE for cell and tissue proteome analysis are

generally based on increasing levels of protein and peptide separation coupled with

amino acid sequence analysis by tandem MS. One-dimensional liquid chromatography

(1D-LC) can be used to separate proteins based on their size (mass), pI (charge), or hydrophobicity. The most commonly used 1D LC method is reverse phase chromatography, which separates proteins based on their hydrophobicity. In proteomic studies, 1D LC has been used primarily for peptide separation before MS analysis, but it can also be used for protein separation of complex lysates from cells or tissue before enzymatic digestion and MS [131]. In two dimensional liquid chromatography (2D-LC), proteins are separated in the first dimension by isoelectric chromatography (pI) (or SCX-strong cation exchange chromatography) and in the second dimension by hydrophobicity (reversed phase) [132], thereby increasing the degree of protein fractionation and decreasing sample complexity.

LC-MS has evolved into a powerful procedure for detailed identification as well as quantification of complex proteomic samples offering the possibility to isolate and sequence hundreds of selected peptides from one sample. Increasingly, proteomic investigators are employing a strategy based on proteolysis of proteins followed by analysis of the complex peptide mixture by LC-MS/MS. This approach is referred to as "shotgun" or multidimensional protein identification technology- i.e. "MudPIT" and was first described by Yates and co-workers [133]. Typical MudPIT approaches use SCX followed by reverse phase chromatography interfacing directly with ESI-MS, dramatically cutting down on analysis time. Recently this MudPit approach was applied to analyze the global proteome of the KATO III human gastric carcinoma cell line. This analysis led to the identification of 1966 uniquely expressed proteins contributing to the characterization of human gastric carcinoma [134]. A caveat to this type of analysis should be mentioned. Since samples must be initially digested with trypsin or another

protease before analysis, this results in a vast increase in complexity of the results making it more difficult to unambiguously reassemble peptide sequences into their precursor proteins. This is especially true in higher eukaryotic organisms, because a single distinct peptide sequence can be represented in several distinct biologically active protein isoforms.

### 1.3.3 Protein Arrays

Traditionally, immunohistochemistry (IHC) has been a technique commonly used for profiling protein distributions in tissue. In this approach antibodies are needed to detect specific proteins and usually only one protein can be detected in a single experiment. The use of protein arrays can facilitate the detection of multiple proteins in a single experiment. A protein microarray consists of antibodies, proteins, protein fragments, peptides, aptamers or carbohydrate elements that are coated or immobilized in a grid-like pattern on small surfaces. There are mainly two types of protein microarrays: analytical and functional [135, 136]. Analytical or detection protein microarrays are used to profile and quantitate antibodies or proteins, and frequently consist of antibodies directed against a defined set of proteins from cells or tissues [137]. These antibodies are robotically spotted onto a solid support such as a glass slide. The slides are then probed with cell or tissue lysates. In contrast to MS pattern analysis, protein microarrays start with a limited, but specific, knowledge of the identities of important signaling molecules in the cancer cell. With protein microarrays it is possible to measure the activated (*e.g.,* phosphorylated or cleaved) form of key signal proteins and thereby estimate whether the designated signal node is "in use" at the time the proteins are extracted from the cell. The

greatest challenge in the use of antibody arrays is obtaining antibodies against all the proteins that comprise the human proteome. At this time antibodies are available for a mere fraction of the proteome. Reverse-phase protein microarrays, are based on the opposite configuration from an antibody array. Cellular proteins (nano or pico liter amounts) to be assessed are robotically spotted onto a nitrocellulose backed slide. Subsequently, each slide can be probed with an antibody that can be detected by fluorescent, colorimetric or chemiluminescent assays. The signal intensity of each array spot is proportional to the concentration of the analyte member within the population of proteins immobilized on the spot. Relative quantitative comparisons of protein concentrations can be made within or between multiple study cases. Investigations performed by Paweletz, *et al.* demonstrate the utility of reverse phase protein arrays to monitor proteins expressed during disease progression [138]. Protein arrays technologies may uncover molecules with specific post translational modifications differentially expressed in a disease state, but primarily they are used for the validation and quantitation of existing biomarkers. They are therefore not useful tools in the discovery of novel markers. Furthermore, the expression and analysis of proteins is carried out in artificial environments relative to the cell and these environments may not have physiological relevance to the biological system under study.

### 1.3.4 New Methods for Tissue Proteomics and Biomarker Discovery.

A major shortcoming associated with the early detection and treatment of cancer is the lack of sensitive and robust technology to detect the molecular signatures of cancer cells from minute quantities of available tissues or serum. New methodologies for tissue

protein profiling such as LCM combined with MALDI mass spectrometry have been used

by our laboratory and others for the discovery of protein markers in complex tissues [125,

127, 139, 140] . This combination of techniques permits simultaneous examination of

hundreds of proteins from a nearly pure cell population removed from a heterogeneous

sample, however large sample requirements and the time consuming step of

microdissection, as mentioned above, will most likely prevent the implementation of this

technique beyond discovery and into the realm of clinical diagnostics. A recent

applications of MALDI MS which addresses the problems of high through-put and

sample requirements is its use to profile and image proteins directly from thin tissue

sections [141, 142]. This technique, known as MALDI imaging mass spectrometry

(MALDI IMS) was pioneered by Richard Caprioli at Vanderbilt University [143]. The

method bypasses the need for microdissection and solubilization of tissue proteins prior

to analysis. MALDI-IMS methodology employs the following scheme (reviewed in [144]

and outlined in Figure 4): A matrix solution, such as sinapinic acid (SPA), is directly

deposited onto tissue sections, and the soluble proteins are extracted from the tissue and

co-crystallize with the matrix. Protonated protein ions are formed by irradiating the

matrix with a pulsed laser directly on the tissue and are separated by m/z in a MALDI-

TOF mass spectrometer. Protein species in the mass range of 2,000-100,000 Da are then

detected in the mass spectra. If matrix is applied uniformly across the tissue section,

desorption can be targeted to specific "points" in a grid pattern and the data rasterized.

The resulting spectra can then be used to generate two-dimensional molecular maps of

hundreds of peptides and proteins directly from the surface of a tissue section. These

molecular maps display the relative abundance and spatial distribution of the protein and
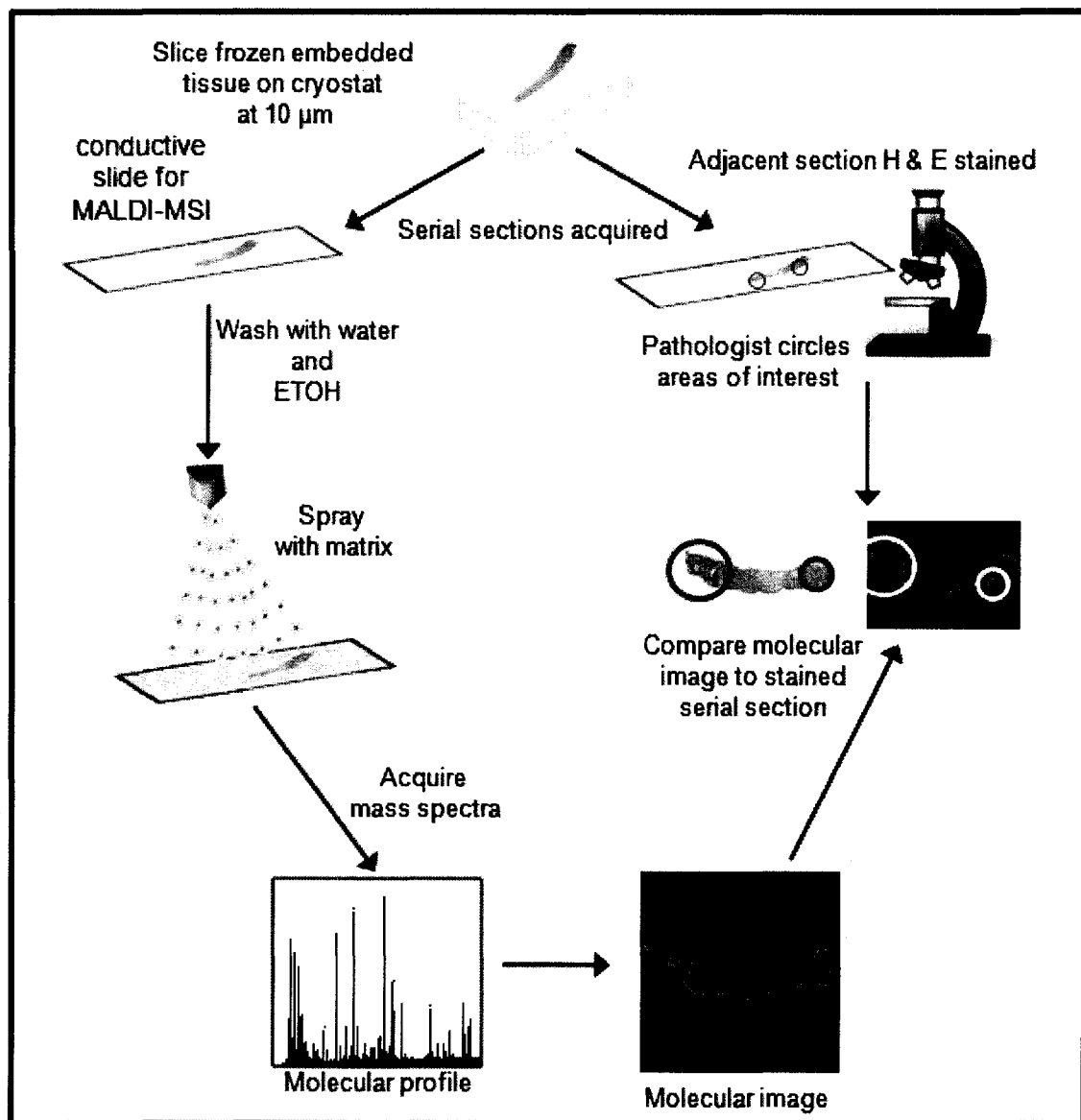
**Figure 4.** Graphic representation of MALDI-IMS protocols using frozen tissue.

peptide molecules.

Several recent studies underscore the potential of MALDI-IMS for clinical histopathology applications. Protein expression profiles obtained from tissue could discriminate lung cancer subtype [145]. Tumor histology, therapeutic response, and patient survival were shown to correlate with the protein expression patterns obtained from direct tissue analysis in breast tumors [146, 147]. Protein expression patterns and images were also found to correlate with brain tumor histology and patient survival [148]. Similar discovery efforts using MALDI-IMS have yielded potential candidates in ovarian, colon and prostate cancer [149-151].

MALDI-IMS also has utility in the examination the distribution of small molecules and peptides in tissue sections [152, 153]. Many compounds that are biologically or pharmacologically relevant are less than 1 kDa in size and thus fall into the broad category of small molecules Levels of drugs such as chemotherapeutic agents or hormonal therapies can be measured directly from a tissue biopsy to assess the level of delivery to a particular organ site [154], opening new possibilities for the measurement of concomitant protein changes in specific tissues after systemic drug administration. The spatial distribution of peptides in a tissue section can also be examined via MALDI-IMS by spotting the section with small volumes of a trypsin solution to carry out in situ protease digestion. Sequence determination of the tryptic fragments is performed using on-tissue MALDI MS/MS analysis directly from the individual digest spots. This protocol enables protein identification directly from tissue while preserving the spatial integrity of the sample. This procedure was demonstrated with the identification of several proteins in the coronal sections of a rat brain [155].

Upregulation of proteolytic activity is a feature of malignant cells [156]. Cancer development is essentially a tissue remodeling process in which normal tissue is substituted with cancer tissue. A crucial role in this process is attributed to proteolytic degradation of the extracellular matrix (ECM). Degradation of ECM proteins is initiated by proteases, secreted by different cell types, participating in tumor cell invasion [156]. Therefore the examination of endogenous peptides in PCa tissue via MALDI-IMS may help determine clues to tumor initiation and progression pathways. Recently MALDI-IMS became available on instruments that allow the measurement of mass signals with very high resolution and precision, namely Fourier transform mass spectrometers (FT-MS) [157, 158]. The spatial distributions of biomolecules differing in mass by less than 0.1 Da can be resolved, using FTICR. This represents a mass resolution not attainable with other MALDI-TOF platforms allowing for the analysis of small metabolites and lipid molecules.

MALDI-MSI has extraordinary benefits as a discovery tool because one does not need to know, in advance, the specific proteins that have changed in a comparative study. Furthermore, the cellular origins and relative concentrations of the biomarkers across the tissue section can be assessed. Once a marker of interest is identified, its precise location, concentration, regulation and function may be investigated, to help understand disease progression at the molecular level. However, critical questions remain regarding the integration of this technique with clinical decision making. The information obtained from MALDI-IMS should significantly augment and enhance existing clinical pathology practices, but not replace them. Obtaining protein biomarkers which are specific for a disease or different stages of a disease would greatly benefit the ability of physicians,

surgeons and pathologists to accurately provide patients with a "personalized" diagnosis and prognosis. The use of this new technology for the advancement of such endeavors holds great promise.

# CHAPTER II

## DISSERTATION RATIONALE AND SUMMARY OF AIMS

The objective of this research proposal is the application and investigation of MALDI-IMS to clinical diagnostics in the examination of prostate cancer tissue. The goal of this clinical/translational approach is to provide a molecular assessment of tumor progression obtained from surgery specimens, with the potential to identify tumor subpopulations and predict patient survival beyond the current histologically determined cellular phenotypes.

Routine diagnostic pathology represents the gold standard and plays an integral role in the diagnosis and prognosis of cancer. Because therapeutic decisions are based on the presumed reliability of the pathology diagnosis, a misdiagnosis can result in unnecessary, harmful and aggressive therapy or inadequate treatment. Unfortunately, medical studies over the last two decades have demonstrated that this gold standard is not consistently reliable. In fact, multiple studies in various cancers have demonstrated discrepancy rates of up to 30% with an average of approximately 10% [159]. Traditionally, pathologists use histopathological images of biopsy samples removed from patients, examine them under a microscope, and make judgments based on their personal experience. While examining such tissues, a pathologist assesses the deviations in the cell structures and/or the change in the distribution of the cells across the tissue. However, this judgment is subjective, and leads to considerable variability [160, 161]. Furthermore, cancer staging provides only probabilities of the course of disease for any individual patient. There still remains a mysterious heterogeneity of outcomes for patients with

cancers of apparently equivalent type, stage and grade. While some recurrences may be due to an incompletely removed tumor or occult micrometastasis, in other cases the recurrence occurs in genetically altered cells in a field surrounding the area from which the tumor was excised [162, 163]. This field of genetically altered cells is defined as a precancerous group of epithelial cells of monoclonal origin [164].

Prostate cancer is a major health burden throughout the world being the most common cancer among men in most developed countries. The molecular pathology of PCa is complex, and the pathways and acquired molecular alterations which are involved in the initiation and progression of prostate tumors are still largely unknown. It is presently not possible to predict aggressiveness in PCa and many tumors with similar histopathological features do not behave similarly. Clearly new molecular markers of PCa are needed to improve and assist pathologists in cancer diagnosis/prognosis.

Malignant transformation initiates alterations in protein expression. These alterations can be monitored at the protein level, *in situ* both qualitatively and quantitatively with a recently developed technique, known as matrix-assisted laser desorption/ionization imaging mass spectrometry (MALDI-IMS). This technique holds promise for the discovery of new molecular markers by examining the protein signatures present in tissue. **The *central hypothesis* of this dissertation is that discrete protein mediators of tumor-host interactions in prostate tumor tissues which are involved in PCa initiation and progression, including metastasis can be identified using MALDI-IMS.** Our central hypothesis will be tested and our overall research objective will be achieved by pursuing the following specific aims.

**AIM 1**: The application of MALDI-IMS to prostate cancer diagnosis and prognosis. The goals of this Aim are:

A. Optimization of MALDI-IMS techniques to existing clinical pathology laboratory practices. This includes enhancing the reproducibility of matrix deposition techniques and new fixation methods which preserve both morphology and proteins.

B. Identification of tumor specific protein expression patterns in prostate tissue. Comparison of the protein expression patterns of primary PCa tumor to surrounding normal tissue will elucidate the tumor microenvironment. The protein patterns will be analyzed with software to create classification algorithms which can distinguish between tumor subtypes on the basis of pathology. Images of specific *m/z* signal will be constructed by plotting the relative ion intensities of a given *m/z* signal over all the spots, providing a plot of the spatial distribution of that protein within the tissue. These images will also be examined for their ability to provide diagnostic information.

C. Identification of protein expression patterns in primary prostate tumor tissue indicative of metastatic disease. Using a cohort of patients presenting with similar risk factors but no extra-prostatic disease at the time of their prostatectomy, profiles and images of PCa lesions from patients with micrometastatic disease will be compared.

**AIM 2**: Sequence identification and characterization of potential biomarkers for clinical diagnostics. This Aim entails:

A. Using fractionation and MALDI-TOF MS/MS (LIFT) methods for protein

sequence determination, the identities of the proteins and endogenous peptides

discovered in Aim 1 will be determined. The sequence identity of the

differentially expressed proteins in normal and diseased tissue will also help

elucidate key pathways that are disregulated in PCa.

B. In-situ trypsin digestion on tissue sections will be employed for the validation

(from Aim 2A) and identification of proteins and peptides present in both PCa

and benign adjacent tissue. MALDI-TOF MS/MS will be used for sequence

identification.

C. Validation of the identities of biomarkers discovered will be determined

orthogonally with Western blot analysis and immunohistochemistry

D. Characterization of biomarkers identified and their role in cancer initiation and/or

progression by the examination of related molecules. This will be performed

using imunohistochemistry and/or Western blot techniques.

**AIM 3:** Evaluation of the clinical utility of MALDI-IMS biomarkers. The goals of this
Aim are:

A. Using a cohort of surgery specimens the clinical utility of biomarkers and protein

expression patterns found and identified in Aims 1 and 2 will be evaluated. Tissue

samples will be blinded and the diagnosis based on MALDI IMS imaging and

spectral analysis will be compared with diagnosis made by clinical laboratory

pathologists.

# CHAPTER III

# AIM 1: THE APPLICATION OF MALDI-IMS TO PROSTATE CANCER DIAGNOSIS AND PROGNOSIS

## 3.1 Introduction

Prostate cancer is the most common cancer, other than skin cancers, in American

men. The American Cancer Society estimates that during 2008 about 186,320 new cases

of prostate cancer will be diagnosed in the United States [30]. In addition, prostate

cancer is the only tumor for which diagnosis is exclusively based on biopsies, placing a

large burden on the ability of pathologists to both detect and predict the course of the

disease. Current markers poorly predict early disease development and tumor

aggressiveness [71]. If you add the fact that PCa is usually heterogeneous and multifocal,

with diverse clinical and morphologic manifestations, it is clear that here is a desperate

need for molecular markers to aid pathologists. Currently, surprisingly little is known

about early molecular alterations in prostate cancer, but several studies have found that

considerable molecular changes precede morphologically detectable malignant

transformation of prostate epithelial tissues [165]. The correlation of molecular

information to histopathological structures offers tremendous potential for improved

characterization of PCa leading to novel strategies in the clinical management of prostate

cancer.

Cancer biomarker discovery has been and continues to be an active and

productive area of research and scientists are using ever more sophisticated and

innovative technologies in this effort. Unlike traditional biomarker approaches to obtain

proteomic information, mass spectrometry provides for an extremely rapid and potentially high-throughput platform for biomarker discovery. This powerful technology can identify all proteins and their posttranslational modifications in disease conditions, and hence will greatly accelerate progress toward novel diagnostic and prognostic tools to track early disease. The use of MALDI-IMS and profiling to obtain such molecular information in the form of protein and peptide distributions greatly enhances the ability to identify potential candidates for new specific biomarkers. In their groundbreaking study, Caprioli and Carbone showed that proteomic patterns obtained directly from small amounts of fresh frozen lung-tumor tissue could be used to accurately classify and predict histological groups as well as nodal involvement and survival in resected non-small-cell lung cancer [145]. Similar results were obtained for ovarian cancer in which peptide profiling by direct MALDI analysis of 25 ovarian carcinomas (stages III and IV) and 23 benign tissues identified several peptides observed to be present only in carcinoma compared to benign samples [166]. The most prevalent peptide was identified as a fragment of immunoproteasome PA28. Specific to prostate tissue, MALDI-IMS revealed a specific expression pattern that was temporally associated with prostate development in an animal model [167] and in a separate study a protein expression pattern was associated with pathogenesis of prostate cancer in a cohort of 22 prostate tissue samples [150].

A major advantage of MALDI-IMS is the avoidance of time-consuming extraction, purification or separation steps, which have the potential for producing artifacts [104]. The reliable and sensitive detection of changes to the proteome in tissue samples is an important challenge and will require standardization and optimization of methodologies. The second most important challenge is the integration of MALDI-IMS

into existing clinical pathology laboratory practices. All of the protocols developed to date for protein analysis by MALDI-IMS have been optimized for freshly frozen tissue specimens. Snap-freezing of tissue samples is ideal from a protein stand point, because no processing is involved and, when performed rapidly, avoids protein degradation through proteolysis. However, frozen tissue is often difficult to process and store for most pathology labs. Historically, tissue samples analyzed in pathology laboratories undergo formalin fixation, dehydration through graded alcohol series, and paraffin embedding. Although the morphology of formalin fixed tissues is superior with respect to fresh frozen samples, the molecular cross-linking by formalin renders proteomic analysis almost impossible [168].

A recently introduced histologic fixative (Universal Molecular Fixative, UMFix) has been shown to preserve macromolecules (DNA, RNA and proteins) in tissue at ambient temperature [169, 170]. A recent study found that the intensity of immunohistochemical reactions for most cytoplasmic antigens was generally equal or stronger in UMFix treated tissues when compared to formalin fixed tissues [171]. Therefore UMFix would seem an ideal choice for the processing of clinical pathology specimens for MALDI-MSI, but protocols for sample preparation, storage and data collection need to be optimized and evaluated. Another important aspect of sample preparation is the homogeneous deposition of the MALDI matrix on the tissue sample in such a way as to avoid significant lateral migration of proteins on the surface of the section. The matrix can either be deposited as individual spots or spray coated as a homogeneous layer. Evaluation and optimization of matrix deposition is crucial to provide consistent results in diagnostic clinical applications.

In Aim I we refine and optimize sample preparation and MALDI-IMS protocols for specific molecular imaging of prostate tissue with emphasis placed on compatibility with current clinical pathology methodologies, by using fixed tissue. An initial cohort of PCa and normal tissues was used to standardize existing protocols. We compared protein profiles of bulk tumor to surrounding normal tissue and profile the tumor microenvironment to probe tumor-host interactions in this initial data set. Additionally, we contrast protein profiles of metastatic lesions with surrounding normal tissue and in tissue obtained from matched patients with similar risk factors who did not develop extra-prostatic disease. The imaging and protein profiling of these tissues has provided us with a critical evaluation as to the utility of the method and capacity to resolve the protein signals from different cell types in close proximity. The comparison of the protein profiles and images generated using MALDI-IMS in a large cohort of prostate cells with different pathological sub-types enabled us to detect PCa in tissue samples.

## 3.2 Materials and Methods

### Materials

Acetonitrile, ethanol, high-performance liquid chromatography (HPLC) grade water, 3,5-dimethoxy-4-hydroxycinnamic acid (sinapinic acid-SPA) were purchased from Sigma Chemical Co. (St. Louis, MO). (HCCA) α-cyano-4-hydroxycinnamic acid was purchased from Bruker Daltonic. Tri-fluoroacetic acid (TFA) was purchased from Pierce Biotechnology, (Rockfold, IL). UMFix (Sakura Finetek USA, Inc.) is a mixture of methanol and polyethylene glycol at a predetermined ratio as previously described (US patent application number 10/141, 780).

**Patients and Tissue Samples**

Patients were consented prior to undergoing radical prostatectomy at Sentara

Norfolk General Hospital. Study protocols were approved by the institutional review

board at EVMS. The age range of the patients was 46-69 with a mean age of 57 years

who underwent surgery between 2003 and 2008. A total of 59 patients were recruited for

this study. Two cored specimens were harvested from each prostate immediately after

removal of the organ. One core was fixed in formalin or UMFix and paraffin embedded

and the other was embedded in OCT (optimal cutting temperature compound, Sakura

Finetek USA) and frozen at 80°C. A total of 72 frozen tissue blocks were acquired from

prostatectomy tissue. The frozen blocks yielded 36 sections of benign tissue (distal from

tumor site), 36 sections of PCa containing tissue (Gleason grades 6-10) with 25 harboring

benign adjacent tissue. Additionally, 12 tissues collected from patients who developed

metastatic disease after their surgery and 7 matched tissues from patients presenting with

similar risk factors but no metastatic disease were harvested for this study. Cryo-

sectioning was performed on a Microm HM 505E cryostat at -20°C. A serial cryosection

at 8µm was stained with hematoxylin and eosin [172] as a guide, and analyzed by a

pathologist to determine tissue morphology. Two additional serial sections at 10µm were

mounted on conductive Indium-Tin Oxide (ITO) coated glass slides (Bruker Daltonic,

Billerica, MA) and used for MALDI-IMS.

**Processing and Sectioning of Fixed Tissue**

Formalin fixed surgery specimens fixed in 10% neutral buffered formalin and

processed overnight in a standard processing machine [173]. Mirrored tissue blocks from

the same surgery specimen were fixed in the UMFix and processed according to a

recently processed in a V.I.P. tissue processor (Sakura Finetek, Inc., Torrance, CA) as

recommended [174]. Sectioning was performed on a Reichert-Jung microtome model

2030. Initial sections were cut (8μm) and stained with hemotoxylin and eosin for

histopathological evaluation by a pathologist. Serial sections were then made (10μm) and

placed on ITO coated slides for MALDI-IMS. The slides were then de-paraffinized by

heating to 45°C and for 3 minutes followed by xylene treatment for 1 min. The sections

were incubated in 100% followed by 95% ethanol for one minute each and then air dried.

Slides were stored in a dessicator until spray coated with matrix.


**Tissue Section Preparation**

Immediately after sectioning, the ITO coated slides containing OCT embedded

frozen tissue sections were washed and fixed with 70% ethanol and 95% ethanol for 30s

each. A water wash was performed to remove residual embedding media followed by a

repeat of the ethanol washes of 70% and 95%. Slides were air dried and stored in a

dessicator for 1 hour before matrix deposition. A matrix solution of sinapinic acid (10

mg/ml) containing 75% acetonitrile and 0.13% TFA was sprayed uniformly over the

tissue using an automated spraying device, (ImagePrep Bruker Daltonics) which controls

matrix deposition and thickness of the matrix layer. Digital images of the sprayed tissue

sections were acquired with a flatbed scanner prior to MALDI analysis.

**MALDI-IMS Analysis and Image Processing**

Spectra were collected across the entire tissue area using the Ultraflex III

MALDI-TOF/TOF instrument (Bruker Daltonics) with a SmartBeam laser operating at

200 Hz in linear mode over a mass range of 2,000 to 45,000 Daltons. A laser spot

diameter of 50 μm and a raster width of 100 μm were employed. Using the FlexImaging

software (Bruker Daltonic), teaching points were generated to ensure the correct

positioning of the laser for spectral acquisition. The software exports the specific

geometry of the tissue to be analyzed and an instrument specific automated method is

created which generates a grid across the tissue of spots where the laser will acquire data.

A total of 200 laser shots were accumulated and averaged from each laser spot rastered

across the tissue section. Calibration was performed externally using a peptide standard

in the mass range of 700-4500 Da. The intensity of each signal over the entire mass range

acquired is plotted as a function of location on the tissue allowing the visualization of the

location of each *m/z* detected. These images were generated and visualized using Flex

Imaging and Biomap software (available as free software from www. MALDI-MSI.org.).

**Data Processing and Statistical Analysis**

Automated analysis of the spectral data was performed to identify all

differentially expressed peaks between cell types. Spectra derived from defined Regions

of Interest (ROI) in each tissue were exported using the FlexImaging software for profile

analysis. Base-line subtraction, normalization (to total ion current), peak detection, and

spectral alignment were performed using ClinProt. A mass window of 0.3% and a signal

to noise ratio of 3 were selected for peak detection. A genetic algorithm (GA) using k-

nearest neighbors (KNN) was used to obtain a classification between normal and PCa containing tissue. The result of the GA is the peak combination which is proved to separate best between the different classes. Significant differences between groups were determined by Student's $t$ test. A $P$-value of less than 0.01 was considered to indicate statistical significance. The predictive power of the putative biomarker to detect PCa tissue areas was tested using the area under the receiver operator characteristic (ROC) curve using SPSS for Windows. The optimal cut-off point was defined as that point on the ROC curve that maximizes both sensitivity and specificity.


## 3.3 Results

**Optimization of Matrix Deposition**

Recently our laboratory acquired a new device for the spray coating of tissue sections for with matrix for MALDI-IMS. In this device (ImagePrep, Bruker Daltonics), a matrix aerosol is created by vibrational vaporization under controlled conditions. An average droplet size of ~20 μm is generated and all droplet diameters are < 50 μm. For quality control an optical sensor monitors the light scattered from matrix crystals to control the preparation parameters in real-time. These parameters include: deposition periods and intervals, matrix layer thickness, wetness, and drying rate. During the wetting period the scattered light intensity fades while drying increases the intensity due to crystal formation. At complete dryness the signal received by the optical sensor is a direct measure of the thickness of the matrix layer. We evaluated the reproducibility of this instrument using serial sections from the same tissue specimen. As shown in Figure 5, the uniformity of the spray coating is consistent across each sample and duplicate samples
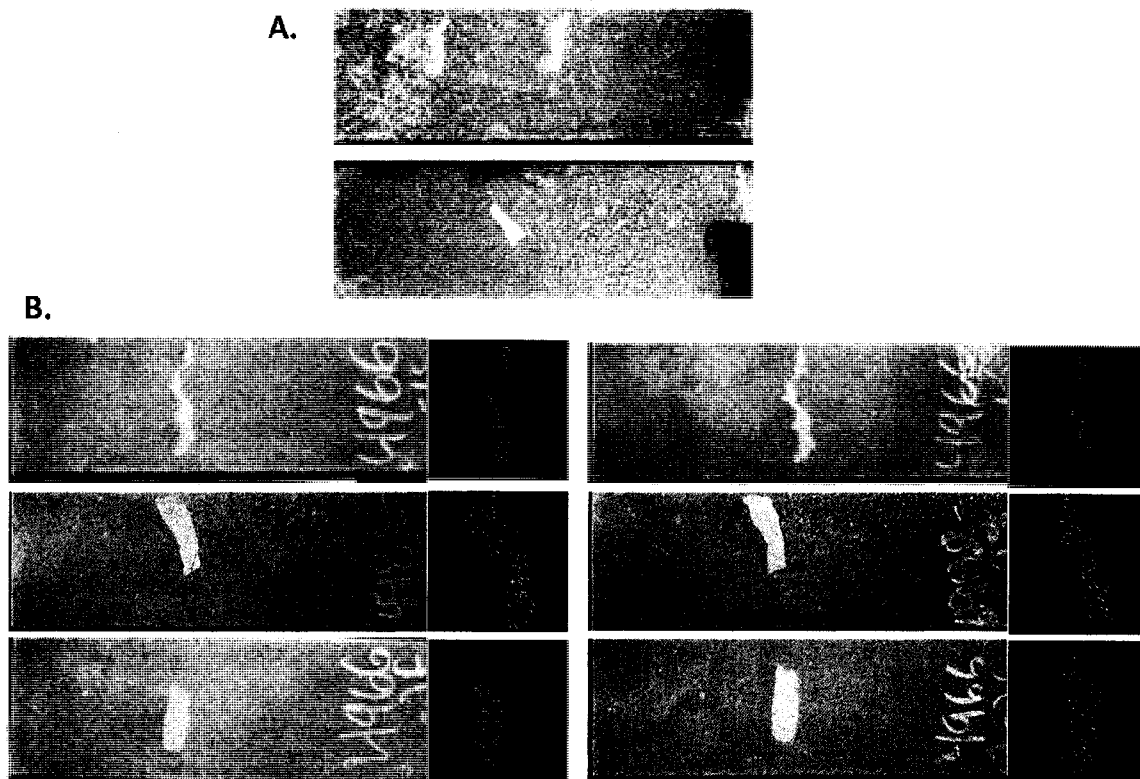
**Figure 5.** Comparison of hand spraying with a TLC sprayer to automated spraying using the ImagePrep device. A.) Two representative slides hand sprayed with SPA matrix (20 passes). B.) Three sets of two serial tissue sections sprayed with the ImagePrep automated spraying device. Also shown are the accompanying MALDI-IMS images of a common $m/z$ value of 11303.5 showing reproducibility of the images produced.

and far superior to hand spraying (a method we evaluated initially using a TLC sprayer).

This reproducibility in matrix coating resulted in reproducibility of spectrum and images

produced across duplicate tissue sections.

**Identification of an Expression Profile that Discriminates between PCa and**

**Adjacent Normal Tissue**

Our investigation into the presence of a PCa specific protein/peptide expression

profile was conducted on a total of 72 frozen prostate tissue samples derived from 59

patients. The patient and tissue sample characteristics of this cohort are presented in

Table 1. Tissue sections were uniformly coated with matrix using the automated spraying

device, and adjacent serial sections were stained with hemotoxylin and eosin (H&E) for

histopathology. Parallel stained slides of each section were read by a genitourinary-

trained pathologist and the regions of interest (ROI) designated. These ROI contained

prostate adenocarcinoma cell populations, benign adjacent epithelial cells, as well as

stroma and benign epithelial cells from tissue specimens without tumor cells present. In

an initial survey experiment we analyzed 22 tissue sections (11 PCa and 11 benign). The

resulting spectra were used to generate two-dimensional molecular maps of the peptides

and proteins present in each tissue section and automated analysis of the spectral data was

performed to identify differentially expressed peaks. Several peptide ions were found to

discriminate PCa from benign tissue (Table 2). Examination by a pathologist reveals

specific regions with designated cell types present in prostate tissue sections (Figure 6A).

In the mass range *m/z* 3000-5000 several differentially expressed ions were detected

which could be used to discriminate between PCa and adjacent benign regions (Figure 6B

inset and Table 2). Of particular note are two peptide ions with an average *m/z* of 4027,

**Table 1.** Patient and Tissue Sample Characteristics

| Characteristics | N |
|---|---|
| Mean age years (range) | 57 (46-69) |
| Mean preoperative PSA ng/ml (range) | 10.2 (3.6-37.5) |
| Tumor volume (%) | 21.3 |
| | |
| *Pathological classification* | |
| pT2a | 8 |
| pT2b | 3 |
| PT2c | 23 |
| PT3a | 20 |
| PT3b | 5 |
| **Total Patients** | **59** |
| | |
| **PCa containing tissue** | 36 |
| *Gleason Score* | |
| 4-6 | 20 |
| 7 | 16 |
| 8-10 | 0 |
| | |
| **Adenosis** | 2 |
| **Benign** | 36 |
| **Total Tissue Samples** | **74** |

**Table 2.** Peaks Used to Discriminate PCa from Benign Adjacent Tissue

| Peaks highly expressed in PCa cells (m/z) | |
|---|---|
| 3373 | |
| 3443 | |
| 3487 | |
| 4027 | |
| 4355 | |
| Peaks highly expressed in benign adjacent cells (m/z) | |
| 4274 | |
| | |
| % Cancer correctly classified | 81.7 |
| % Benign areas correct | 59.8 |
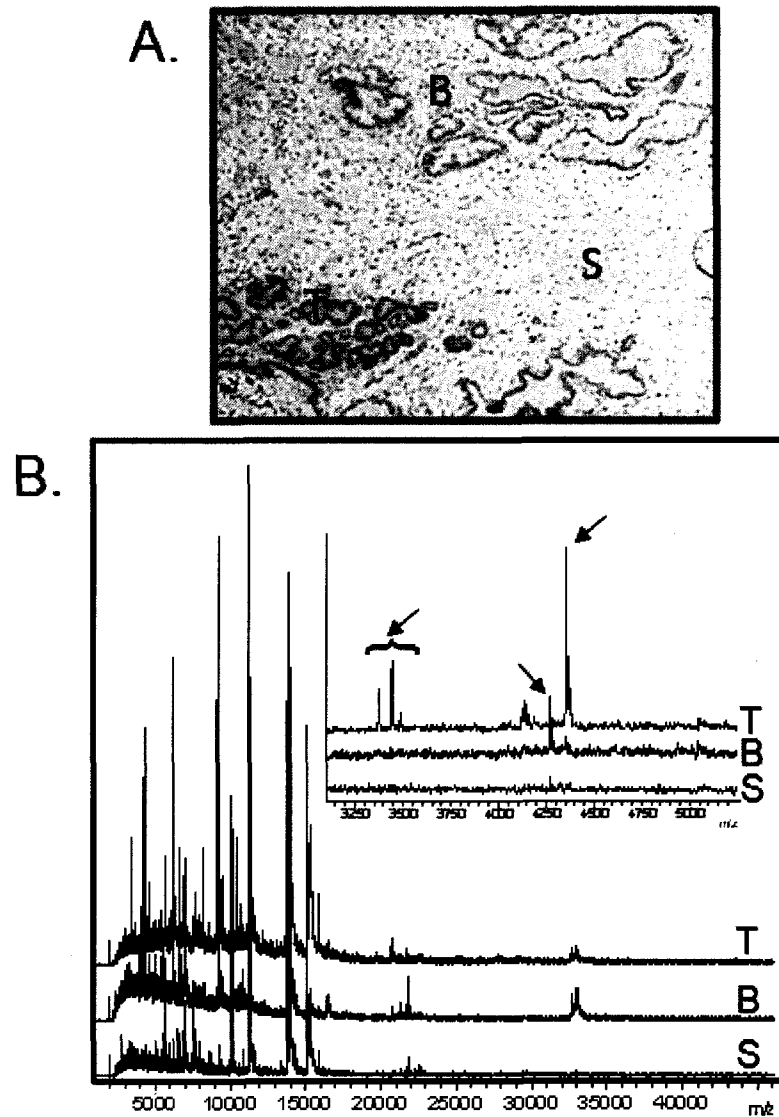
**Figure 6.** Direct tissue mass spectrometric analysis of human prostate tissue reveals cell-specific profiles. Frozen prostate tissue was processed for MALDI imaging and coated with SPA matrix followed by spectra acquisition in linear mode. A) Representative histology image of H & E stained prostate tissue showing areas of prostate adenocarcinoma (T) benign prostate glands (B) and benign stroma (S). B) Resulting spectra acquired from each region indicated showing characteristic profiles for different cell types. Bottom panel inset) Expanded view of the mass range $m/z$ 3000-5300 showing differences in the profiles for each cell type

and 4355 which showed significant over-expression in PCa cells when compared to benign adjacent cells spectra. Three ions over expressed in PCa (3,372, 3,443, and 3,487) are consistent in mass with defensin peptides and may be indicative of infiltrating neutrophils [175, 176]. Another peak at *m/z* 4274 was expressed in benign adjacent epithelial cells and stroma with little or no expression seen in PCa cells. Spectra derived from ROIs designated tumor or benign from the initial 22 tissues examined were used to generate a classification algorithm capable of correctly classifying 85% of PCa tissue areas and 50.2% of benign regions. Selected component ions with significant discriminating power were evaluated in these initial tissues and images derived around the pathology-designated ROI. This allowed for a visual determination of region specific changes in peptide ion expression. Representative examples of images derived from three regionally discriminating ions are shown in Figure 7. An additional classification algorithm using 5 differentially expressed *m/z* values (3443, 3442, 4030, 4275. 4355) was also developed. This algorithm was able to correctly classify 90.3% of the PCa containing regions, but only 64.1% of the benign regions were correctly classified (Table 3).

**MALDI-IMS Utilizing *m/z* 4355 Can Identify PCa Specific Regions of Prostate.**

When we examined the list of differentially expressed peaks from our initial set of 22 tissues, the ion at *m/z* 4355 was the most significantly over-expressed ion, in PCa containing tissue regions ($p = 2.76 \times 10^{-16}$). We therefore wanted to further evaluate the utility of this peak alone for the detection of PCa regions within prostate tissue via MALDI-IMS. Figure 8 is a representative image of a tissue section with one specific
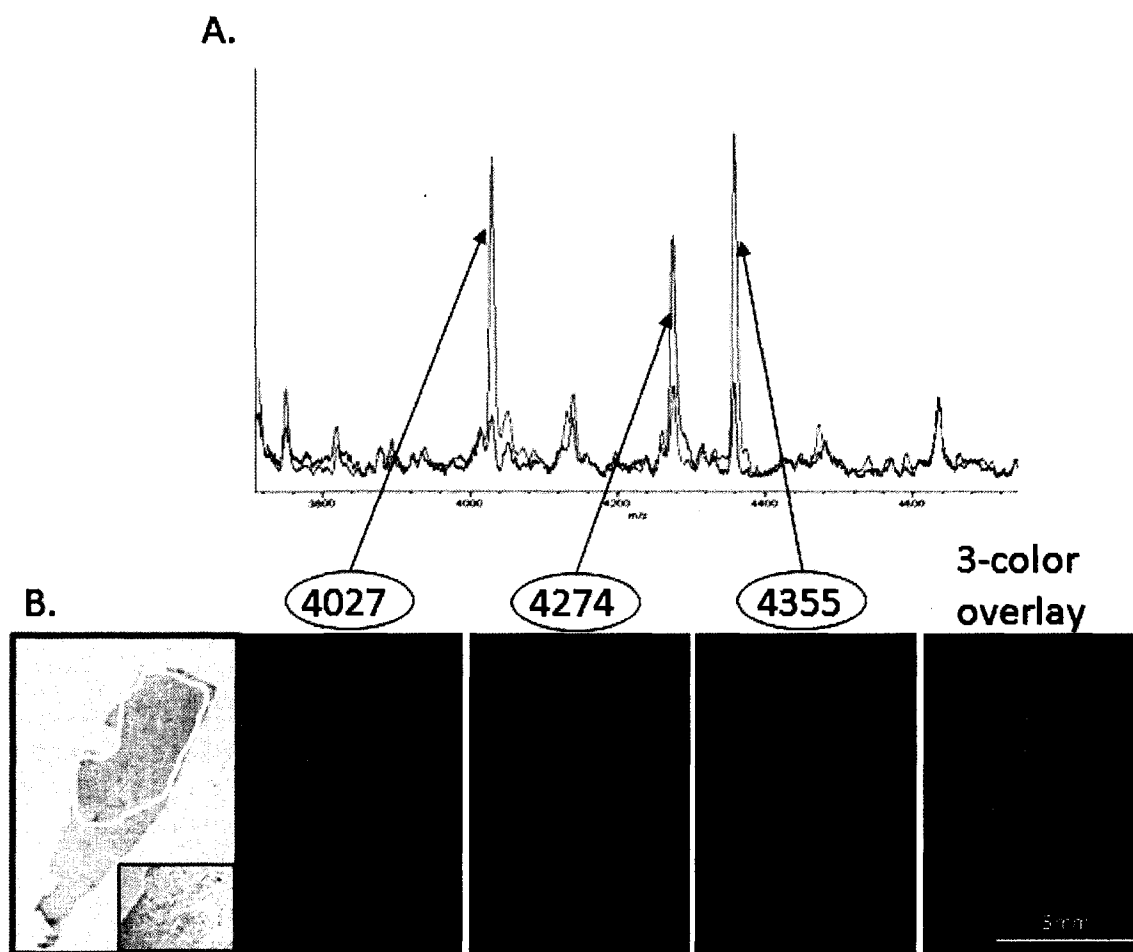
**Figure 7.** MALDI-IMS utilizing specific *m/z* values can identify PCa specific regions within the prostate. Direct profiling of human prostate tissues revealed specific peaks both over and under-expressed in PCa regions. A) Composite spectra showing characteristic profile for PCa regions (top line) and benign adjacent regions (bottom line) indicating the overexpression of 2 peaks at *m/z* 4355 and *m/z* 4027 and underexpression of *m/z* 4274. B) Left- H & E stained histological image of a representative tissue containing an area of PCa circled by a pathologist with a 10X view of the cancerous glands (inset). Right- Corresponding images indicating the expression pattern for each peak shown in a) and the combined image for all three peaks.

**Table 3.** Genetic Algorithm for PCa vs. Benign Tissue Classification

| Peaks used in classifier (m/z) |
| --- |
| 3443 |
| 3488 |
| 4027 |
| 4275 |
| 4355 |
| |
| Correct classification |
| PCa areas:          90.3% |
| Benign Areas      64.1 % |

region of PCa cells and clearly defined adjacent regions of normal prostate glands. A higher magnification view of each cell type can be seen in the insets. Clearly evident from the ion density map, the $m/z$ 4355 peak was highly expressed in the PCa region as compared to the surrounding tissue. Little to no expression is visible in the normal stroma or benign glandular regions. When representative spectra were exported from the specific regions (tumor vs. benign) we can clearly observe a prominent peak at $m/z$ 4355 over-expressed in the PCa obtained profile.

## MALDI-IMS Utilizing $m/z$ 4355 Discriminates between Cancer and Uninvolved Prostate Tissue.

In order to evaluate the differential expression of $m/z$ 4355 between PCa and benign regions we conducted an analysis of the full set of prostate tissue derived from radical prostatectomy. We examined the images produced from the ion density of the $m/z$ 4355 peak following the analysis of 36 PCa and 61 benign tissue sections. The benign tissues were both distal (n=36) and adjacent (n=25) to tumor. Shown in Figure 9 are representative ion images of the expression of the $m/z$ 4355 peak in 4 tissue sections containing PCa (Figure 9 A.-D.) and 4 distal benign sections (Figure 9 e.-H.). The corresponding spectra in the representative region of $m/z$ 4000-4600 are shown in the top panels above each image. High expression (defined as $\geq$ 2x the normalized peak intensity of the benign regions) was visible in each section where PCa cells were present (Figure 9 A. and D.) or visible throughout the tissue when no benign cells were present (Figure. 9 B. and C.). In contrast, little to no expression of the $m/z$ 4355 ion was detected in sections containing benign cells only (Figure 9 E.-H.). In order to illustrate the tissue specific
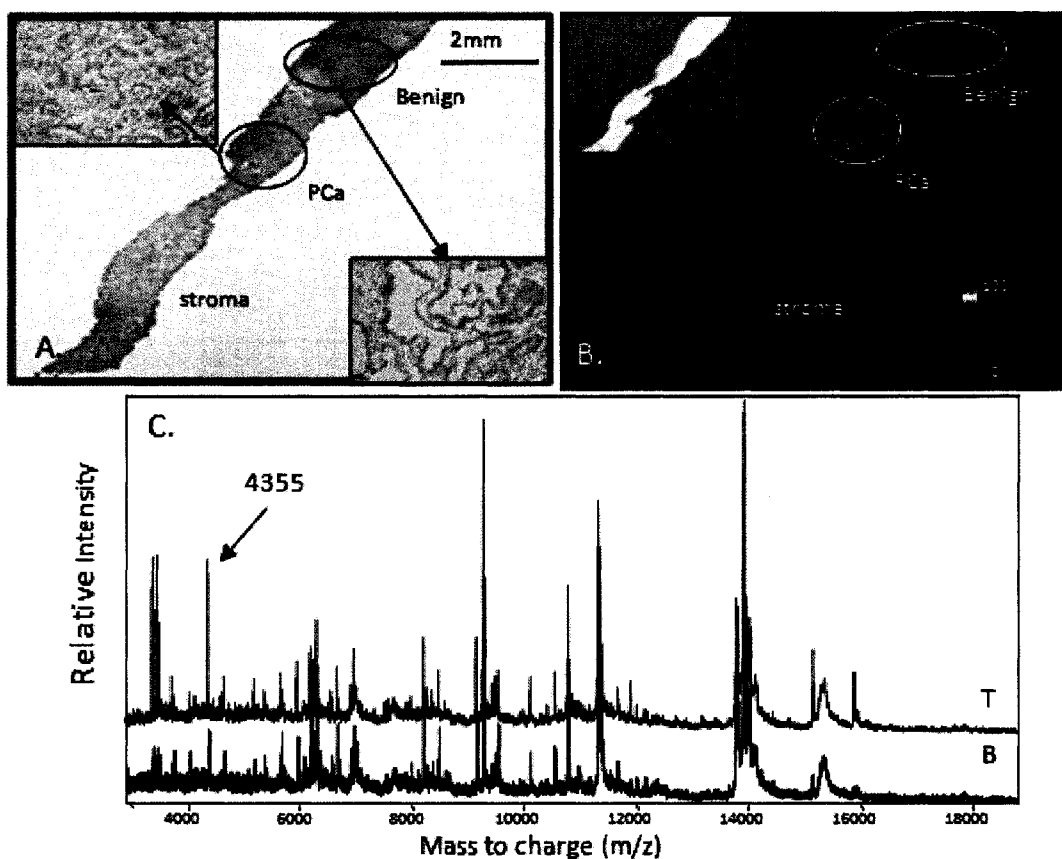
**Figure 8.** MALDI-IMS utilizing *m/z* 4355 can identify PCa specific regions of prostate. A) H & E image of a tissue specimen containing a defined area of PCa glands and benign glands. Magnified (10x) views of each cell type are shown in the insets. B) Resulting 2D ion density map of the tissue showing high expression of a peak at *m/z* 4355 (bottom circle) in the PCa area (inset is a scan of the tissue after matrix deposition). C) Representative spectra obtained in the PCa region from the benign adjacent glandular area displaying differential expression of the ion at *m/z* 4355
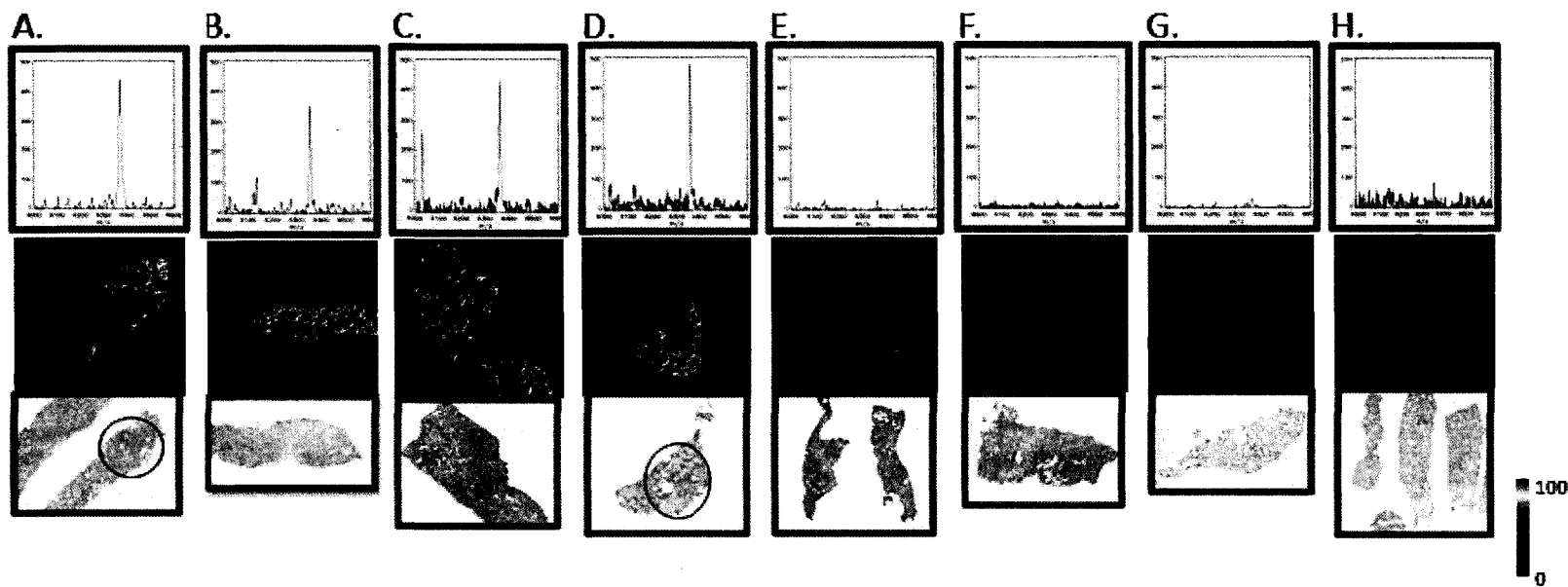
**Figure 9.** MALDI 2D ion density maps of 4 PCa containing tissues and 4 benign prostate tissue specimens. Tissues obtained from 8 patients undergoing radical prostatectomy were processed for MALDI imaging and 2D ion density maps were generated (middle panels) showing expression of the peak at $m/z$ 4355. A-D) Tissue specimens with defined regions of PCa (circled) or throughout the specimen visible from H & E serial sections (bottom panels). Areas in red (bright areas) from the resulting MALDI-IMS indicate high expression of $m/z$ 4355. E-H Benign prostate tissue showing little to no expression of the $m/z$ 4355 peak. Spectra exported from representative regions of each tissue are shown in the $m/z$ range of 4000-4600 and display the $m/z$ 4355 peak profile (top panel). Intensity scale for the images is shown bottom right.

expression of *m/z* 4355, we examined the intensity values with respect to defined tissue regions across the full data set. Intensity values normalized to total ion current for the *m/z* 4355 peak were calculated for each tissue region (PCa, benign adjacent, and benign distal) and plotted (Figure 10). The average intensity of the *m/z* 4355 peak in benign adjacent or distal tissue was 30.2 and 27.6 respectively, whereas for PCa regions the average intensity was 71.8, representing a 2.5 fold increase. A total of 75% (n=26) of the PCa regions exhibited average intensity values for the *m/z* 4355 peak above the average intensity for benign regions. A ROC curve calculated from the average normalized intensity of each ROI (distal benign vs. PCa) is shown in Figure 11. The optimal cutoff point for using the *m/z* 4355 peak as a biomarker for PCa in tissue sections was a normalized average intensity value of 27. This cutoff point was associated with a sensitivity of 75.0% and a specificity of 74.3% (AUC 0.834). Of the 25% (n=9) of PCa samples with values at or below the cut-off, two were from tissues containing pseudohyperplastic PCa (characterized by the presence of larger glands with branching and papillary infolding), and one was a specimen with cribriform PCa (relatively large epithelial cell masses perforated by multiple small lumens, Gleason grade 4+3). Interestingly one specimen below the cut-off was from a patient treated with hormone ablation therapy prior to surgery, also a Gleason grade 4+3 (no other patients in the study received pretreatment). Of the remaining 5 tissues with low expression of the ion at *m/z* 4355, three were Gleason grade 3+4, and two were Gleason grade 3+3. No other remarkable morphological differences were seen for these tissue sections.
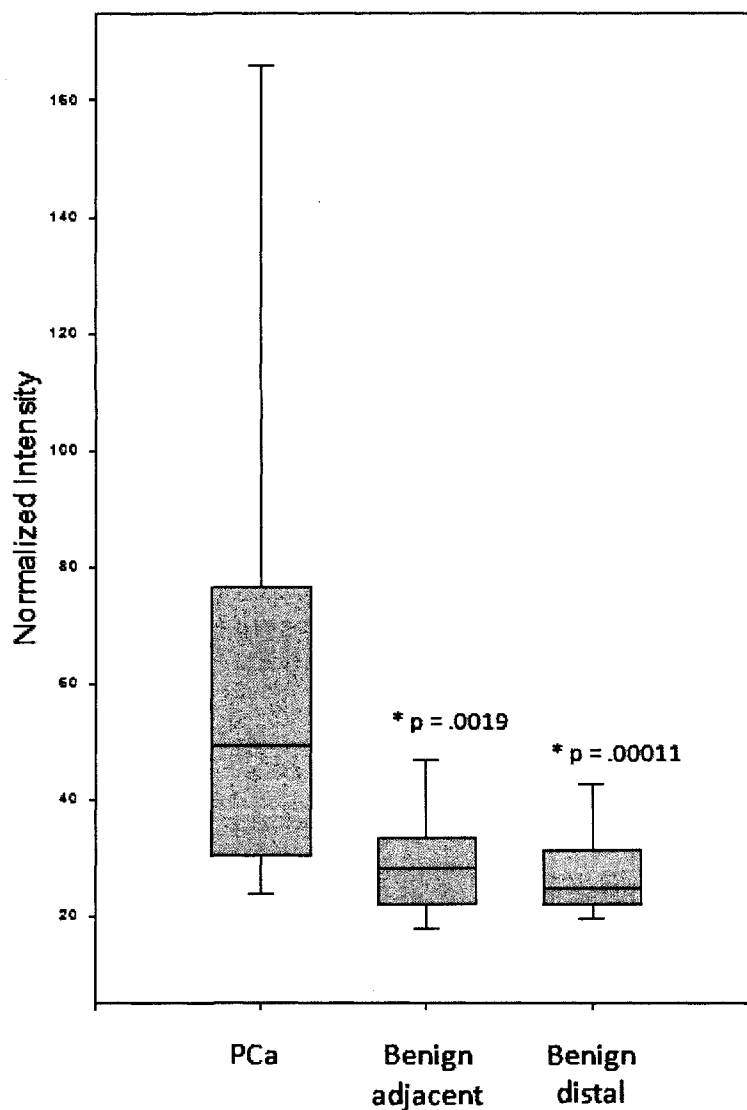
**Figure 10.** Normalized average intensity values for *m/z* 4355 in different prostate tissue areas. A total of 36 PCa containing tissues 25 benign adjacent and 36 distal benign tissues were analyzed via MALDI-IMS. The resulting normalized average intensity values for the *m/z* 4355 peak were plotted for PCa, benign adjacent and benign distal regions. The boundary of the box closest to zero indicates the 25th percentile, a line within the box marks the median, and the boundary of the box farthest from zero indicates the 75th percentile. Whiskers above and below the box indicate the 90th and 10th percentiles. * Significant p value.
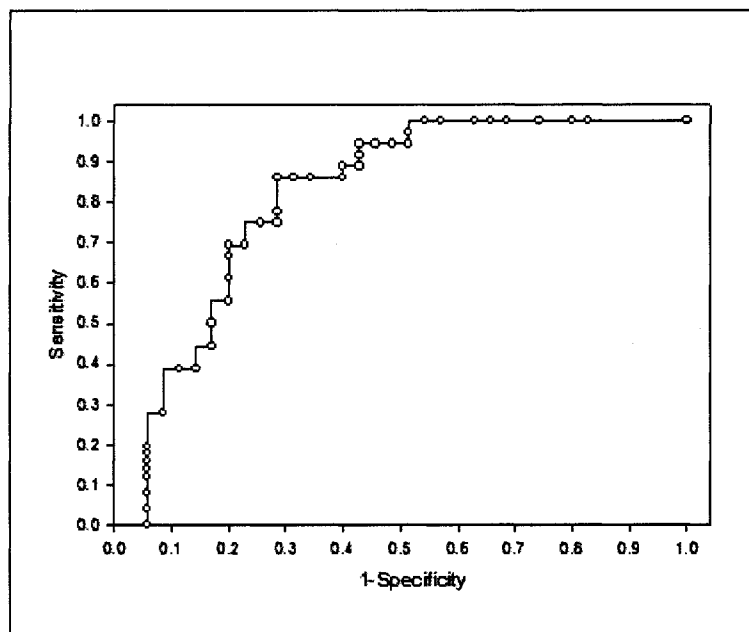
**Figure 11.** ROC curve for *m/z* 4355. The predictive power of the putative biomarker to detect PCa tissue areas was tested using the area under the receiver operator characteristic (ROC) curve. The area under the curve (AUC) = 0.834.

**Specific Morphological Features are Associated with the Expression of m/z 4355 in PCa and atrophic Prostate Glands**

The careful examination of areas expressing the ion at *m/z* 4355 revealed that certain specific morphological features in prostate tissues are associated with this expression. As shown in Figure 12, two representative PCa areas from moderately differentiated tumors exhibiting distinct m/z 4355 expression have infiltrating lymphocytes surrounding the cancerous glands (small arrows). Infiltrating lymphocytes were also observed in one case of proliferative inflammatory atrophy (Figure 13A) and another case of benign tissue where cystic atrophy (Figure13B) was present, both in areas expressing the *m/z* 4355 ion.

**Identification of an Expression Profile using MALDI-IMS for the Detection of Metastatic Disease**

Frozen prostate sections of similar stage disease in which the case/control design is the discovery of metastatic disease after surgery in the case group were analyzed for protein expression differences using MALDI-IMS. We concentrated on differential expression patterns of the tumor tissue regions between case and control. We have examined 12 PCa tissue samples harvested from patients with micro-metastatic disease and 7 tissues from patients with PCa and similar risk factors (PSA level, Gleason score) but no metastatic disease. From this dataset we have generated a list of top discriminating spectral peaks that are presented in Table 4. We then plotted several of the *m/z* for image generation and subsequently compared the images to the mirrored histologically stained and pathology read sections. In Figure 14 representative images from MALDI-IMS show two peaks (4030 and 5364) found to be highly expressed in case samples when compared
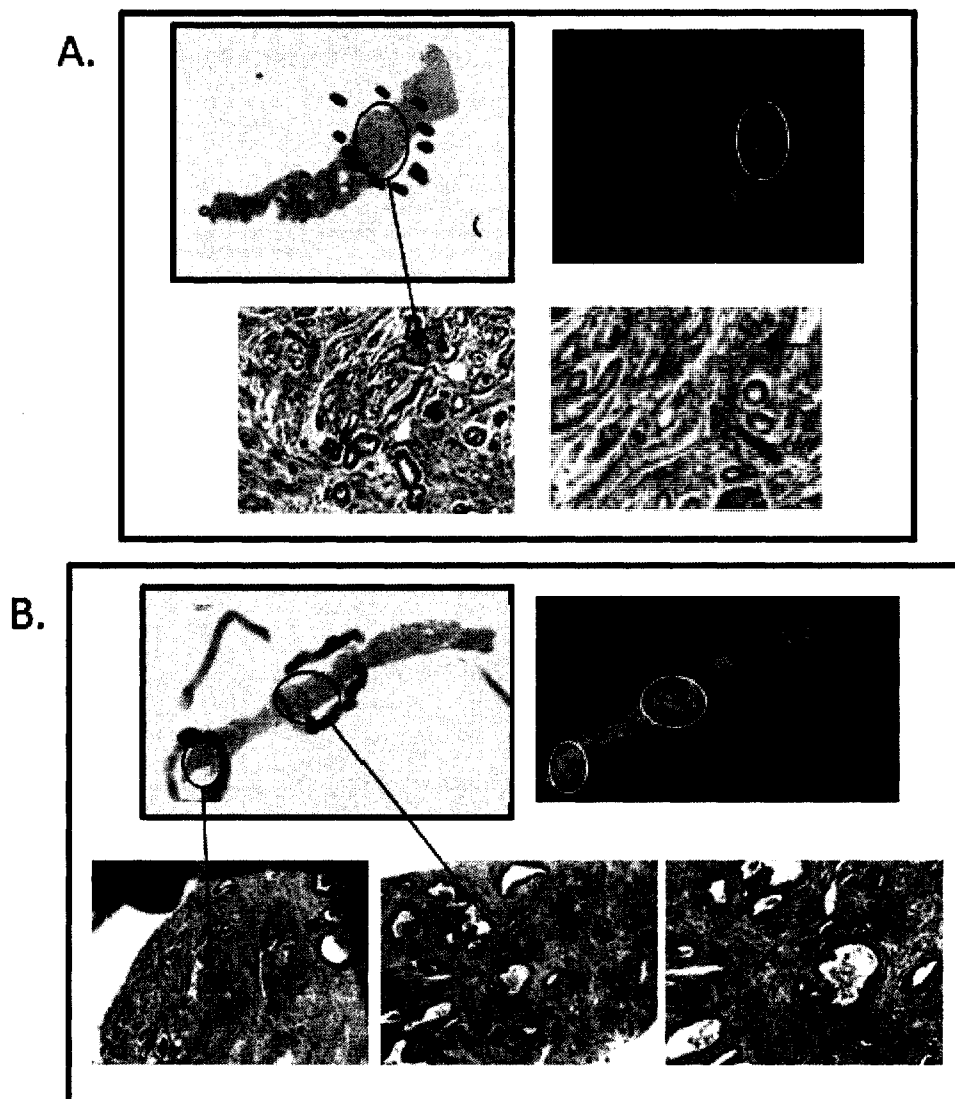
**Figure 12.** Specific morphological features are associated with the expression of the ion at m/z 4355 in PCa tissue. Two tissues with moderately differentiated PCa regions circled in the H&E stained section (top left A and B). High expression of m/z 4355 (circled) as viewed in images produced via MALDI-IMS (top right in each panel) corresponds to regions of PCa with accompanying lymphocytic infiltrates. Bottom images are 10X, views of specific regions from the serial H&E stained section with 20X views of areas containing infiltrating lymphocytes (small arrows).
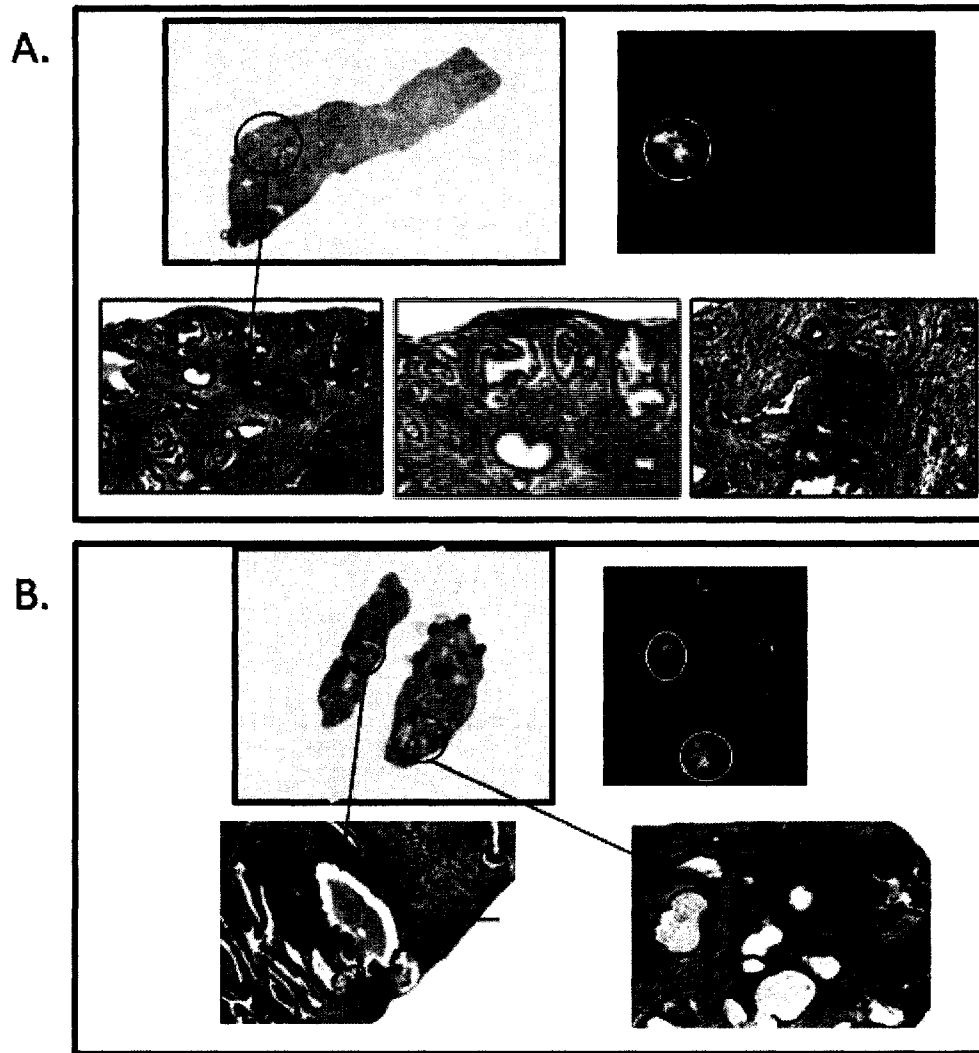
**Figure 13.** Specific morphological features are associated with the expression of the ion at m/z 4355 in non-neoplastic lesions. Two tissues with PIA (A) and atrophic regions (B) circled in the H&E stained section. High expression (circled) of m/z 4355 (top right in each panel) corresponds to regions of atrophy inflammation with accompanying lymphocytic infiltrates. Bottom images are 10X views of specific regions of infiltrating lymphocytes (small arrows).

**Table 4.** Differentially Expressed Peaks in PCa Tissues from Patients with Micro-metastasis

| m/z | normalized intensity | | p-value |
| | Target | Match | |
| --- | --- | --- | --- |
| 4030 | 61.41 | 41.18 | 2.59E-88 |
| 5364 | 61.72 | 42.96 | 3.97E-83 |
| 9533 | 21.32 | 8.4 | 1.13E-79 |
| 6186 | 83.43 | 45.48 | 8.75E-64 |
| 3230 | 31.93 | 65.12 | 6.79E-56 |
| 3817 | 35.17 | 59.12 | 1.57E-52 |
| 3245 | 24.86 | 36.88 | 1.17E-51 |
| 9767 | 25.07 | 8.85 | 3.56E-47 |
| 8963 | 42.24 | 10.78 | 3.59E-46 |
| 9091 | 50.71 | 14.39 | 8.89E-45 |
| 9021 | 17.39 | 6.28 | 1.39E-42 |
| 6344 | 37.64 | 31.13 | 5.49E-39 |
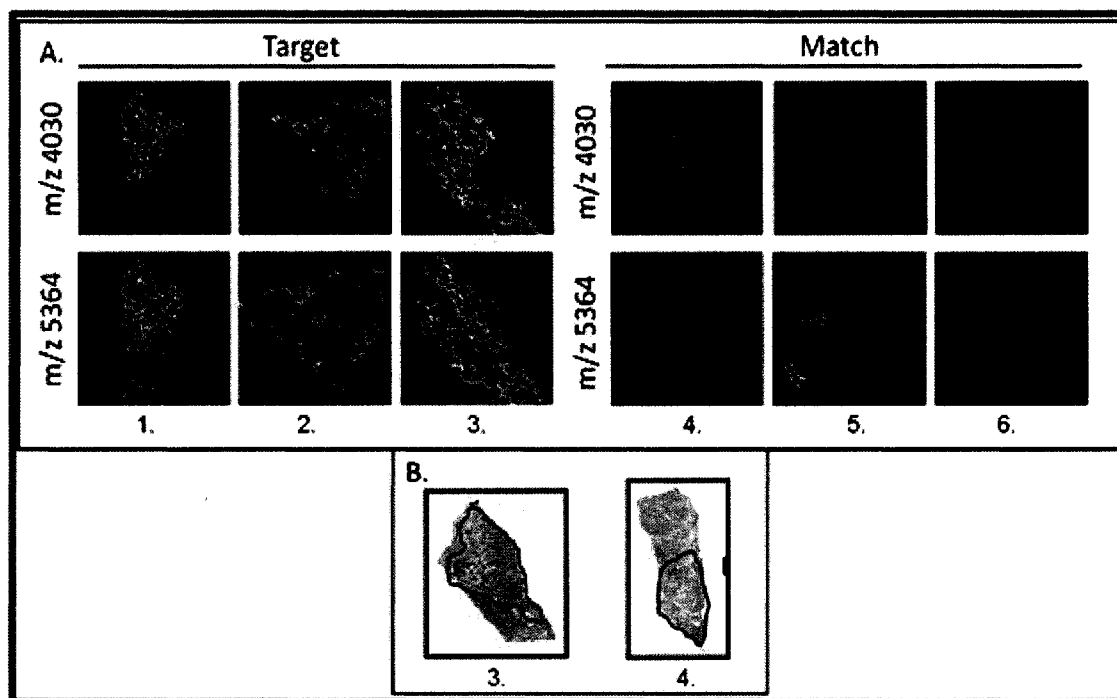
**Figure 14.** MALDI-IMS analysis of PCa containing tissue obtained from micrometastatic patients (target-case) and patients with matching risk factors at the time of surgery (match-control). The expression patterns of two *m/z* values found over-expressed in the target tissues are shown. A) Left-Target tissues showing high expression of *m/z* 4030 (top) and *m/z* 5364 (bottom). Right- Matched tissues showing reduced expression of *m/z* 4030 in all three matched tissues (top), and reduced expression in 2 of 3 for *m/z* 5365 (bottom). B.) H & E of two tissues represented in A.) showing circled areas of PCa with similar morphology and the same Gleason grade of 3+4.

to control specimens. Additionally, the *m/z* 4355 peak was not found to be discriminatory

for these samples as expected since PCa was present in both groups. A 2D peak

distribution view for the two most discriminatory peaks (*m/z* 4030 and *m/z* 5365) is

shown in Figure 15. The samples from patients with metastatic disease are separated from

the matched controls with some overlap in both groups. We next developed a

classification algorithm using 6 differentially expressed peaks (*m/z* 3374, 3751, 3817,

4030, 5364, and 5664). As shown in Table 5, this algorithm was able to correctly classify

the PCa tissues from patients who harbored micrometastatic disease at a rate of 83%.

However, the algorithm's ability to correctly classify tissue samples from patients

without extra-prostatic spread was only 58%.

**MALDI-IMS of fixed tissue**

Fixed tissue provides the best histological morphology, but classical methods

such as formalin fixation cross-link proteins and are therefore not useful for proteomic

analysis. In order to facilitate the use of MALDI-IMS into current clinical laboratory

methods we wanted to determine if the "protein friendly" fixative (UMFix) was

compatible with MALDI imaging. To assess the quality of the spectrometric data and to

better understand the effect of the fixation procedure, profiles and images obtained from

the UMFix processed samples were compared to those obtained from OCT embedded

frozen samples. For the UMFix specimens, after sectioning, paraffin removal and partial

rehydration (protocol shown in Figure 16), MALDI matrix, (SPA) was sprayed on the

tissue following our established protocol using the ImagePrep workstation. We evaluated

prostate tissue treated with UMFix to obtain spectra and images via MALDI-IMS. The

**Table 5.** Genetic Algorithm for Detection of Micrometastatic Disease

| Peaks used in classifier (m/z) |
| --- |
| 3374 |
| 3751 |
| 3817 |
| 4030 |
| 5364 |
| 5663 |
| Correct classification |
| Case: 82.8% |
| Control 58.2 % |
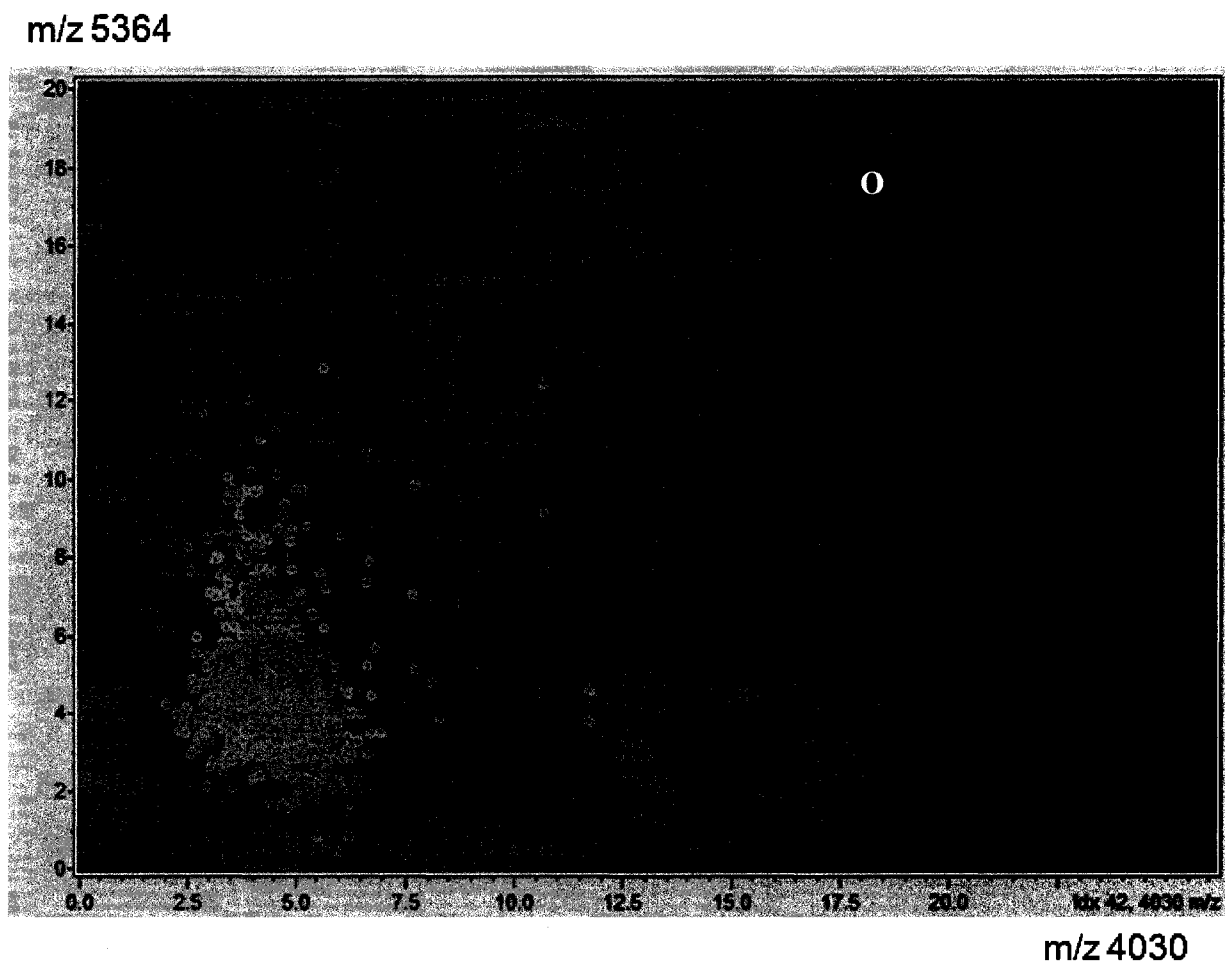
m/z 5364



m/z 4030

**Figure 15.** 2D peak distribution plot of PCa tissue from patients harboring micro-metastatic disease. Individual peak values for Target (case) versus (matched controls) are displayed for the two most discriminatory peaks (*m/z* 5364 and *m/z* 4030).
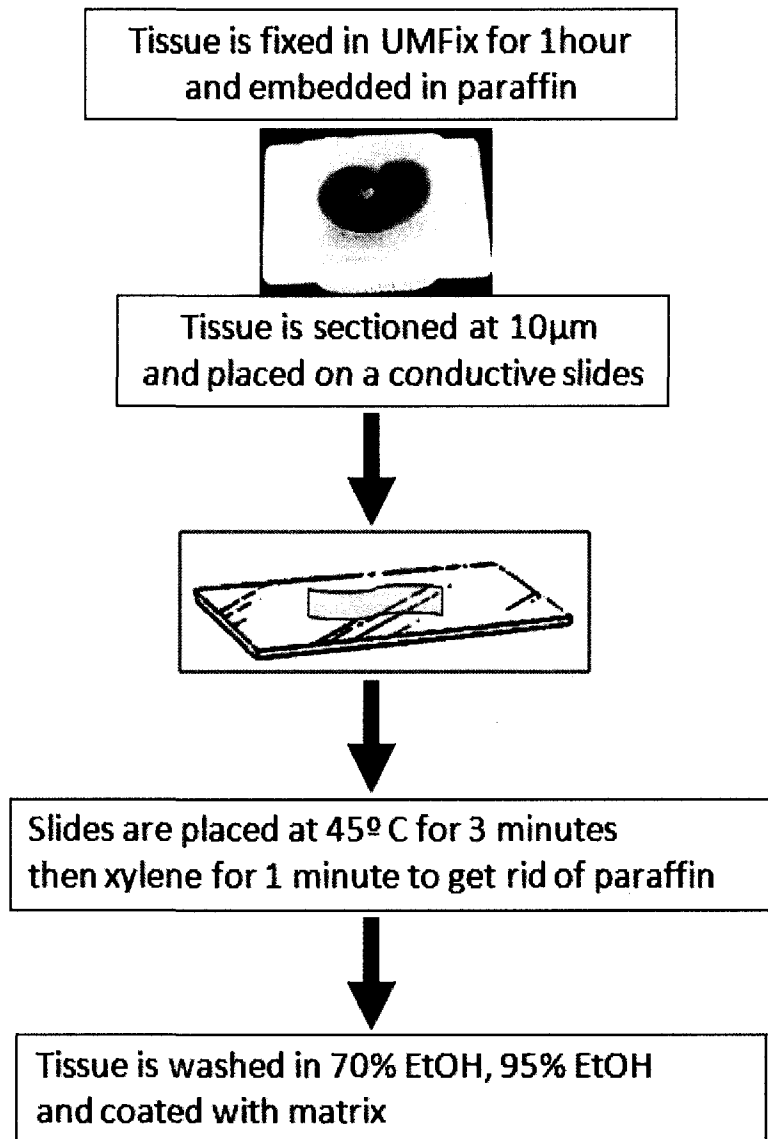
**Figure 16.** Flowchart of processing protocol for UMFix treated tissue before MALDI-IMS.

matched mirrored frozen and formalin fixed tissue was also processed for comparison. Representative spectra resulting from this comparison are shown in Figure 17. As expected, the formalin fixed tissue did not produce any protein peaks. The UMFix treated tissue however produced spectra with signal intensity and peak pattern similar to that obtained from OCT embedded frozen tissue. The minor variations in peak intensities may be due to variations in areas sampled or an unknown modification of proteins during the fixation process. This phenomenon will need to be evaluated and characterized in further studies.

We also examined resulting images from two sets of matched fixed and frozen tissue produced after conversion of the spectra to a 2D ion map using BioMap. As shown in Figure 18, the area of overexpression of the *m/z* 4355 peak in the resulting images corresponds well in both the UMFix and frozen tissue. The areas showing high expression of *m/z* 4355 were designated by a pathologist to be proliferative inflammatory atrophy (PIA) and cystic atrophy. PIA is believed to be a precursor lesion to PCa. These results indicate that the UMFix processed tissue is compatible with the MALDI-IMS and preserves detail in the subsequent images, producing comparable results to frozen tissue.

## 3.4 Discussion

In a previous study we established that SELDI-MS (a variant of MALDI) protein profiles from lysed prostate cells (isolated via LCM ) obtained from different disease states had discriminating peak differences [127]. The results of our current study demonstrate that both the protein profiles as well as the resulting molecular image maps are discriminatory. In this study we employed MALDI-IMS in an attempt to discriminate
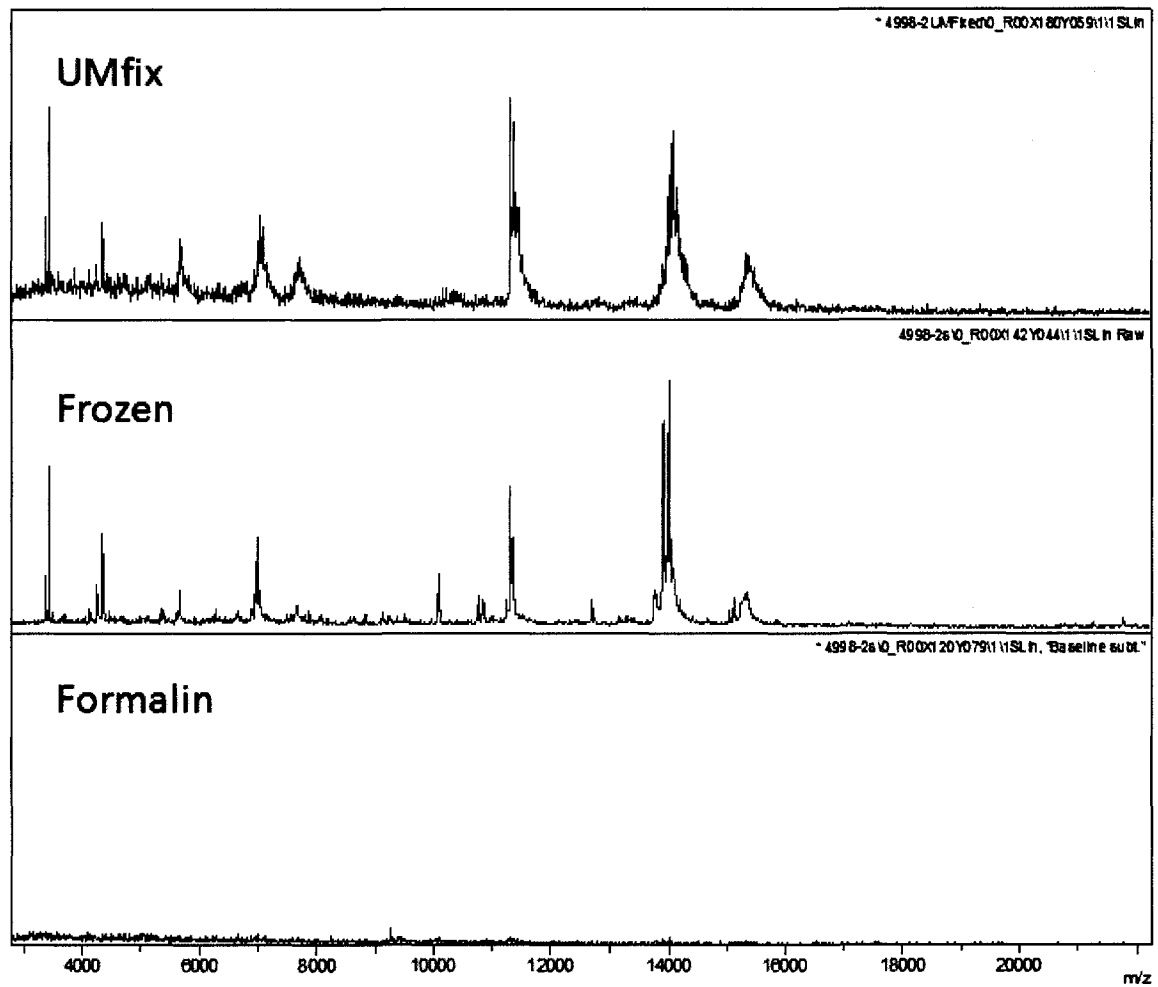
**Figure 17.** Comparison of MALDI-IMS spectra derived from prostate tissue samples which were fixed (UMFix or formalin) or frozen.
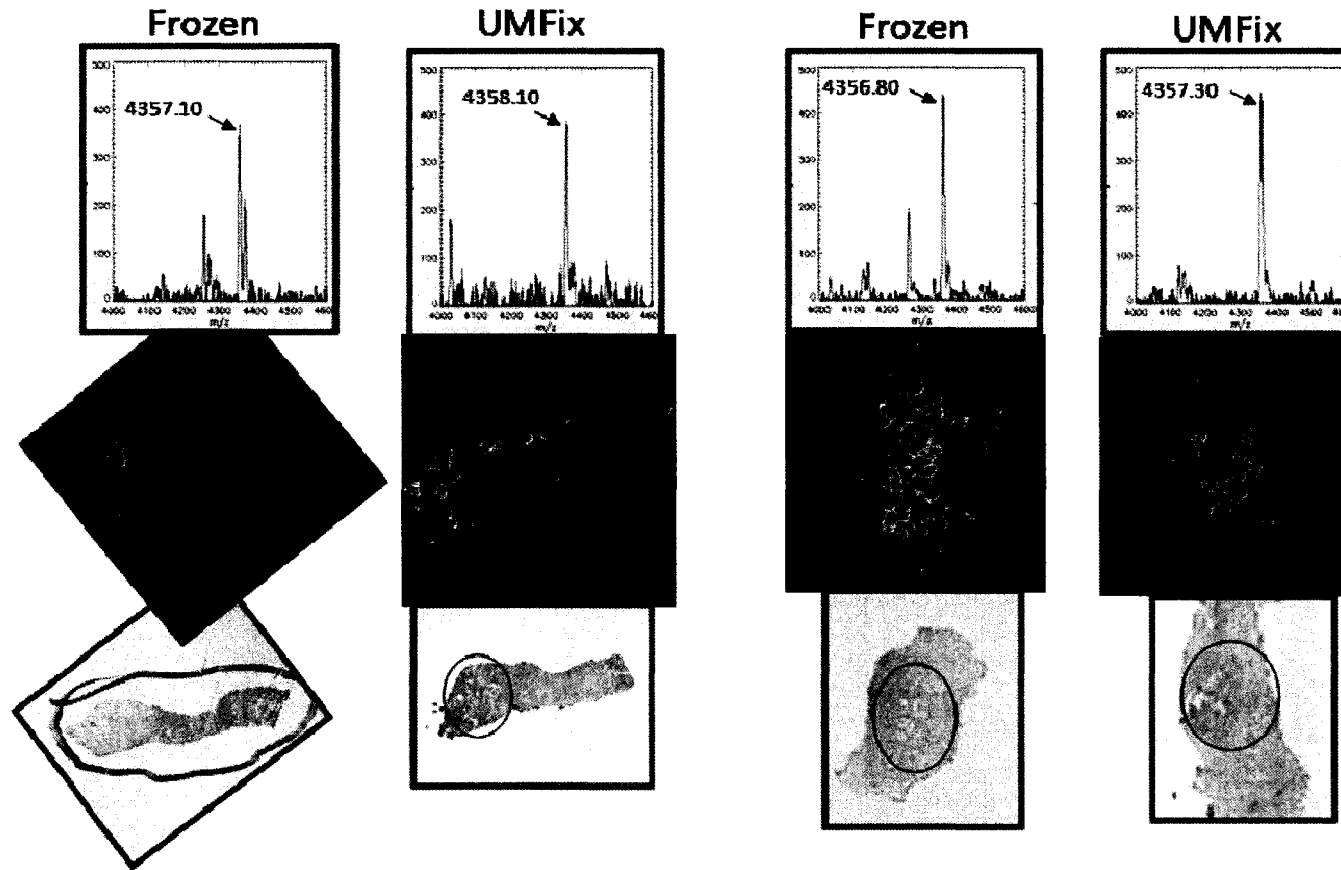
**Figure 18.** Comparison of MALDI-IMS data in frozen and UMFix processed tissue in two pairs of matched prostate tissue samples. Top panels) Representative spectra of the *m/z* 4355 ion. Middle panels) MALDI-IMS image showing high expression of *m/z* 4355 in specific areas of PIA or cystic atrophy (circled) in H & E image (bottom panel).

tumor from benign adjacent prostate tissues. After an initial discovery via profiling in a subset of (11 PCa/11 benign), we tested the performance of selected biomarkers across a large tissue set of 36 PCa and 61 benign tissue sections. The performance of a single biomarker ($m/z$ 4355) was associated with the corresponding image for the detection of PCa. Thus, the expression changes detected in tissues by MALDI-IMS may reflect molecular pathway changes indicative of PCa development. We also show that the commercial fixative, UMFix, preserves expression detail similar to that found in frozen tissue, at least for some markers.

Any new technology will only be useful to patient care if it is adopted by clinicians. In order for MALDI-MSI to be clinically useful it must contribute to the ability of pathologists and surgeons to make accurate diagnosis and prognosis. Since pathologists are familiar with the use of images to make diagnosis, the use of molecular images should translate more readily to this end. This study was undertaken to assess the feasibility of the use of MALDI-IMS for the elucidation of peptide and protein expression differences prostate tissue sections as well as determining the clinical feasibility of this technique to produce images which correlate with histopathology. In addition we have identified a potential marker for prostate cancer which may aid in the detection of prostate cells in a surgery specimen.

A weakness of our study is the lack of high grade PCa tissue to examine the expression of the $m/z$ 4355 peak. There is some indication from our data that the ion at $m/z$ 4355 is reduced in high grade PCa and increased in well differentiated tumors as well as PIA lesions (a putative PCa precursor). Three PCa tissues with a Gleason score of 9 or higher had normalized intensity values below the cut-off value of 27. Unfortunately, we

did not have enough high grade tissue samples to make an accurate estimation of this decrease. Therefore this marker may be a true biomarker of early disease and the tissue changes associated with cancer initiation. Morphological features associated with the expression of the ion at *m/z* 4355 include infiltrating lymphocytes. Moreover the expression of defensin peptides in the spectra derived from PCa areas indicates the presence of neutrophils. Inflammation involves the induction of complex coordinated chemical signals and physiological processes following injury to promote "healing" of damaged tissues. Early responses include increases in vascular permeability and activation, together with the directed migration of leukocytes (neutrophils, monocytes and eosinophils) towards the site of injury for the formation of a new ECM. Our results point to an association of inflammation in the areas with higher expression of the *m/z* 4355 peak both in PCa and atrophic lesions.

Further studies using additional tissue including high Gleason grade tissue are needed to validate and assess the utility of this marker. However, its true usefulness lies in its ability to detect cancer cells in a minute amount of tissue such as in biopsy samples which we are currently undertaking. Sequence identification and enhanced functional analyses of the *m/z* 4355 peaks and other differentially expressed protein markers will not only advance our understanding of the patho-mechanisms and aid in elucidating potential drug targets, but may also serve as diagnostic and prognostic tools for better patient care.

Although clinically localized prostate cancer can be treated with androgen ablation, surgical resection or radiation, its transition to metastatic disease is almost uniformly fatal. The molecular differences between metastatic prostate cancer and localized prostate cancer have not been well established. Before rational therapies can be

developed to target this lethal form of prostate cancer, the molecular alterations associated with the transition of indolent to an aggressive PCa phenotype need to be revealed. From our MALDI-IMS analysis, we have identified several $m/z$ values which are differentially expressed in tissues derived from patients harboring metastatic disease at the time of surgery to remove their prostate. The sequence identification of these peaks should elucidate the molecular hallmarks associated with aggressive characteristics. As no test performs perfectly, sensitivity, specificity and cost become trade-offs in the application of diagnostics to disease management. The classification algorithm developed was helpful, in that it correctly identified 83% of tissue samples from micrometastatic patients. Unfortunately in 42% of the control PCa tissues, our algorithm was incorrect in classifying PCa from patients with organ confined disease. The combination of this algorithm with other screening methods may potentially increase its usefulness and a trade-off of sensitivity to specificity could benefit patients at risk for the development of metastatic PCa. Preoperative identification of patients with metastatic disease would be helpful in sparing men from the morbidity of a radical prostatectomy that would be ineffective or for selecting patients best suited for clinical trials of new therapies.

Clearly for this and other tissue-based markers the greatest utility will be realized in the actual biopsy sample. To that end, our study investigating the commercially available UMFix approach developed at the University of Miami (33) is critically important. We have demonstrated that UMFix processed tissue is highly compatible with MALDI-IMS methods and the resulting data and images closely correlate with those collected from traditional methods employing frozen tissue. This makes the transition for this new technology into current clinical pathology practice much more feasible and will

facilitate its incorporation at a much improved pace. Future studies will need to parallel extensive analysis of the quality retained for clinical analysis via morphology and immunostaining. Ultimately, such changes in the tissue fixation routinely conducted by pathology will require either a commitment to move away from highly toxic formalin-based approaches toward less toxic alcohol preparations and/or the discovery of a biomarker specific to non-formalin tissues that revolutionizes clinical diagnostics.

# CHAPTER IV

## AIM 2: SEQUENCE IDENTIFICATION AND CHARACTERIZATION OF POTENTIAL BIOMARKERS FOR CLINICAL DIAGNOSTICS

### 4.1 Introduction

MALDI-IMS experiments logically lead to the sequence identification of the low molecular weight protein species that show tissue location-specific or disease-related changes. This has been one of the more difficult hurdles to overcome for MALDI-IMS and remains one of the most challenging aspects to protein biomarker discovery in general. Once a biomarker is conclusively identified, a more sensitive immunological or enzyme-based assay may then be developed to accurately determine and measure the molecule of interest in normal and disease samples [25, 177, 178]. Thus, deciphering the chemical identity of protein biomarkers may facilitate more robust and sensitive tests to detect, monitor and possibly target these new protein biomarkers in cancer.

As the molecular weight of a compound increases, its physical properties places limits on the utility of a mass spectrometer to detect it with high resolution [179]. As mass increases, the natural isotopic envelope distributes the population of molecules across multiple species, resulting in broader peaks. This is not a result of an instrumental limitation but is a fundamental property of biomolecules and is therefore insurmountable. Additionally, high molecular weight molecules require a larger amount of energy to ionize than low molecular weight species and therefore the ability to detect these molecules is decreased. Because of the inefficiency of MALDI –TOF mass spectrometers to resolve [101] and detect higher molecular weight compounds [180] most signals

detected are below *m/z* 30,000. However, the localization of larger proteins may be facilitated by the use of *in situ* digestion of the proteins in a tissue section. The smaller peptide fragments generated by such enzymatic cleavage are much easier to detect by MALDI-IMS, and should still represent the abundance of the parent protein. Furthermore, the spatial positions of the parent protein can be inferred from the localization of the fragment [149, 155] in reflectron mode. MALDI-TOF instruments with reflector technology offer the possibility to measure in linear mode as well as in reflectron mode. In reflectron mode, all incoming ions are reaccelerated after deceleration to achieve an increase in resolution making peptide analysis possible. The resulting peptides can be visualized to provide spectra for profiling, but they can also be directly sequence identified via MALDI-TOF tandem MS.

The analysis of mass spectra and identification of proteins is usually performed by searching within protein or DNA databases using different search algorithms. Therefore, complete protein or genome databases are required as only proteins of organisms with already sequenced genomes can be analyzed this way. The fragments generated from a tandem MS analysis provide amino acid sequence information to identify the peptide. In the majority of mass spectrometers, this can only be performed in a limited mass range (usually 600–4500 Da) [108]. Unfortunately, many low abundant markers fall below the level of sensitivity currently available in MALDI-TOF MS/MS instruments for direct tissue analysis. If this is the case, the only hope currently for identification is to take a small amount of tissue that relates to the area of interest and perform a standard proteomic analysis using cell and tissue lysates.

Traditional approaches to biomarker purification and sequencing using tissue lysates include liquid chromatography followed by MS (LC-MS) as well as traditional SDS PAGE followed by gel band excision and tryptic digestion. In this type of experiment, care must be taken to ensure that the peptide or protein species detected in the direct tissue analysis are being adequately represented in tissue lysates. Methods of microdissection such as LCM can be an important first step in creating a lysate representative of cells containing the biomarker of interest. However, fractionation schemes, almost always necessary for the simplification of complex protein mixtures before MS/MS analysis, increase the sample amount requirements and consequently the time needed to obtain enough material using LCM. Bulk tissue lysates can be used as an alternative if the tissue contains greater than 90% of the cell population of interest.

Any sequence identification of potential biomarkers via mass spectrometry should also be confirmed using affinity detection methods such as Western blot or immunohistochemistry. For many human proteins commercially available antibodies make this kind of confirmation experiment routine and rapid. For peptides or proteins for which no antibody is available or for unknown proteins from species without a complete database, antibodies must be generated to verify results.

In this Aim we purified and identified the sequence of the ion *m/z* 4355. Using basic chromatography capture, we reduced the complexity of prostate tissue lysates to enable the use of MALDI-TOF tandem MS (LIFT). Using direct *in-situ* trypsinization the sequence was also verified by the detection of specific peptide fragments. Finally, the identity of the biomarker protein was verified using immunohistochemistry and Western

blot analysis. Additional protein species present in prostate tissues were also sequence identified.

## 4.2 Materials and Methods

### Materials

Rabbit monoclonal antibody to MEKK2 (EP626Y) was purchased from Abcam, Cambridge, MA. Rabbit polyclonal antibody to MEK 5 (RB0932) was purchased from Abgent, San Diego, CA.

### Tissue and cell culture lysates

Tissue lysates were prepared from bulk frozen prostate tissue ($\sim$0.5mm$^3$) by homogenizing the samples in a small dounce tube on ice with a solution of 20mM Hepes, 1% Triton-X 100 (1ml). Lysates were then sonicated at room temperature for 15 minutes and spun down at 14,000 rpm for 2 minutes to remove cellular debris. The lysates were then subjected to fractionation using weak cationic exchanger (WCX) magnetic beads (Bruker Daltonic) according to the supplier's specifications. The bound peptides and proteins were eluted in 20 µl of elution buffer. Five microliters of this eluate was lyophilized and resuspended in 5 µl of CHCA matrix in 50% acetonitrile with 0.1% TFA. Lysates from the prostate cancer cell lines (Du145, LnCap and PC-3) were prepared from $10^6$ cells in a lysis buffer containing 0.3% SDS, 3%DTT and 30mM Tris pH 7.5

## MALDI-MS/MS and Protein Identification

One microliter of each tissue lysate mixed with matrix was then spotted on a steel MALDI target. The mass profiles were recorded by MALDI MS using the same acquisition parameters as for tissue imaging. Data was collected on the UltraFlex III in reflectron mode to verify the presence of the peak of interest. MS/MS analysis of the peak was then performed in LIFT mode. An optimized high mass LIFT method was used and externally calibrated with fragments from a peptide standard with parent masses in the mass range of 700-4500 Da . A parent mass (monoisotopic mass as determined in reflectron mode) was selected and LIFT analysis (MS/MS) was performed in the Ultraflex TOF-TOF. Peaks were labeled using FlexAnalysis software and opened in BioTools 3.1 (Bruker Daltonic) The MS/MS spectrum sequence analysis and database search was performed using MASCOT 2.2.03 with the following settings: MS Tolerance: 70 ppm  MS/MS Tolerance: 1.0 Da, no enzyme designation , serine acetlyation, using the National Center for Biotechnology Information database for human sequences with 20,080,125 entries.

Trypsin digestion was performed on the tissue slices (10μm) by spotting 0.5μl of a solution of 0.769μg/ul trypsin in 50mM Ammonium bicarbonate pH. 8.0. The tissue slices were then incubated at 37°C for 2 hours. Following trypsin treatment the tissue sections were spray coated with CHCA (7mg/ml in 50% acetonitrile, 0.2% TFA). Data was collected across the tissue in reflectron mode.

**Immunohistochemistry**

Immunostaining of UMFix treated paraffin-embedded and frozen, specimens was performed by the avidin-biotin peroxidase complex method using the Vectastain Elite ABC kit (Vector, Burlingame, CA). Blocking was performed with an avidin-biotin blocking kit (Vector Laboratories, catalog number SP-2001). Fixed and frozen tissues were then treated with 0.3% hydrogen peroxide to block endogenous peroxide activity for 15 minutes. Sections were incubated in normal goat serum to block nonspecific binding for 20 minutes at room temperature. Sections were incubated with rabbit monoclonal antibody to MEKK2 diluted 1:50 in PBS or rabbit polyclonal antibody to MEK5 for 1 hour at room temperature. This antibody reacts with the N-terminal portion of MEKK2. Sections were then treated with biotinylated goat anti-rabbit immunoglobulin G (IgG), followed by treatment with avidin-biotin-peroxidase complex, and stained with IMPACT DAB peroxidase substrate (Vector Labs) according to the supplier's protocol. Counterstaining was performed with Mayer's hematoxylin.

**Western Blot Analysis**

A total of 30-100μg of protein was separated on a 4-12% SDS-PAGE gel and transferred by semi-dry transfer method to PVDF membranes (Immobilon-P, Millipore, Billerica, MA). The membranes were then incubated in Odyssey™ blocking buffer diluted 1:1 in PBS for 1 h at room temperature. Incubation with rabbit monoclonal antibody to MEKK2 (EP626Y) diluted 1:1000 in blocking buffer was performed overnight at 4°C with gentle shaking. Blots were then washed four times with 5 min incubations in PBS and 0.1% Tween 20 (PBST). The secondary antibody, Alexa Fluor

IRDye 800cw goat anti-rabbit IgG (# 926-32211), was diluted 1:5000 with blocking

buffer, 0.1% Tween 20, and 0.01% SDS. The membrane was incubated with 10 ml of this

solution with gentle rotational mixing at room temperature for 1 h protected from light.

The membranes were then washed in PBST as before, washed in PBS and scanned with

the Odyssey infrared imaging system (LI-COR, Lincoln, NE).


## 4.3 Results

**Sequence Identification of *m/z* 4355 as a fragment of MEKK2**

Having established the differential expression of a peptide ion at *m/z* 4355 in specific

Aim 1, we next set out to sequence it. Lysates were prepared from 4 tissue samples; 2

PCa and 2 benign prostate. These tissues were examined in the initial MALDI-IMS

analysis and found to have high or low expression of the peak at *m/z* 4355. Protein

lysates were incubated with weak cationic (WCX) magnetic beads and eluted fractions

were shown to be enriched for the *m/z* 4355 peak as measured by MALDI-TOF. As seen

in Figure 19, the peptide ion captured from the WCX fractionation of the PCa tissue

lysate matches the mass detected directly from the tissue within an error of 0.26 Da,

whereas no peptide ion was detected at this *m/z* in the enriched lysate from benign tissue.

The PCa lysate was then concentrated via lyophilization and prepared for MS/MS

analysis as described above. Figure 20 displays the fragmentation pattern of the parent

ion (*m/z* 4350.4), in which it can be seen that the spectra contained many large internal

fragments observable in the TOF/TOF analysis. The fragmentation series gave a

MASCOT top score of 67 (1.0 Da, 70 ppm), with scores ≥ 63 indicating extensive

homology, and matched to a fragment of MEKK2 (Swiss-Prot entry Q9Y2U5) with S-

acetylation at the N-terminal of the peptide (Figure 21). Out of 129 observed fragment peaks, 126 could be accurately assigned to theoretical fragments of MEKK2. This sequence represents amino acid residues 26-61 in the 619 amino acid full-length sequence and lies within the PB1-domain of the molecule.

In order to further establish that the *m/z* 4355 ion derived from tissue is a fragment of MEKK2 we performed an on-tissue digest to analyze for the presence of predicted MEKK2 tryptic fragments. A tissue section previously found to have high expression of the *m/z* 4355 peak in a PCa region was used for this analysis. Serial sections of the same tissue region were harvested and analyzed. One of the mirror sections was trypsin treated while the adjacent mirror section was untreated and used as a control. Ion density maps were also generated using the indicated theoretical tryptic peptides. As seen in Figure 22, specific theoretical masses of the predicted MEKK2 fragment after trypsinization could be detected in the trypsin treated PCa tissue. The in-tissue trypsin-generated fragments matching the theoretical digest masses were not present in the mirror untreated section of the same PCa tissue (Figure 22C). Furthermore, trypsin digestion of benign tissue sections did not generate fragment ions corresponding to theoretical MEKK2 cleavage products (Figure 22B). Unfortunately, the peptides were not of sufficient abundance to perform tandem MS. We also show a representative ion density map image derived from the parental 4355 *m/z* as a comparison to images derived from the tryptic peptides (Figure 22A). This analysis demonstrates that both the parental peptide and predicted peptide fragments display concordant tissue expression.

## Other Proteins Sequenced from Prostate Tissue

In our efforts to sequence the ion at $m/z$ 4355, we were also able to sequence many other proteins expressed in prostate tissue using MALDI-TOF tandem MS. While we cannot make a determination on the comparative expression levels of these peptides and proteins in PCa versus benign tissue, their presence and the ability to sequence them directly from the tissue samples represents an important step in both biomarker discovery and identification. The results of this effort can be seen in Table 6. Using both the bulk PCa tissue lysate and the WCX fractionated lysate we were able to identify 4 additional proteins. Actin and hemoglobin are common proteins found in tissue, and alpha-1 antitrypsin is an abundant serum protein. Direct tissue trypsin digestion enabled the sequencing of abundant and less abundant proteins. A total of 20 additional proteins were sequenced from the trypsinized tissue. Of note are transgelin (found in benign and PCa tissue) and prokineticin-1 (found in PCa tissue). Transgelin (also known as SM22) is found in vascular and visceral smooth muscle and is an early marker of smooth muscle differentiation [181]. It is also present in fibroblasts, and some epithelium where expression is likely driven by TGF-beta1 [182]. Prokineticins (PK-1 and PK-2) are a novel family of secreted peptides with diverse regulatory roles, one of which is their capacity to modulate immunity and promote angiogenesis [183, 184]. Prokineticin-1 (PK1) is also known as endocrine gland-derived vascular endothelial growth factor (EG-VEGF).

**MEKK2 is Overexpressed in PCa Specific Regions of the Prostate**

We examined the expression of MEKK2 in PCa tissue using immunohistochemistry specific for expression of MEKK2. PCa containing and adjacent uninvolved frozen tissues were stained for the detection of MEKK2. The antibody used is specific for the N-terminal portion of the MEKK2 protein where the PB1 domain is located and our fragment lies [185]. As seen in Figure 23A, MEKK2 staining correlates with the presence of PCa in the tissue section. Additional prostate tissues were also stained and magnified views of the stained PCa glands can be seen in Figure 23B. All prostate tissues examined showed high levels of MEKK2 within involved tissue with a predominantly cytoplasmic expression pattern. In contrast benign glands displayed much reduced MEKK2 expression that was only slightly above background levels obtained with no primary antibody.

Samples of high grade PCa can be difficult to obtain due to the success of early detection screening practices. We were able to obtain a total of three poorly differentiated tissue samples and observed reduced expression of both the *m/z* 4355 ion and MEKK2 in these three cases. As shown in Figure 24, overall very little of the ion at *m/z* 4355 is present in two cases of PCa with Gleason scores of 4+5 and one case with a Gleason score of 4+4. The IHC staining for MEKK2 of another tissue sample from the same prostate (Gleason 4+4) can be seen in Figure 25. Overall there is not a large amount of *m/z* 4355 ion present or MEKK2 staining evident. However, a small foci of *m/z* 4355 expression is visible in the MALDI-IMS image (red area). This foci corresponds to the same area which produced dark staining for MEKK2 evident in the intra-luminal space of one gland.
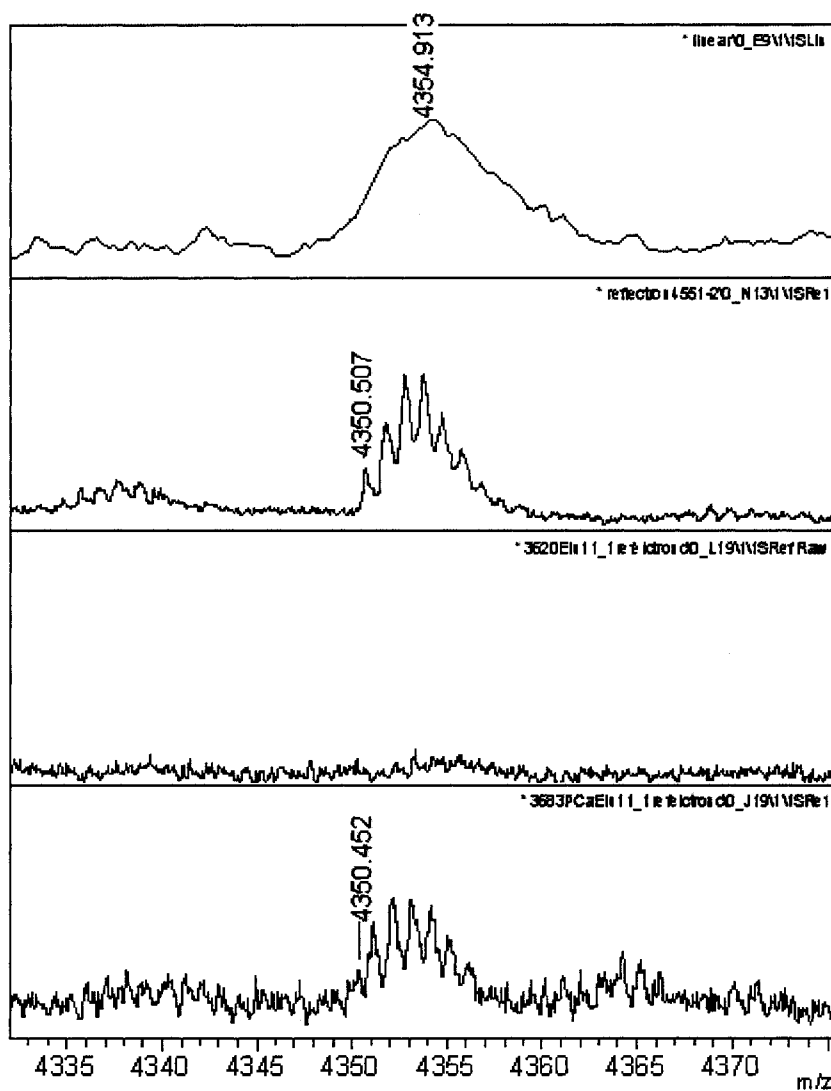
**Figure 19.** Purification of PCa biomarker at m/z 4355. Representative spectra from direct acquisition from tissue showing the peak profile of *m/z* 4355 in: A)-linear mode B)-reflectron mode. Also shown are the reflectron mode spectra from the corresponding tissue lysates from benign tissue (C), and PCa containing tissue (D)
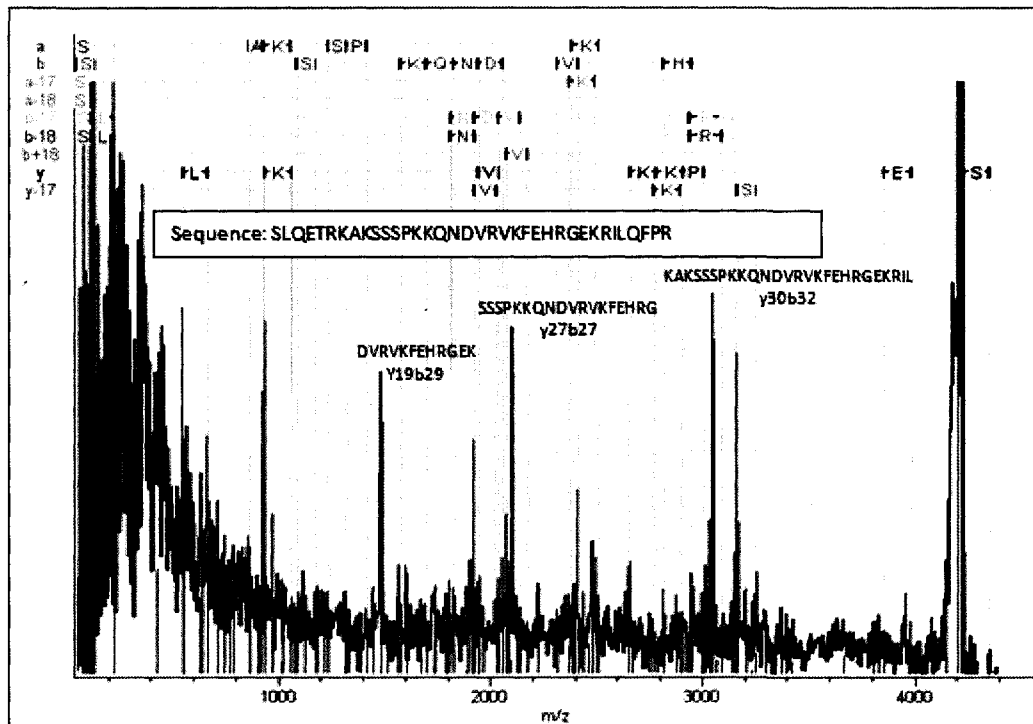
**Figure 20.** Sequence identification of biomarker peak *m/z* 4355. MS/MS spectra of monoisotopic peak of *m/z* 4355 (m/z 4350.4) from prostate tissue lysate collected using TOF/TOF LIFT. Peaks attributed to internal fragments are labeled. Out of 129 peaks 126 were assigned. A Mascot search identified the sequence as matching to the PB-1 domain of MEKK2.

**Probability Based Mowse Score**

Individual ions scores > 44 indicate peptides with significant homology.

Individual ions scores > 63 indicate identity or extensive homology (p<0.05).

Human Mitogen Activated Protein Kinase Kinase Kinase 2 Phox Domain (Map3k2-Phox) Variable modifications: N-Acetyl (S)

No enzyme cleavage specificity

Sequence Coverage: 36%

Matched peptides shown in Bold Red

[1] SMSLQETRKA KSSSPKKQNDVRVKFEH RGEKRILQFPRPV
KLEDLRSKAKIAFGQSMDLHYTNNELVIPLTTQDDLDKAV
ELLDRSIHMKSLKILLVING [101]

**Figure 21.** Protein sequence identity of *m/z* 4355 ion. A Mascot search identified the sequence as matching to the PB-1 domain of MEKK2 representing sequence coverage of 36% for this region.

**A.**

PCa tissue

m/z 4355

**B.**

| PCa | Control | Benign |
|---|---|---|

S*LQETR (775.4 Da)

QNDVR (631.3 Da)

FEHR (588.3 Da)

ILQFPR (773.5 Da)

+Trypsin    -Trypsin    +Trypsin

**C.**

+Trypsin

631.327

-Trypsin

**D.** S*LQETRKAKSSSPKKQNDVRVKFEHRGEKRILQFPR
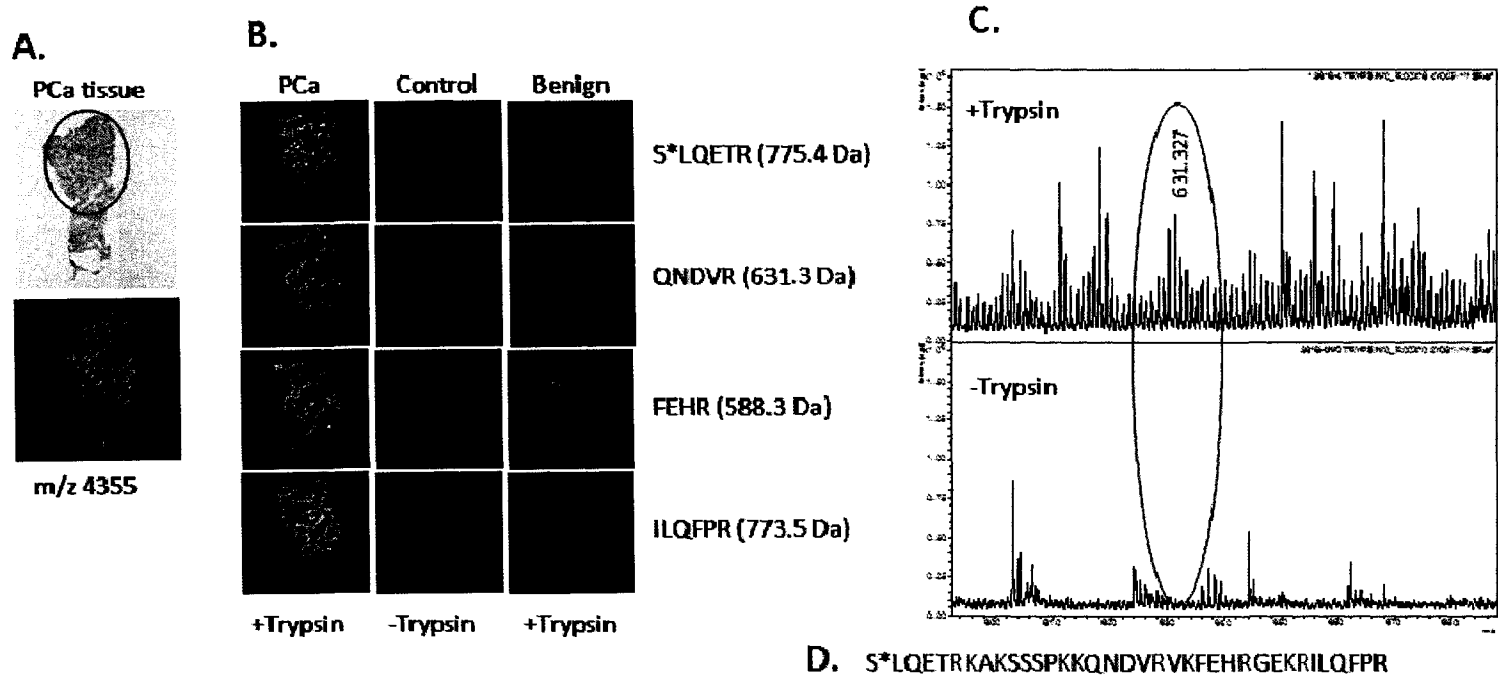
**Figure 22.** On-tissue trypsin digestion of PCa tissue detects predicted peptides of MEKK2 fragment. A) H & E stained image of PCa tissue with a region of adenocarcinoma circled (top), and MALDI-IMS showing spatial distribution of parent ion at m/z 4355 (bottom). B) After trypsin treatment on the tissue, 4 predicted fragments corresponding to the MEKK2 fragment sequenced were detected in the PCa tissue. Control is an identical section of PCa tissue without trypsin treatment. A benign section of prostate tissue was also trypsin treated. C) Representative spectra from trypsinized (top) and non-trypsinized (bottom) PCa tissue showing the presence of an ion at m/z 631.3 in the trypsin treated tissue only. D) The sequence of the peptide corresponding to the m/z 4355 is shown below for reference with trypsin cleavage sites (R and K) shown.

**Expression of MEKK2 in Prostate Cancer Cell Lines and Tissues**

Western blot analysis was performed on PCa and benign tissue extracts and 3

prostate cancer cell lines (Du145, LnCap, PC-3). LNCaP cells originate from a lymph

node metastatic lesion of human PCa and Du145 and PC-3 are human prostate

adenocarcinoma cell lines metastatic to the brain and bone respectively. The antibody

used was the same as that employed in the above IHC analysis for MEKK2 expression.

The relative expression of MEKK2 in these systems is shown in Figure 26. All three

prostate cell lines showed strong expression of full length MEKK2 (70kDa). This

analysis revealed higher MEKK2 expression in the PCa tissues when compared to the

expression seen in the benign tissues. Densitometry analysis indicated a 4.4 fold

increased expression of MEKK2 in PCa tissue compared to benign tissue.


**MEK5 Expressed in PCa and Benign Prostatic Tissue.**

To investigate members of the ERK5 pathway downstream from MEKK2, we

also performed IHC for MEK5 in 3 PCa and 3 benign prostate tissues. As seen in Figure

27, MEKK2 expression correlates with MEK5 expression however there are distinct

abundance differences with respect to Gleason grade. MEKK2 expression in the

moderately differentiated PCa (Gleason 3+4) is higher than MEK5. Conversely, MEK5

expression appears somewhat higher in the higher grade PCa tissue (Gleason 4+4 and

4+5). Additionally, MEKK2 expression is barely detectable in benign prostate, but

MEK5 nuclear staining can be seen in a few glands. In cases with cystic atrophy MEKK2

and MEK5 staining is evident in the intra-luminal spaces. The MEK5 staining of the

luminal cells appears to be both cytoplasmic and nuclear, whereas MEKK2 staining is predominately cytoplasmic.

## 4.4 Discussion

We have identified the ion at *m/z* 4355 found to be differentially expressed in PCa tissue as a fragment of MEKK2 and confirmed the differential expression of this protein between tumor and benign tissue using immunohistochemistry and Western blot analysis. MEKK2 is a member of a mitogen activated protein kinase cascade (MAPK) and is designated as a MAP kinase kinase kinase or MAP3K. Mitogen-activated protein kinase (MAPK) signaling cascades are among the most widespread signaling mechanisms involved in eukaryotic cell regulation. MAPKs are activated through a module that includes a MAPK, a MAPK kinase (MAPKK), and a MAPKK kinase (MAP3K). Thus a MAPK cascade consists of three sequential protein kinase reactions which finally lead to the phosphorylation of defined MAPK substrates (e.g., transcription factors, other protein kinases, phospholipases, cytoskeleton- associated proteins) on serine/threonine residues [186-188]. Biochemical and genetic studies have demonstrated that MAP3Ks are crucial in relaying distinct cell-surface signals through various downstream MAPK pathways [187]. The MAP3Ks are the most numerous of the core kinase elements. The challenge is in defining the specific upstream inputs and cellular functions mediated by each. Additionally, MAP3Ks have been found to be highly promiscuous, interacting with and activating a number of downstream components and are the major players in the coordination, localization, duration and magnitude of MAPK activation in response to cell stress and inflammation [189]. The in vivo functions of MEKK2 have been studied in

**Table 6.** Sequence Identification of Protein Peaks Found in Prostate Tissue

| Peaks identified from bulk PCa tissue lysates | | Expect | MASCOT score |
|---|---|---|---|
| 1617.8 | Actin α-2 | 0.022 | 60 |
| 2952.4 | Actin α-1 | 0.00053 | 79 |
| 3586.6 | Hemoglobin subunit-α | $6.3 \times 10^{-8}$ | 112 |
| | | | |
| **Peaks identified from WCX purified PCa lysate** | | | |
| 4133.4 | Alpha-1-antitrypsin | $6.0 \times 10^{-6}$ | 75 |
| 4350.4 | MEKK2 | 0.0011 | 80 |
| | | | |
| **Peaks identified from trypsinized benign prostate tissue** | | | |
| 854.6 | Dynein-heavy chain | 0.047 | 13 |
| 993.5 | Calponin I | 0.031 | 32 |
| 1032.6 | amyloid β A4 precursor protein-binding | 0.0017 | 41 |
| 1046.7 | 28s mitochondrial ribosomal protein S2 | 0.03 | 17 |
| 1055.5 | Kinesin-like protein | 0.044 | 23 |
| 1155.5 | GDNF family receptor-α like | 0.0099 | 40 |
| 1209.8 | USP6 N-terminal like protein | 0.0023 | 41 |
| 1354.6 | Actin smooth muscle | 0.00026 | 55 |
| 1408.6 | Transgelin | $3.0 \times 10^{-6}$ | 72 |
| 4130.1 | Phosphoinositide-3 kinase regulatory subunit | 0.033 | 15 |
| 1790.9 | Actin smooth muscle | 0.00014 | 54 |
| 1932.9 | Cartiladge acidic protein 1 | 0.0098 | 35 |
| 2088.7 | Desmin | $1.8 \times 10^{-6}$ | 74 |
| 3458.5 | Poly [ADP-ribose] polymerase 12 | 0.018 | 27 |
| | | | |
| **Peaks identified from trypsinized PCa tissue** | | | |
| 656.1 | Myosin phosphatase targeting subunit | 0.011 | 25 |
| 976.5 | Actin smooth muscle | 0.00049 | 49 |
| 1198.9 | Actin smooth muscle | 0.0022 | 39 |
| 1209.7 | Prokineticin-1 | 0.044 | 29 |
| 1407.9 | Transgelin | 0.00021 | 52 |
| 1978.3 | (D)J recombination-activating protein 2 | 0.00098 | 46 |

different physiologic systems, including MEKK2 knockout mice and cells. The pathways

in which MEKK2 plays a part can be seen in Figure 28. Studies have shown that MEKK2

regulates T-cell function [190-192], controls cytokine gene expression in mast cells and

mediates epidermal growth factor (EGF) receptor and fibroblast growth factor-2 (FGF-2)

receptor signals [193, 194], and plays a role in rheumatoid arthritis [195, 196]. In

addition, MEKK2 activation is critical for c-Jun-N-terminal kinase (JNK) activation and

TNF-α production [197].

MEKK2 and MEKK3 are two closely related MAP3Ks belonging to the

MEKK/STE11 subfamily which are expressed in multiple tissues and are also potent

activators of the NFkB, ERK5 and JNK pathways [192, 198]. In fact, MEKK2 is one of

only two of the 20 known MAP3Ks, the other being MEKK3, which regulate the

mitogen/extracellular-signal-regulated kinase kinase 5/ extracellular signal-regulated

kinase-5 (MEK5/ERK5) pathway [199-201]. Growth factors and oxidative/osmotic

stress stimulate a three-tier ERK-5 kinase module consisting of MEKK2/3, MEK5 and

ERK5. MEKK2 and MEKK3 contain PB1 (Phox-Bem1p) domains that selectively

heterodimerize with the MEK5 PB1 domain to form a functional MEKK2 (or MEKK3)–

MEK5- ERK5 ternary complex [202, 203]. PB1 sequences are

dimerization/oligomerization domains present in adaptor and scaffold proteins as well as

kinases [204]. PB1 domain-dependent MEKK2/3-MEK5 heterodimers provide a spatially

organized signaling complex primed to activate ERK5 in response to activation of

MEKK2 or MEKK3 [200]. No other MAPK cascade has been shown to form such a

complex. Interestingly, the *m/z* 4355 represents a peptide fragment that lies within the

PB1 domain and may reflect molecular pathway changes indicative of PCa development.

ERK5 signaling is a critical pathway in the regulation of cell invasion under "normal" conditions to support immune surveillance as well as during tumor metastasis (reviewed in [205]). Indeed, the ERK5 pathway has been implicated in high grade prostate cancer. Specifically, an increase in MEK5 expression was associated with metastatic prostate cancer, cell proliferation, MMP-9 expression and cell invasion [206]. Strong MEK5 expression was also found to correlate with the presence of bony metastases and less favorable disease-specific survival. An additional report found significant correlation between ERK5 cytoplasmic overexpression, Gleason sum score and less favorable disease-specific survival [207]. The authors also found that ERK5 nuclear expression is significantly associated with the transition from hormone-sensitive to hormone insensitive disease. Our studies have also found MEK5 expression in PCa tissue detected via immunohistochemistry. MEK5 protein expression correlated with MEKK2 expression although the level of expression varied with PCa Gleason score. Cases of well to moderately differentiated PCa showed a higher level of MEKK2 expression as compared to MEK5. The situation was reversed in high grade or poorly differentiated PCa in that MEKK2 levels decreased and MEK5 expression increased. This is in agreement with previous studies in which MEK5 was over-expressed in high grade PCa. We also detected MEK5 expression in some benign prostate tissues, especially in atrophic glands, although not at the level seen in high grade PCa. Overall MEKK2 staining was predominately cytoplasmic and MEK5 staining was predominately nuclear. This is consistent with a recent study in which MEK5 is localized in the nucleus of HeLa and Rat-1 cells both before and after stimulation [208]. This study also reported that in resting cells, MEKK2 was localized all over the cell, and upon stimulation of the

cells with EGF there was an enrichment in the nuclear localization of MEKK2.

Since MEK5 lies downstream of MEKK2 in the ERK5 pathway, our findings imply that the ERK5 pathway is highly active in PCa cells. Although ERK5 and MEK5 have been shown to correlate with high grade PCa disease, this is the first time MEKK2 has been shown to discriminate between cancer and normal prostate tissues. Unfortunately, we were unsuccessful in our attempt to perform Western blot analysis for MEK5 and ERK5 (data not shown). Since MEKK2 has been shown to also play a part in both the ERK1/2, JNK, and p38 and pathways, as well as NFκB activation, further studies are needed to determine the exact role MEKK2 is playing with regard to carcinogenesis and which pathway(s) are increasingly activated.

Several studies have found MEKK2 over-expression in the synovial tissue and cultured synovocytes of arthritis patients [196, 209]. In vitro kinase assays have shown that MEKK2 kinase activity is increased by cytokines in synoviocytes [196]. MEKK2 seems to play an important role in cytokine production and is known to directly phosphorylate and activate Ikappa B kinases, playing a role in the pro-inflammatory transcription factor nuclear factor kappa B (NFκB) signaling pathway by controlling the late phase of its induction [210]. Furthermore it has also been shown that ERK5 may enhance NFκB activity by enhancing p65 nuclear localization [211]. Thus the increase in MEKK2 protein levels may increase NFκB activity directly or indirectly through its role in activating ERK5 signaling.

As mentioned before, inflammatory disorders harbor a greatly increased risk for cancer development, owing primarily to the pro-growth environment generated by

A.

| H&E | MEKK2 stained | Control |

B. PCa    Benign
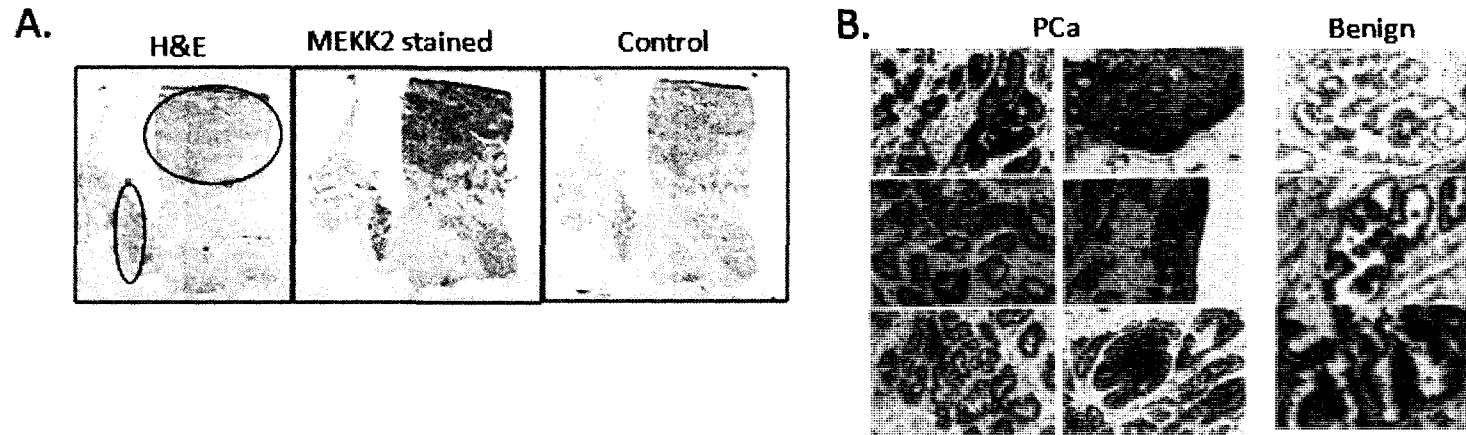
**Figure 23.** MEKK2 expression in prostate tissue. A) Immunohistochemical analysis of frozen prostate tissue sections. H&E stained prostate tissue with regions of PCa circled (left panel). MEKK2 stained serial section showing staining in PCa regions (middle panel). Control section without primary antibody (right panel). B) Representative areas of MEKK2 staining from 6 PCa and 3 benign adjacent tissues showing strong expression of MEKK2 in adenocarcinoma cells and little expression in benign glands.
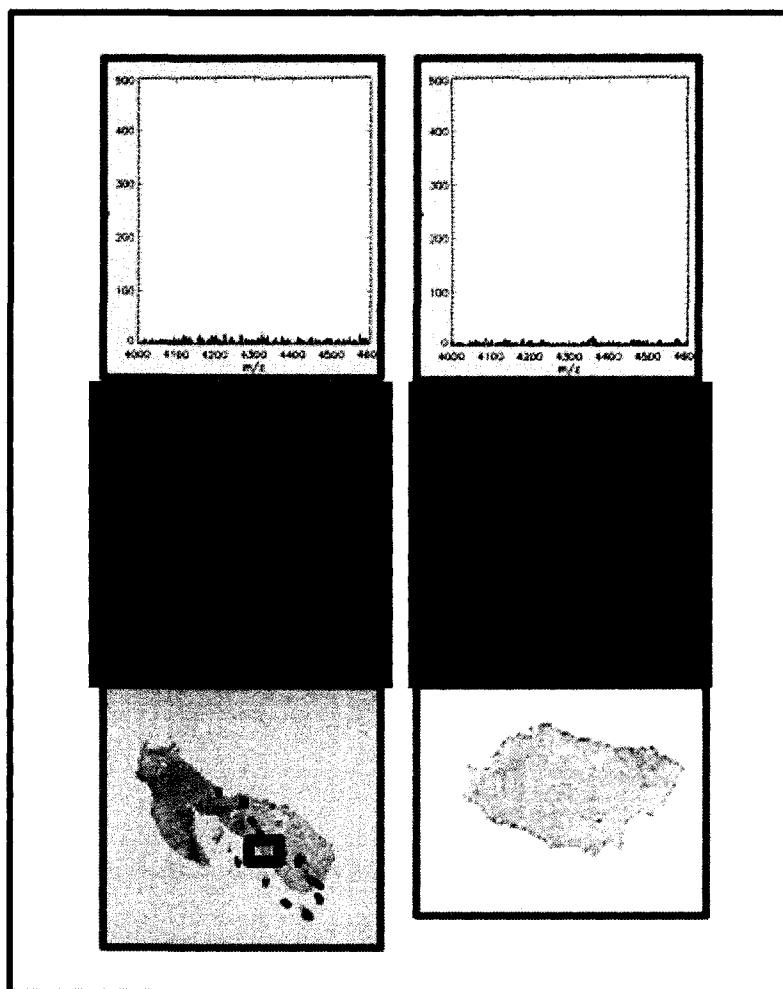
**Figure 24.** Representative MALDI-IMS from High Grade PCa. Two frozen PCa tissue samples, both with a Gleason score of 4+5 were processed for MALDI-IMS. Top panels show the absence of a peak at *m/z* 4355 and the middle panels show no expression visible in the resulting MALDI-IMS images. Bottom panels are the H&E stained tissue images.
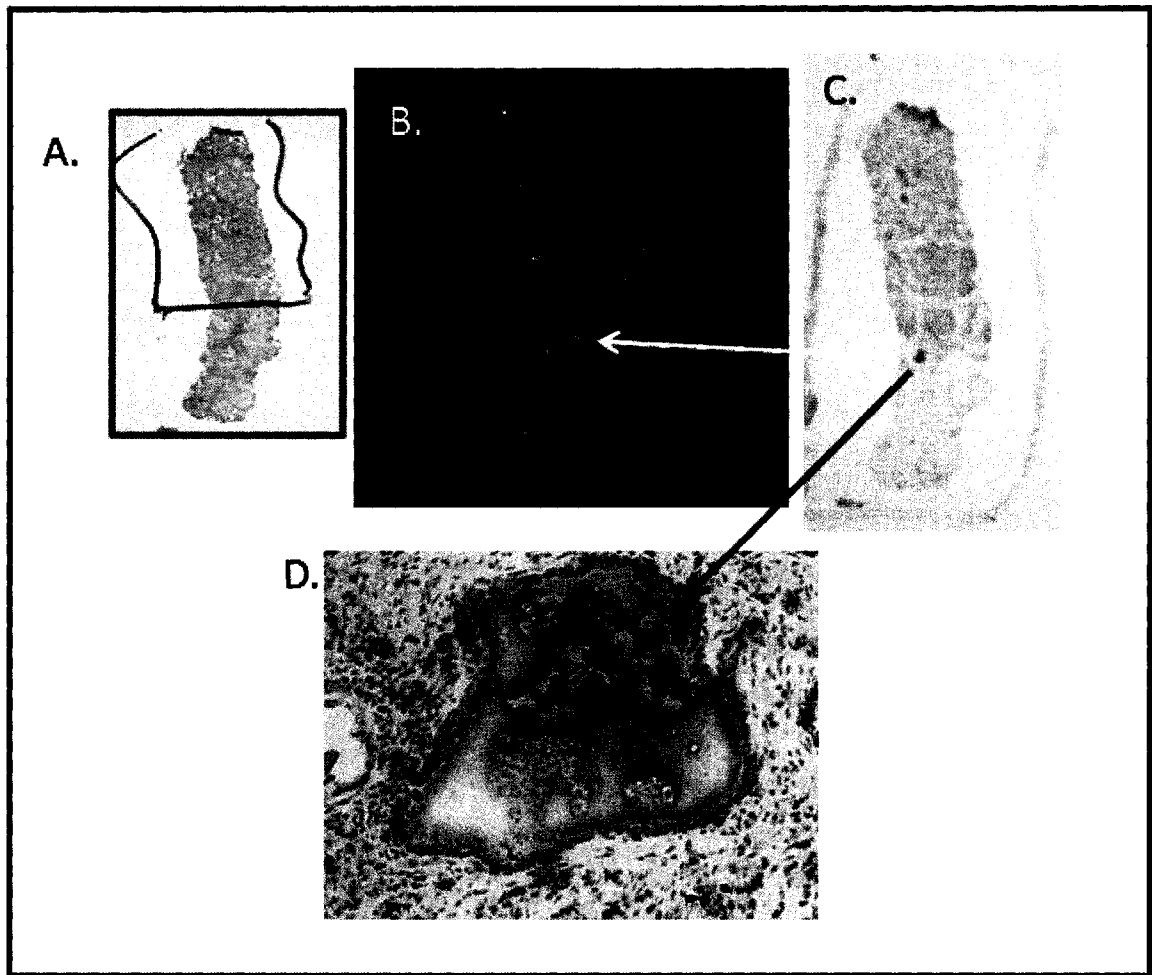
**Figure 25.** MALDI-IMS of *m/z* 4355 and IHC for MEKK2 in High Grade PCa. One frozen PCa tissue sample with a Gleason score of 4+4 was processed for MALDI-IMS. A) H&E stained section with area of PCa circled. B) Resulting MALDI-IMS image with a small area of high expression of the ion at *m/z* 4355 which correlates with intense MEKK2 staining of the same area in a serial section shown in (C.). D.) 10X view of the area with intense MEKK2 staining showing intra-luminal expression.
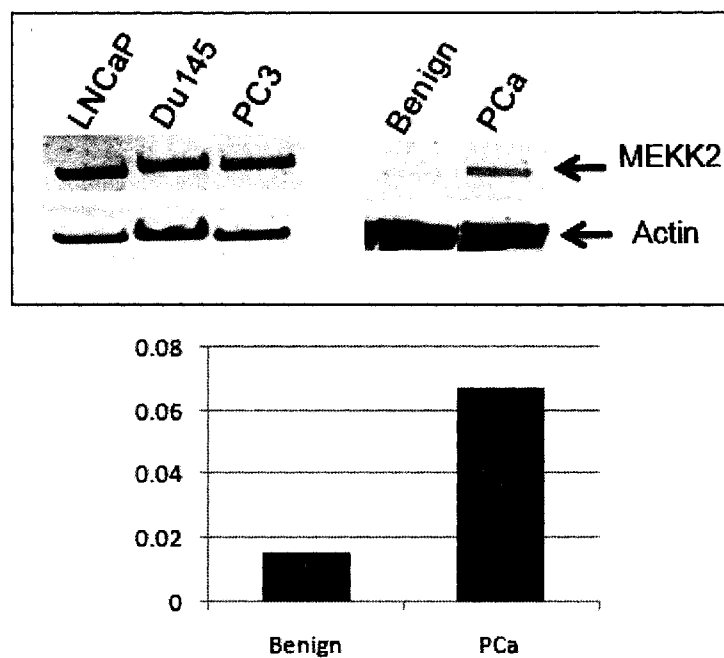
**Figure 26.** Western blot analysis for expression of MEKK2. Western blot of the indicated PCa cell lines (30ug) and tissue lysates (100ug) was performed using an antibody to the N-terminal region of MEKK2. Actin was used as a loading control. The bottom panel is the densitometric quantitation of the MEKK2 bands for benign and PCa tissue lysates.
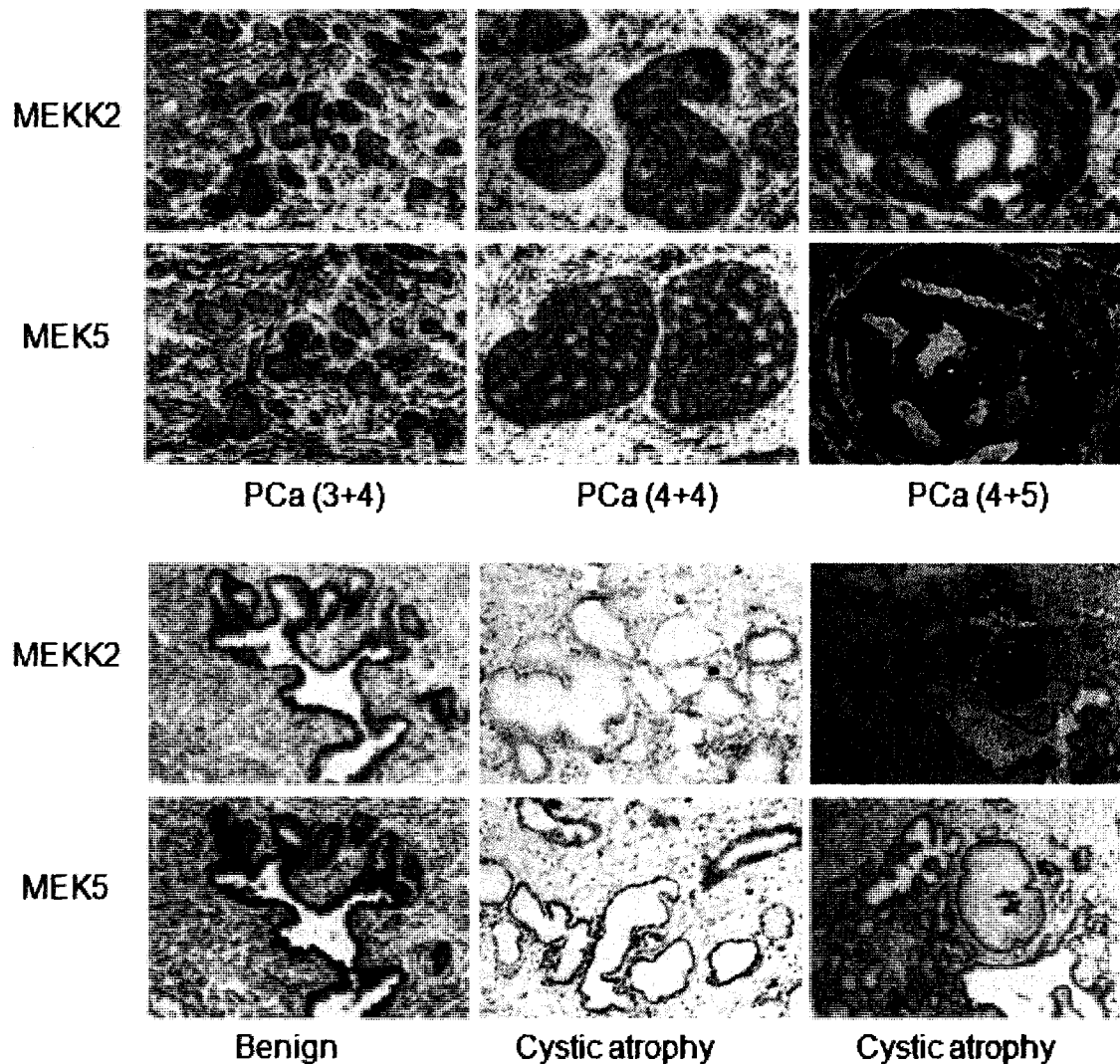
**Figure 27.** Comparison of MEKK2 and MEK5 expression in prostate tissue. Immunohistochemistry was performed. on three PCa tissues with increasing Gleason scores (top panels) and three benign tissues, two with cystic atrophy (bottom panels). MEKK2 expression in reduced in the higher grade PCa lesions compared to the lesions with Gleason grade 3+4, whereas MEK5 expression is increased. Minimal expression of MEKK2 and MEK5 is visible in the benign prostate epithelial cells. MEKK2 and MEK5 are also expressed intra-luminally in two cases of cystic atrophy. Note the cytoplasmic expression of MEKK2 and the nuclear expression of MEK5.
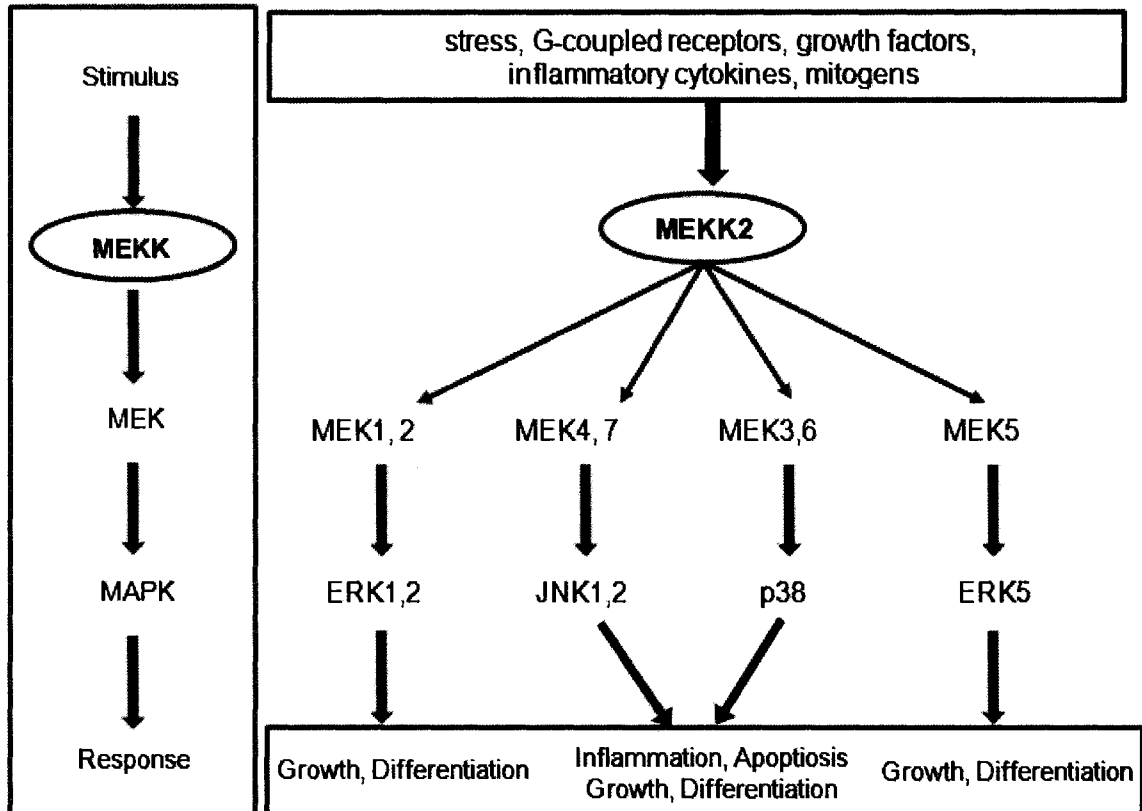
**Figure 28.** MAPK pathways in which MEKK2 plays a role. MEKK2 plays a role in the ERK 1,2, JNK 1, 2, p38 and ERK5 pathways. Leading to growth, differentiation, inflammation and apoptosis depending on which pathway and cell system is activated.

activated inflammatory cells [212]. Since NFκB has been identified as an important molecule linking chronic inflammation [213] and cancer it is tempting to speculate about the contribution of MEKK2 to inflammation and the development of prostate cancer, because of its contribution to both NFκB and JNK activation. Indeed our study has uncovered over-expression of MEKK2 in proliferative inflammatory lesions of the prostate (PIA) and lesions exhibiting cystic atrophy. Inflammatory responsive cells have previously been found juxtaposed to PIA lesions. These include mononuclear and/or polymorphonuclear inflammatory cells in both the epithelial and stromal compartments, and sometimes, abundant macrophages and/or neutrophils in the glandular lumen or epithelium [214]. Macrophages may be present in the lumen of PIA lesions to engulf epithelial cells damaged by infection, oxidants, autoimmunity or hypoxia. In turn macrophages and neutrophils secrete cytokines, tumor necrosis factor and reactive nitrogen species leading to an environment susceptible to chronic infection.

The examination of high grade PCa tissue samples in our study found a reduction of detectable MEKK2 in both MALDI-IMS (*m/z* 4355) results and IHC staining. Interestingly, in prostate cancer as in many other malignancies, an overall reduction in tumor stroma indicates a more malignant pathological grade [215]. It is conceivable that an overall reduction in specific stromal cells within high-grade lesions leads to reduced potential for specific stromal cell mononuclear cell interactions that are supportive of antitumor cytotoxic activities and secretion of pro-inflammatory mediators. It has been established that in the tumor microenvironment, there is a delicate balance between antitumor immunity and tumor-originated proinflammatory activity, which weakens antitumor immunity [216]. The inflammatory milieu is occupied by cells such as resident

and recruited macrophages, dendritic cells, T cells, and NK cells [217]. Among these, tumor-associated macrophages (TAMs) and T cells are frequently the prominent leukocytes present in a tumor [212, 218]. The infiltrated immune cells can exert paradoxical effects during cancer development [219]. These effects depend on different mediators that are released by host inflammatory cells, cancer cells, as well as fibroblasts and endothelial cells. When host-mediated antitumor immunity is stronger than tumor-mediated immunosuppressive activity, tumor cells can be eliminated [220]. Conversely, when host-mediated antitumor activity is weaker than tumor-mediated immunosuppressive activity, tumor cells undergo immune escape and grow rapidly [220]. Given the fact that some of the tissue we examined contained only high grade adenocarcinoma cells, the potential for interaction with immune cells is greatly reduced. Indeed, we did not observe many infiltrating lymphocytes in the high grade PCa tissues examined, leading to speculation that there is no longer a mechanism whereby an inflammatory response is potentiated, leading to a possible reduction in MEKK2 expression.

Our sequence identification of other proteins directly from trypsinized tissue yielded some interesting results. Transgelin (SM22) has been widely reported to be abnormally expressed in many solid tumors [221]. Recent evidence suggests that transgelin acts as a tumor suppressor and its expression has been found to be reduced in high grade prostate, breast and colon cancers [222, 223]. Transgelin also represses MMP-9 expression, by reducing AP-1-dependent trans-activation of the gene by way of compromised ERK activation [181]. Diminished transgelin expression in several cancers may therefore be responsible for elevated MMP-9 expression evident in some tumors. In

our study, transgelin was identified from both PCa and benign tissue. Further studies for the determination of the relative expression levels of this protein and/or peptide using MALDI-IMS may reveal altered expression levels. Another protein sequenced in this study found only from PCa tissue is PK-1 or EG-VEGF. PK-1 does not belong to the VEGF family but instead is a member of a structurally related class of peptides which includes the digestive enzyme colipase [224]. PK1 and -2 exert their physiological functions through G-protein-coupled receptors recently identified and named PK receptor type 1 (PKR1) and type 2 (PK-R2) [183]. These receptors are activated by nanomolar concentrations of recombinant PK. Activation of PK receptors induces calcium mobilization, induction of phosphoinositide turnover, and activation of MAPK signaling pathways [225]. PK-1 is a key mediator of angiogenesis and exposure of human or mouse hematopoietic stem cells to PK-1 results in significant increases in total leukocyte, neutrophil, and monocyte counts [226]. Emerging evidence indicates that prokineticins are associated with pathologies of the reproductive and nervous systems, myocardial infarction as well as tumorigenesis (reviewed in [184]). A recent study demonstrated that prokineticins and their receptors are expressed in human prostate and that their levels increased with prostate malignancy [227]. This may imply that PK1 could be involved in prostate carcinogenesis, probably in the regulation of angiogenesis. Therefore, PK-1 may be an interesting biomarker warranting further investigation.

The identification of a peptide fragment of MEKK2 leads to speculation as to how this fragment was formed. It is possible that this fragment is a degradation product formed during tissue processing. Prostate tissues are known to have a general increase in overall proteolytic activity during tumor progression, especially in the metalloprotease

and cysteine protease classes [228]. Serine proteases are also highly abundant in prostate tissues (i.e. PSA and other members of the kallikrein family) [229]. Since the MEKK2 fragment we sequenced has a serine at the N-terminus the increased presence of the fragment in areas of cancer could be a result of non-specific cleavage of the full-length MEKK2 protein by a serine protease occurring either as a natural process or after tissue harvest. Over-expression of the full-length MEKK2 (70kDa) was visible in the PCa tissue lysate in our Western blot however, so not all of the protein is cleaved. Alternatively, the fragment could be generated from the targeted and specific cleavage of MEKK2 due to an unknown disease specific mechanism. For example, MEKK2 is a substrate of Smurf1, an E3 ubiquitin ligase. Smurf1 physically interacts with MEKK2 and promotes the ubiquitination and turnover of MEKK2 to promote osteoblast activity and bone homeostasis [230]. Proteasome degradation of ubiquitin-targeted proteins is an important mechanism that negatively controls activated signaling pathways. Another study found that following TNF-α stimulation of human embryonic kidney cells, XIAP (a regulatory protein of NFκB) interacts with and ubiquitinates MEKK2, promoting a second wave of nuclear translocation that leads to prolonged NFκB activation [231]. This opens up the intriguing possibility that NFκB activation and therefore the inflammatory stimulus is perpetuated in early tumor development. Further functional studies of MEKK2 in prostate tissue will be needed to access the regulatory mechanism (if any) that lead to the generation of the fragment we are detecting in early prostate cancer.

# CHAPTER V

# AIM 3: EVALUATION OF THE CLINICAL UTILITY OF

# MALDI-IMS BIOMARKERS

## 5.1 Introduction

The ultimate hurdle for any new biomarker is validation. In some respects,

biomarker validation is more arduous than discovery [232]. Unfortunately, the literature

is full of novel marker candidates that did not stand up to validation [233]. Biomarker

validation faces several big challenges. One is the biological variability of patients'

samples. Another issue is that single biomarkers are unlikely to provide the sensitivity

and specificity needed for most clinical applications given the substantial heterogeneity

among cancers. It is therefore unrealistic to expect that a single biomarker will provide

information about tissue type and malignant transformation throughout the various stages

of tumor development and progression. Therefore, panels of biomarkers are needed. This

makes the validation of a single biomarker all the more challenging. Furthermore, in

order for cancer biomarker tests to be used effectively in a clinical setting, their clinical

risks and benefits must be assessed. For example, if a biomarker detects disease early,

there are several reasons why it might not have an overall benefit for the screened

population [234]. These include ineffective treatments for detected tumors and

difficulties with implementing the biomarker detection in clinical laboratories (ease of

use or prohibitive economic factors). For studies where the identities of the biomarkers

are known, results should be validated using an independent sample set, either using the

original technique or an alternative assay such as an immune-based assay or array. For

studies using computer-based models of profiles in which the identity of the biomarkers is unknown, it is essential that the model be validated with an independent test set of samples analyzed during a completely separate time period [235]. There are three common ways biomarkers are validated: 1) validation to confirm results, 2) validation to expand utility, and 3) validation to determine clinical usefulness. Most discovery laboratories can perform the first two validation tasks however the third task usually requires several laboratories and many hundreds of samples.

In this Aim we use a cohort of surgery specimens to evaluate the clinical utility of the *m/z* 4355:MEKK2 fragment biomarker and protein expression patterns. A new cohort of tissue samples were analyzed blinded and the diagnosis based on MALDI MSI imaging werecompared with the diagnosis made by clinical laboratory pathologists. The classification algorithms developed in Aim 1 using multiple *m/z* values were also used for the classification of the tissue samples as PCa or benign or metastatic.


## 5.2 Materials and Methods

### Sample selection and processing

Twenty five tissue samples from prostatectomy specimens were collected and embedded in OCT and processed as described in Aim 1. Regions of interest were circled by a pathologist on the serial sections stained with Hemotoxylin and Eosin. In addition, 8 UMFix treated tissues were also collected and processed as previously described. Tissue sections were mounted on ITO coated slides and prepared with SPA matrix using the same protocols used in Aim1. All tissue diagnoses were blinded to the investigator until after the collection of the data and export of the spectra.

**MALDI-IMS**

MALDI-IMS was performed as previously described in Aim1. Images were
acquired using both BioMAP and Flex-Imaging.

**Classification of Tissue Specimens**

Spectra were exported from regions of interest and classified using ClinProt tools
software and the algorithms developed in Aim1. The normalized intensity values of the
$m/z$ 4355 (MEKK2 peak) were also calculated using ClinProt tools for each blinded
tissue sample. The classification results of both the algorithms and the ROC cut-off
values for the $m/z$ 4355 peak were compared to the diagnosis made by the clinical
laboratory pathologists.

**5.3 Results**

**Classification of Blinded Dataset**

A total of 29 frozen tissue areas representing 10 PCa, 10 benign distal and 9
benign adjacent samples were analyzed using MALDI-IMS. Additionally 8 UMFix
processed tissues (4 PCa and 4 benign) were also analyzed for validation. These
specimens were blinded to the investigator during the data collection and analysis phase.
A genetic algorithm using 5 peaks from the initial cohort was tested in its ability to
correctly classify blinded tissue samples. In the initial study cohort a high percentage of
PCa regions were correctly classified (90.3%), but the algorithm did not perform well on
the classification of benign tissues with only 64.1% correctly classified. For the blinded
samples, (9/10) 90% of the PCa tissues were correctly classified, whereas, only (3/19)

15.8% of the benign tissues were classified correctly (see Table 7). For the UMFix treated samples once again the genetic algorithm did not perform well in the classification of the benign samples. As seen in Table 8, in a total of 8 UMFix treated tissues, 62.5% of the samples were correctly classified. All of the UMFix treated PCa tissues (4/4) were classified correctly, however only 1/4 (25%) of the benign tissues were classified as benign.

The use of a cut-off value derived from the normalized intensity value of the ion at $m/z$ 4355 (MEKK2 fragment) performed much better in classifying the frozen blinded samples. As shown in Table 7, using a cut-off of value of 27 for normalized intensity derived from the ROC analysis, 82.7% of all the blinded samples were classified correctly. This represents a correct classification of 80% for PCa tissue areas, and 84.2% for benign areas (both adjacent and distal). Additionally, all of the 8 UMFix blinded tissues were classified correctly using this ROC cut-off value indicating that the fixed tissue preserves the peak intensity as well as the frozen tissue (Table 8).

## 5.4 Discussion

The validation of the biomarkers discovered in Aim 1 and 2 of this project were tested in an independent set of samples. Using a genetic algorithm and normalized intensity values for $m/z$ 4355 (MEKK2 fragment) developed from the initial study cohort the classification of the blinded samples was determined and compared to the pathologist's histopathological diagnosis. The performance of the genetic algorithm to correctly classify the samples was much poorer than the use of normalized intensity

**Table 7.** Frozen Blinded Sample Classification Based on Normalized Intensity of *m/z* 4355 and Classification Algorithm

| Tissue | *m/z* 4355 Norm. Int.* | Classification | Pathology Diagnosis | Correct | Algorithm class. | Correct |
|---|---|---|---|---|---|---|
| 4340-2 | 19.0 | Benign | Benign Dist. | Yes | Benign | Yes |
| 4422-2 | 13.9 | Benign | Benign Dist. | Yes | PCa | No |
| 4597-1 | 20.3 | Benign | Benign Dist. | Yes | PCa | No |
| 4608-1 | 17.5 | Benign | Benign Dist. | Yes | Benign | Yes |
| 4691-2 | 25.6 | Benign | Benign Dist. | Yes | PCa | No |
| 4735-1 | 24.1 | Benign | Benign Dist. | Yes | PCa | No |
| 4903-1a | 114.1 | PCa | PCa | Yes | PCa | Yes |
| 4903-1b | 56.1 | PCa | Benign Adj. | No | PCa | No |
| 4903-2a | 48.2 | PCa | PCa | Yes | PCa | Yes |
| 4903-2b | 24.6 | Benign | Benign Adj. | Yes | PCa | No |
| 4928-2 | 25.1 | Benign | Benign Adj. | Yes | PCa | No |
| 4941-1 | 24.9 | Benign | Benign Dist. | Yes | Benign | Yes |
| 4941-2a | 48.5 | PCa | PCa | Yes | Benign | No |
| 4941-2b | 29.8 | PCa | Benign Adj. | No | PCa | No |
| 4964-2 | 17.7 | Benign | Benign Dist. | Yes | PCa | No |
| 4966-1a | 76.9 | PCa | PCa | Yes | PCa | Yes |
| 4966-1b | 20.9 | Benign | Benign Adj. | Yes | PCa | No |
| 4966-2a | 33.9 | PCa | PCa | Yes | PCa | Yes |
| 4966-2b | 22.4 | Benign | Benign Adj. | Yes | PCa | No |
| 4974-1 | 57.0 | PCa | Benign Dist. | No | PCa | No |
| 4982-1a | 42.4 | PCa | PCa | Yes | PCa | Yes |
| 4982-1b | 22.0 | Benign | Benign Adj. | Yes | PCa | No |
| 4982-2 | 46.2 | PCa | PCa | Yes | PCa | Yes |
| 4989-1a | 35.9 | PCa | PCa | Yes | PCa | Yes |
| 4989-1b | 19.1 | Benign | Benign Adj. | Yes | PCa | No |
| 4994-1 | 24.2 | Benign | PCa | No | PCa | Yes |
| 4998-1a | 26.7 | Benign | PCa | No | PCa | Yes |
| 4998-1b | 21.9 | Benign | Benign Adj. | Yes | PCa | No |
| 5023-3 | 17.9 | Benign | Benign Dist. | Yes | PCa | No |

| | | | Total Correct | 82.7% | Total Correct | 41.4% |
|---|---|---|---|---|---|---|
| | | | PCa | 80.0% | PCa | 90.0% |
| | | | Benign | 84.2% | Benign | 15.8% |

*Any value above 27 was considered indicative of PCa. This value was based on the optimal cut-off from the ROC curve. Bengn Dist= benign distal, Benign Adj.=benign adjacent

**Table 8.** UMFix Blinded Sample Classification Based on Normalized Intensity of *m/z* 4355 and Classification Algorithm

| Tissue | *m/z* 4355 Norm. Int.* | Classification | Pathology Diagnosis | Correct | Algorithm class. | Correct |
|---|---|---|---|---|---|---|
| 4869-1 | 22.4 | Benign | Benign | Yes | Benign | Yes |
| 4885-2 | 19.5 | Benign | Benign | Yes | PCa | No |
| 4889-1 | 54.3 | PCa | PCa | Yes | PCa | Yes |
| 4913-1 | 22.0 | Benign | Benign | Yes | PCa | No |
| 4935-1 | 19.6 | Benign | Benign | Yes | PCa | No |
| 4987-1 | 64.5 | PCa | PCa | Yes | PCa | Yes |
| 4992-2 | 38.7 | PCa | PCa | Yes | PCa | Yes |
| 4994-1 | 49.7 | PCa | PCa | Yes | PCa | Yes |

| | | Total Correct | 100.0% | Total Correct | 62.5% |
|---|---|---|---|---|---|
| | | PCa | 100.0% | PCa | 100.0% |
| | | Benign | 100.0% | Benign | 25.0% |

*Any value above 27 was considered indicative of PCa. This value was based on the optimal cut-off from the ROC curve.

values. The apparent lack of specificity for the benign tissues in the blinded dataset points out the weakness of a genetic algorithm to classify this type of data. Genetic algorithms were initially employed for genomic microarray experiments and have been adapted for proteomic dataset analyses [236, 237]. A genetic algorithm (GA) seeks to find a collection of markers that separate cases and controls. Here the markers correspond to the measurements at a given set of $m/z$ values derived from the tissue specimen. Our study employed a total of 36 PCa and 61 benign data for the training set. Typical spectra produced from any individual tissue location produces from 50-200 peaks or features. In multivariate predictive analysis, a statistical model or algorithm can be overfitted if it has too many features for the number and type of cases in the training set [238]. This can result in a model that fits the training data set very well but does poorly when applied to other data as we saw in our blinded set. Another potential problem is that our data analysis method involves exporting individual spectra from any given ROI. Based on the size of the ROI, the number of exported spectra may be small or large. However, the genetic algorithm does not average or take a consensus of each ROI, but treats each spectrum as an individual. Therefore variations in the data may result in inaccurate representation of features in each ROI.

Using the averaged normalized intensity value of the ion at $m/z$ 4355 provided a much better classification of the blinded tissue samples. One explanation for this improved result is connected to how the data was calculated. After the spectra from each ROI are exported, a normalized intensity value for each peak or feature was calculated. The normalized intensity values from each individual spectrum were then averaged across all of the representative spectra contained in any given ROI. This seems to provide

a better representation and relative quantitation used for the classification. Indeed the normalized intensity values were very consistent for benign and PCa tissue areas in both frozen and UMFix processed tissue. Clearly better methods of quantitation and feature selection are needed to improve the performance of different algorithms for their application in MALDI-IMS experimental data sets. In reality, a sophisticated classification system based on the use of both image and spectral feature selection will probably provide the best classification model for this new technology. New methods capable of combining different computational modules for processing histology images have been developed recently [239]. A combination of these methods with other classification algorithms should improve our results. Other classification algorithms which have been used for MS data include Linear Discrimination Analysis (LDA), Support Vector Machine (SVM), Classification and Regression Trees, Random Forest, and Neural Networks [240]. Ultimately, each classification model may need to be evaluated as to its applicability to MALDI-IMS data and a consensus classification could be determined by combining two or more methods. The MALDI-IMS data generated in future planned studies will provide the basis for adapting these new methods and optimization of existing classification algorithms.

# CHAPTER VI

# CONCLUSIONS AND FUTURE DIRECTIONS

## 6.1 AIM 1: The application of MALDI-IMS to prostate cancer diagnosis and prognosis.

A. Our optimization of MALDI-IMS techniques determined that the use of an automated spraying device for matrix coating of tissue sections is far superior to hand spraying for reproducibility and consistency across multiple samples. Additionally, our results show that UMFix processed tissue is compatible with MALDI-IMS in that both the spectral qualities and images produced were comparable to those obtained from frozen tissue specimens.

B. MALDI-IMS analysis of the study cohort of a total of 36 PCa and 61 benign tissue sections derived from 59 patients resulted in the discovery of a protein expression profile which discriminated PCa from uninvolved prostate tissue. The visual representation of expressed discriminatory peaks resulted in images in which distinct areas of PCa could be identified. A genetic algorithm was developed using 5 m/z values (3443, 3442, 4030, 4275, 4355) which could correctly classify 90.3% of the PCa containing regions, and 64.1% of the benign regions. The most differentially expressed peak (m/z 4355: $p = 2.76 \times 10^{-16}$) highly expressed in PCa tissue areas, was found to be discriminatory on its own, with a normalized intensity value 2.5 fold above benign tissue expression. In a ROC analysis, the optimal cutoff point for using the *m/z* 4355 peak as a biomarker for PCa in tissue sections was a normalized average intensity value of 27. This cutoff point was associated with a sensitivity of 75.0% and a specificity of 74.3% (AUC 0.834). It was

also determined that tissue areas exhibiting distinct *m/z* 4355 expression also have infiltrating lymphocytes surrounding cancerous glands as well as in areas designated as proliferative inflammatory atrophy or cystic atrophy.

C. The examination of tissue derived from patients harboring micrometastatic disease (n=12 *case*) resulted in the discovery of a unique expression profile differing from matched PCa tissue harvested from patients with similar risk factors (n=7 *control*). We developed a classification algorithm using 6 differentially expressed peaks (*m/z* 3374, 3751, 3817, 4030, 5364, and 5664) which was able to correctly classify the *case* PCa tissues from benign at a rate of 83%. However, the algorithm's ability to correctly classify tissue samples from patients without extra-prostatic spread (*control*) was only 58%.

## 6.2  Future Directions of Aim I

In Aim 1 we successfully optimized and refined MALDI-IMS methods, bringing this technology one step closer to clinical utility. The use of UMFix for tissue fixation allows the same tissue sample to be used for both patho-histological determination as well as MALDI-IMS analysis. Our results have shown that UMFix is compatible with MALDI-IMS analysis, and one aspect of future studies will focus on the long term storage effects on tissue in this fixative and subsequent MALDI-IMS data quality.

The identification of a specific protein expression pattern for PCa tissue areas resulted in images which closely match regions of interest circled by a pathologist. Any new technology will only be useful to patient care if it is adopted by clinicians. In order

for MALDI-IMS to be clinically useful it must contribute to the ability of pathologists and surgeons to make accurate diagnosis and prognosis. Since pathologists are familiar with the use of images to make diagnosis, the use of molecular images should translate readily to this end. The greatest utility of tissue assessed biomarkers is restricted to decisions made in pathology using biopsy or surgical material.

In the collection of biopsy specimens for an initial diagnosis of prostate cancer, sampling variables often play a part. Sampling variables result mainly from the lack of accurate imaging techniques to identify and sample specific lesions. Thus, while ultrasound guidance allows for systematic sampling of the prostate, small tumors can be missed, especially in large hypertrophic prostates. Once sampled, each core is completely embedded in paraffin, however, the detection rate is affected by analytical variables such as the number of cores embedded in each block [241] and the number of sections prepared from each block. The blocks are not serially and completely sectioned to exhaustion, and thus some tissue remains unexamined in the paraffin blocks. In addition, differing thresholds for atypical lesions, assessment of Gleason score, and diagnosis of small cancers are also sources of analytical variability. Second-opinion reviews suggest that reclassification of a malignant to benign lesion occurs in 1-2% of cases and in up to 10% of cases a change in Gleason score affecting clinical decision making may occur [242, 243]. The use of MALDI-IMS may aid the pathologist in these cases. To that end, we have begun using UMFix to process prostate biopsy specimens in close collaboration with the pathology group at Sentara Norfolk General Hospital. The future MALDI-IMS analysis of these tissues will enable us to determine if both the

expression profile and normalized intensity of *m/z* 4355 will be useful clinically for the diagnosis of PCa.

The most helpful utility of this technology could be in the assessment of biopsy specimens for the prognosis of metastatic disease. Radical prostatectomy when performed on individuals with metastatic disease is contraindicated due to the over-riding need for systemic therapy. Removal of the primary tumor has no clear accepted advantage for survival following the indication of extracapsular metastatic disease, and can result in potentially adverse surgical complications [75]. Typically, individuals suffer from impotence, incontinence and urinary obstruction to varying degrees of severity. Thus, if metastatic disease were to be identified, radical prostatectomy would not be performed. Our future studies will include a larger cohort of metastatic patients and the examination of biopsy specimens from patients who later develop metastatic disease. These types of tissue will be invaluable for the determination of a specific prognostic protein expression profile determined at the time of biopsy, or after prostatectomy.

It is clear from our study that better methods of data analysis are needed for the interpretation and processing of MALDI-IMS data. The exportation of spectra from regions of interest defined for each tissue examined requires thousands of spectra to be imported into other programs for analysis. The software package available to us (ClinProt tools) was inadequate in that each analysis (peak finding and algorithm generation) took up to 48 hours of computer run-time. Additionally, the handling of such data needs to be refined in such a way that each ROI is treated as a group and not individual spectra. The use of genetic algorithms for the classification of our data yielded high sensitivity, but

low specificity in both PCa vs. Benign, as well as metastatic case vs. control. Clearly better models are needed. We are currently consulting with computer analysis specialists in the development of improved software packages for data handling and model generation in MALDI-IMS.

## 6.3 AIM 2: Sequence identification and characterization of potential biomarkers for clinical diagnostics.

A. The identification of the most discriminatory ion overexpressed in PCa tissues has enabled us to further characterize the molecular landscape of prostate tumors. This ion peak ($m/z$ 4355) was identified as a fragment of MEKK2. This identification was achieved using a WCX fractioned bulk tissue lysate. After confirmation of the spectral patterns in PCa vs. benign lysates, the $m/z$ 4355 ion was sequenced using high mass LIFT MS/MS.

B. The use of trypsin digestion directly on tissue sections confirmed the presence of MEKK2 specific peptides in PCa tissue. These peptides were not detected from benign tissue or control PCa tissue without trypsin treatment. In addition, "in situ" trypsin digestion also enabled the sequence identification of several other molecules present in both benign and tumor tissue. Most of the molecules identified were high abundant proteins, however two molecules sequenced (transgelin and prokineticin-1) are less abundant proteins and indicate that this method could be useful in the sequence identification of disease relates proteins or peptides directly from tissue sections.

C. The high expression of MEKK2 was confirmed in PCa tissues via immunohistochemistry and Western blot. Staining was confined to epithelial cells and was primarily cytoplasmic. Western blot analysis revealed MEKK2 full length expression (70KDa) in three prostate cancer cell lines and higher expression was detected in PCa bulk tissue lysates when compared to benign. The expression level was calculated to be greater than 4 fold higher in cancer tissues relative to benign tissues.

D. To determine the possible activation of the ERK5 pathway in prostate tissue, we investigated the expression levels of the downstream partner of MEKK2, MEK5. Immunohistochemical staining revealed concordant expression of MEK5 and MEKK2, although the level of expression of the two molecules varied with Gleason grade. MEK5 expression levels appeared to increase with increasing Gleason score. Conversely, MEKK2 expression levels were higher in well to moderately differentiated tumors and lower in high grade tumors.

## 6.4 Future Directions of Aim 2

The main accomplishment of this Aim was the sequence identification of the *m/z* 4355 peak as a fragment of MEKK2. This was significant due to the fact that ions above 4000 Da are usually very difficult to sequence using the LIFT MS/MS technology. In the future we hope to further optimize high mass LIFT to enable the identification of molecules in the range of 4000-6000 Da. Molecules of this size are not readily separated by SDS-PAGE and will therefore need to be sequenced using tandem MS. We hope to sequence identify other proteins/peptides found to be differentially expressed in PCa

tissues. A major focus will be the identification of ions found to be significant in primary PCa samples from patients harboring micro-metastatic disease. These molecules should help us determine the molecular pathways activated in more aggressive tumor types.

To further determine the clinical significance of MEKK2 expression, a larger cohort of samples will be used to examine MEKK2 expression in tissues using IHC. We have a large bank of formalin-fixed prostate tissues representing all stages and grades. To this end, since MEKK2 immunostaining of fixed tissues produced high background in our hands, the conditions will need to be optimized. The analysis of archived samples with complete pathology and outcome will allow us to pinpoint which type of tissues and cells overexpress MEKK2 and provide additional clues as to its role in PCa development and progression. This information will also help with the validation of MEKK2 as a biomarker for PCa using MALDI-IMS. Other future projects will address the mechanistic basis for the formation of the MEKK2 fragment in prostate cancer cells. Since the antibody used in our study recognizes the N-terminal portion of MEKK2 (where the PB-1 domain is located), it should also bind the fragment we detected. At least two other antibodies to MEKK2 are available commercially which recognize epitopes in the C-terminus. Immunohistochemical staining using these antibodies will help us to determine if our fragment or the whole protein can be used as a biomarker.

Additional future studies will examine the role of MEKK2 activation with respect to ERK5 activity and tumor progression. We were unsuccessful in performing Western blot analysis for ERK5 and MEK5. Therefore, we will evaluate different antibodies for these experiments. Future investigations into MEKK2 will also be performed at the transcript level. Using RT-PCR of microdissected prostate cells, we will determine the

level of MEKK2, MEK5 and ERK5 mRNA in these cell lysates. Finally, the role of MEKK2 in PCa will be examined in different prostate cancer cell lines with varying degrees of aggressiveness. Recently, MEKK2 containing plasmids and siRNA have been made available commercially. Using these tools, we hope to examine the effect of both MEKK2 over-expression as well as knockdown in prostate cancer cell lines or other appropriate cell systems.

The identification of proteins directly from tissue sections is a major hurdle in the area of MALDI-IMS. Our discovery of transgelin and prokineticin-1 in prostate tissues is compelling. However, these identifications will need to be confirmed and the expression levels in each tissue will need to be determined. In the future we hope to use the direct application of trypsin to profile peptides in tissue (reflectron mode MALDI) in a similar fashion to protein profiling (linear mode MALDI). This will enable us to visualize peptides from higher molecular weight proteins and hopefully detect more differentially expressed molecules. We are currently experimenting with different methods to deposit trypsin on tissue. The manual spotting method will not provide adequate reproducibility and therefore spraying trypsin on tissue before the spray coating of matrix will be performed. Several recent studies have examined the use of trypsin digestion and MALDI-IMS of formalin fixed paraffin embedded tissues (FFPE) [149, 244]. This method usually involves a procedure of heat induced antigen retrieval in presence of EDTA followed by on target trypsin hydrolysis [168]. Using our large tissue bank of FFPE tissues for MALDI peptide profiling should aid in the discovery of new biomarkers for PCa.

Most patients with metastatic PCa initially respond to androgen ablation therapy. However, the cancer often recurs as an androgen-independent tumor which is difficult to treat [41]. Thus, the progression from androgen-dependence to androgen independence is a critical step in the development of prostate cancer, yet the molecular mechanisms for this conversion are poorly understood. MAPK signaling pathways have been shown to regulate steroid receptor activation and localization through receptor phosphorylation [245]. Using tissue from patients with both AR dependent and AR independent tumors we hope to examine the expression levels of MEKK2 and its downstream partners.

TArgeted multiplex MS IMaging (TAMSIM) [246] is a new method which combines IHC and MALD-IMS for imaging multiple candidate antigens simultaneously. The TAMSIM strategy is based on the indirect detection of a probe via a reporter group or "Tag-Mass" indicator that is a small molecule of known mass which is easily detectable using MALDI-MS. This method has been applied in obtaining specific images of proteins using tagged secondary antibodies [247]. Recent improvements to this strategy have tagged primary antibodies with second generation photocleavable tags which are more stable and act as their own matrix [248]. Tagged antibodies specifically bind to their target protein in the tissue with sensitivity in the fmole range. The tag is cleaved from the antibody, desorbed with a laser pulse, and sized by MALDI-MS. This method permits specific analysis of proteins of high or low molecular weight in tissue sections and the images created by TAMSIM have shown good correlation with classical IHC. Any antigen for which a suitable antibody exists can potentially be studied and multiple antigens can be imaged simultaneously. Our future studies will use this strategy for the detection and quantitation of MEKK2 in prostate tissues.

## 6.5 AIM 3: Evaluation of the clinical utility of MALDI-IMS biomarkers

A. The validation of the biomarkers discovered in Aim 1 was partially successful. Using a genetic algorithm designed with 6 of the most discriminating $m/z$ values, the correct classification of frozen PCa tissues was 90%, but only 15.8 % of the normal tissues were classified as benign. This was also the case for UMFixed tissues in which 100% of the blinded PCa samples were correctly classified, but only 25% of the benign samples were classified correctly. The classification of blinded samples was much more successful when using the normalized intensity cut-off value, derived from the ROC analysis, for the $m/z$ 4355 peak (MEKK2). For the frozen tissue specimens, 80% of PCA tissues and 84.2% of benign tissues were classified correctly. All of the UMFix processed tissue samples (4 PCa and 4 benign) were classified correctly using the normalized intensity cut-off.

## 6.6 Future Directions of Aim 3

Our validation of the biomarkers discovered in Aim 1 and sequenced in Aim2 was performed on a small cohort of samples collected at EVMS. We will abandon the use of a genetic algorithm and use other classification methods as well as the normalized intensity for the $m/z$ ion at 4355. Future studies will evaluate MEKK2 (as detected using MALDI-IMS) using a larger cohort (at least 100 from each disease group) of tissues collected from other institutions as well as other organ sites. These studies will help us determine if there is sufficient evidence for potential clinical utility of our biomarker(s) to warrant further investment in true clinical validation study using hundreds or even thousands of samples.

If the images produced from MALDI-IMS do not provide enough detail or cannot be adequately quantitated in a much larger data set, it may ultimately be necessary to move to IHC for clinical validation. Once other candidate *m/z* values are sequence identified, a panel of markers could be used for classification via MALDI-IMS or IHC. Multicolor images of tissue sections depicting the expression of multiple biomarkers can then be used diagnostically.

Finally, we will determine if any of the biomarkers discovered and validated in tissue samples make their way into proximal fluids of serum. Our laboratory is currently using expressed prostatic secretions (EPS) for the discovery of new biomarkers. EPS is obtained by prostate massage, which can be performed during a digital rectal examination or before radical prostatectomy [249]. We will examine the MALDI spectra obtained from EPS for *m/z* peaks which match those obtained from MALDI-IMS. Sequence identification of these peaks will determine if the same or similar proteins can be detected in this proximal fluid allowing for a less invasive screening procedure.

## 6.7 Concluding Remarks

The goal of proteomic analysis of tissue samples is to determine the overall set of proteins that are important in normal cellular physiology or altered by a disease process. There are two basic questions in the field of tissue proteomic studies: (1) can proteomic alternations in cancer cells be reliably measured in tissue? and (2) do the derived proteomic signatures correlate with biological state, clinical behavior, or therapeutic

response? Using MALDI-IMS we have successfully answered both of these questions. Our analysis detected discriminating protein expression differences in PCa tissue as compared to benign tissue. The work reported here represents the first stage in the proteomic analysis prostate cancer, revealing a specific aberration in a MAP kinase cascade. This can be viewed as a small step toward the translation of proteomics into the realm of clinical diagnostics.

Changes in components of critical signaling cascades produce a diversity of disease states, depending on the specific tissues in which they are disrupted. Moreover, changes in different components may ultimately lead to common clinical manifestations reflecting a final common pathway to disease. Once identified and their role in disease defined, the ability to disrupt a specific signaling function and, thereby, interrupt the molecular mechanisms underlying pathology becomes a primary focus for individualized disease management. This practice is already in use today in the treatment of some tumors. For example, MAPK kinase targeted therapy is the focus of cancer drugs such as Gleevec (Imatinib), and Iressa [250]. Molecular profiling (genetic and proteomic) may someday augment and customize a histological diagnosis with the equivalent of a circuit diagram of altered genes and protein signaling pathways for a patient's tumor. This functional map of a patient's tumor cells will then become the starting point for individualized molecular therapy. In the same fashion, proteomic analysis could also be used to monitor the individual's response to that therapy. In oncology, there are many proofs of principle for personalized medicine, and many more are emerging. Although much of its promise remains unproven to date, the foundations of personalized medicine

appear solid and evidence is accumulating rapidly pointing to its growing importance in

clinical care.

# REFERENCES

1. Finn, W.G., *Diagnostic pathology and laboratory medicine in the age of "omics": a paper from the 2006 William Beaumont Hospital Symposium on Molecular Pathology.* Journal of Molecular Diagnostics, 2007. **9**(4): p. 431-6.

2. Allemani, C., et al., *Prognostic value of morphology and hormone receptor status in breast cancer - a population-based study.* British Journal of Cancer, 2004. **91**(7): p. 1263-8.

3. Hadjisavvas, A., et al., *Correlation between morphology, immunohistochemistry and molecular pathology in hereditary and sporadic breast cancer cases.* Ultrastructural Pathology, 2002. **26**(4): p. 237-44.

4. Loberg, R.D., et al., *The lethal phenotype of cancer: the molecular basis of death due to malignancy.* CA Cancer J Clin, 2007. **57**(4): p. 225-41.

5. Gofrit, O.N., et al., *Predicting the risk of patients with biopsy Gleason score 6 to harbor a higher grade cancer.* Journal of Urology, 2007. **178**(5): p. 1925-8.

6. Slaughter, D.P., H.W. Southwick, and W. Smejkal, *Field cancerization in oral stratified squamous epithelium; clinical implications of multicentric origin.* Cancer, 1953. **6**(5): p. 963-8.

7. Schneider, S., et al., *[Molecular genetic markers for prostate cancer. Evidence in fine needle biopsies for improved confirmation of the diagnosis].* Urologe A, 2008. **47**(9): p. 1208-11.

8. Larson, P.S., et al., *Loss of heterozygosity or allele imbalance in histologically normal breast epithelium is distinct from loss of heterozygosity or allele imbalance in co-existing carcinomas.* Am J Pathol, 2002. **161**(1): p. 283-90.

9. Tuxhorn, J.A., et al., *Reactive stroma in human prostate cancer: induction of myofibroblast phenotype and extracellular matrix remodeling.* Clin Cancer Res, 2002. **8**(9): p. 2912-23.

10. Tuxhorn, J.A., G.E. Ayala, and D.R. Rowley, *Reactive stroma in prostate cancer progression.* Journal of Urology, 2001. **166**(6): p. 2472-83.

11. Elenbaas, B. and R.A. Weinberg, *Heterotypic signaling between epithelial tumor cells and fibroblasts in carcinoma formation.* Experimental Cell Research, 2001. **264**(1): p. 169-84.

12. Tlsty, T.D. and L.M. Coussens, *Tumor stroma and regulation of cancer development.* Annu Rev Pathol, 2006. **1**: p. 119-50.

13. Mueller, M.M. and N.E. Fusenig, *Friends or foes - bipolar effects of the tumour stroma in cancer.* Nat Rev Cancer, 2004. **4**(11): p. 839-49.

14. Tuxhorn, J.A., et al., *Reactive stroma in human prostate cancer: induction of myofibroblast phenotype and extracellular matrix remodeling.* Clinical Cancer Research, 2002. **8**(9): p. 2912-23.

15. Allinen, M., et al., *Molecular characterization of the tumor microenvironment in breast cancer.* Cancer Cell, 2004. **6**(1): p. 17-32.

16. Folkman, J., P. Hahnfeldt, and L. Hlatky, *Cancer: looking outside the genome.* Nature Reviews Molecular Cell Biology, 2000. **1**(1): p. 76-9.

17. Anderson, L. and J. Seilhamer, *A comparison of selected mRNA and protein abundances in human liver.* Electrophoresis, 1997. **18**(3-4): p. 533-7.

18. Black, D.L., *Mechanisms of alternative pre-messenger RNA splicing.* Annual Review of Biochemistry, 2003. **72**: p. 291-336.

19. Schaub, M. and W. Keller, *RNA editing by adenosine deaminases generates RNA and protein diversity.* Biochimie, 2002. **84**(8): p. 791-803.

20. Krueger, K.E. and S. Srivastava, *Posttranslational protein modifications: current implications for cancer detection, prevention, and therapeutics.* Molecular & Cellular Proteomics, 2006. **5**(10): p. 1799-810.

21. Cho, W.C., *Contribution of oncoproteomics to cancer biomarker discovery.* Molecular Cancer, 2007. **6**: p. 25.

22. Cho, W.C. and C.H. Cheng, *Oncoproteomics: current trends and future perspectives.* Expert Review of Proteomics, 2007. **4**(3): p. 401-10.

23. van 't Veer, L.J., et al., *Gene expression profiling predicts clinical outcome of breast cancer.* Nature, 2002. **415**(6871): p. 530-6.

24. Pritzker, K.P., *Cancer biomarkers: easier said than done.* Clin Chem, 2002. **48**(8): p. 1147-50.

25. Zangar, R.C., et al., *A rational approach for discovering and validating cancer markers in very small samples using mass spectrometry and ELISA microarrays.* Dis Markers, 2004. **20**(3): p. 135-48.

26. Posadas, E.M., et al., *Proteomic analysis for the early detection and rational treatment of cancer--realistic hope?* Ann Oncol, 2005. **16**(1): p. 16-22.

27. Rubin, E., *Essential Pathology.* Lippencott Williams and Wilkins, Philadelphia, 2001.

28. Fournier, G., et al., *[Prostate cancer: Diagnosis and staging].* Ann Urol (Paris), 2004. **38**(5): p. 207-24.

29. Donovan, J.L., et al., *Screening for prostate cancer in the UK. Seems to be creeping in by the back door.[see comment].* BMJ, 2001. **323**(7316): p. 763-4.

30. *Cancer Facts and Figures.* American Cancer Society Atlanta 2005.

31. Kolonel, L.N., D. Altshuler, and B.E. Henderson, *The multiethnic cohort study: exploring genes, lifestyle and cancer risk.* Nature Reviews. Cancer, 2004. **4**(7): p. 519-27.

32. Jones, R.A., S.M. Underwood, and B.M. Rivers, *Reducing prostate cancer morbidity and mortality in African American men: issues and challenges.* Clinical Journal of Oncology Nursing, 2007. **11**(6): p. 865-72.

33. Powell, I.J., *Epidemiology and pathophysiology of prostate cancer in African-American men.* Journal of Urology, 2007. **177**(2): p. 444-9.

34. Wallace, T.A., et al., *Tumor immunobiological differences in prostate cancer between African-American and European-American men.* Cancer Research, 2008. **68**(3): p. 927-36.

35. Gronberg, H., et al., *Cancer risk in families with hereditary prostate carcinoma.* Cancer, 2000. **89**(6): p. 1315-21.

36. Nelson, W.G., et al., *The role of inflammation in the pathogenesis of prostate cancer.* Journal of Urology, 2004. **172**(5 Pt 2): p. S6-11; discussion S11-2.

37. Whittemore, A.S., et al., *Prostate cancer in relation to diet, physical activity, and body size in blacks, whites, and Asians in the United States and Canada.[see comment].* Journal of the National Cancer Institute, 1995. **87**(9): p. 652-61.

38.   Chan, J.M., P.H. Gann, and E.L. Giovannucci, *Role of diet in prostate cancer development and progression.* Journal of Clinical Oncology, 2005. **23**(32): p. 8152-60.

39.   Platz, E.A., S.K. Clinton, and E. Giovannucci, *Association between plasma cholesterol and prostate cancer in the PSA era.* International Journal of Cancer, 2008. **123**(7): p. 1693-8.

40.   Wu, K., et al., *Dietary patterns and risk of prostate cancer in U.S. men.* Cancer Epidemiology, Biomarkers & Prevention, 2006. **15**(1): p. 167-71.

41.   Heinlein, C.A. and C. Chang, *Androgen receptor in prostate cancer.* Endocrine Reviews, 2004. **25**(2): p. 276-308.

42.   Strief, D.M., *An overview of prostate cancer: diagnosis and treatment.* Urologic Nursing, 2007. **27**(6): p. 475-9; quiz 480.

43.   Haas, G.P. and W.A. Sakr, *Epidemiology of prostate cancer.* CA: a Cancer Journal for Clinicians, 1997. **47**(5): p. 273-87.

44.   Puppo, P., et al., *Role of transurethral resection of the prostate and biopsy of the peripheral zone in the same session after repeated negative biopsies in the diagnosis of prostate cancer.* Eur Urol, 2006. **49**(5): p. 873-8.

45.   Bostwick, D.G., A. Pacelli, and A. Lopez-Beltran, *Molecular biology of prostatic intraepithelial neoplasia.* Prostate, 1996. **29**(2): p. 117-34.

46.   Bostwick, D.G. and J. Qian, *High-grade prostatic intraepithelial neoplasia.* Modern Pathology, 2004. **17**(3): p. 360-79.

47.   Qian, J., P. Wollan, and D.G. Bostwick, *The extent and multicentricity of high-grade prostatic intraepithelial neoplasia in clinically localized prostatic adenocarcinoma.* Human Pathology, 1997. **28**(2): p. 143-8.

48.   Schlesinger, C., D.G. Bostwick, and K.A. Iczkowski, *High-grade prostatic intraepithelial neoplasia and atypical small acinar proliferation: predictive value for cancer in current practice. [erratum appears in Am J Surg Pathol. 2005 Nov;29(11):1548].* American Journal of Surgical Pathology, 2005. **29**(9): p. 1201-7.

49.   De Marzo, A.M., et al., *Proliferative inflammatory atrophy of the prostate: implications for prostatic carcinogenesis.* American Journal of Pathology, 1999. **155**(6): p. 1985-92.

50.   Gonzalgo, M.L. and W.B. Isaacs, *Molecular pathways to prostate cancer.* Journal of Urology, 2003. **170**(6 Pt 1): p. 2444-52.

51.   Lucia, M.S. and K.C. Torkko, *Inflammation as a target for prostate cancer chemoprevention: pathological and laboratory rationale. [see comment].* Journal of Urology, 2004. **171**(2 Pt 2): p. S30-4; discussion S35.

52.   Polascik, T.J., J.E. Oesterling, and A.W. Partin, *Prostate specific antigen: a decade of discovery--what we have learned and where we are going. [see comment].* Journal of Urology, 1999. **162**(2): p. 293-306.

53.   Thompson, I.M., et al., *Prevalence of prostate cancer among men with a prostate-specific antigen level < or =4.0 ng per milliliter. [see comment][erratum appears in N Engl J Med. 2004 Sep 30;351(14):1470].* New England Journal of Medicine, 2004. **350**(22): p. 2239-46.

54.     Selley, S., et al., *Diagnosis, management and screening of early localised prostate cancer.* Health Technology Assessment (Winchester, England), 1997. **1**(2): p. i.

55.     Davis, M., et al., *The procedure of transrectal ultrasound guided biopsy of the prostate: a survey of patient preparation and biopsy technique.* Journal of Urology, 2002. **167**(2 Pt 1): p. 566-70.

56.     Egevad, L., et al., *Prognostic value of the Gleason score in prostate cancer.* BJU International, 2002. **89**(6): p. 538-42.

57.     Pinthus, J.H., et al., *Prostate cancers scored as Gleason 6 on prostate biopsy are frequently Gleason 7 tumors at radical prostatectomy: implication on outcome.* Journal of Urology, 2006. **176**(3): p. 979-84; discussion 984.

58.     Ross, J.S., et al., *Morphologic and molecular prognostic markers in prostate cancer.* Advances in Anatomic Pathology, 2002. **9**(2): p. 115-28.

59.     Sun, H., et al., *PTEN modulates cell cycle progression and cell survival by regulating phosphatidylinositol 3,4,5,-trisphosphate and Akt/protein kinase B signaling pathway.* Proceedings of the National Academy of Sciences of the United States of America, 1999. **96**(11): p. 6199-204.

60.     Mulholland, D.J., J. Jiao, and H. Wu, *Hormone refractory prostate cancer: Lessons learned from the PTEN prostate cancer model.* Adv Exp Med Biol, 2008. **617**: p. 87-95.

61.     Sharrocks, A.D., *The ETS-domain transcription factor family.* Nature Reviews Molecular Cell Biology, 2001. **2**(11): p. 827-37.

62.     Mehra, R., et al., *Comprehensive assessment of TMPRSS2 and ETS family gene aberrations in clinically localized prostate cancer.* Modern Pathology, 2007. **20**(5): p. 538-44.

63.     Tomlins, S.A., et al., *Recurrent fusion of TMPRSS2 and ETS transcription factor genes in prostate cancer.[see comment].* Science, 2005. **310**(5748): p. 644-8.

64.     Lin, B., et al., *Prostate-localized and androgen-regulated expression of the membrane-bound serine protease TMPRSS2.* Cancer Research, 1999. **59**(17): p. 4180-4.

65.     Perner, S. and M.A. Rubin, *A variant TMPRSS2 isoform and ERG fusion product in prostate cancer with implications for molecular diagnosis.* Mod Pathol, 2008. **21**(8): p. 1056; author reply 1056-7.

66.     Perner, S., et al., *TMPRSS2-ERG fusion prostate cancer: an early molecular event associated with invasion.* American Journal of Surgical Pathology, 2007. **31**(6): p. 882-8.

67.     Perner, S., et al., *TMPRSS2-ERG fusion prostate cancer: an early molecular event associated with invasion.[see comment].* American Journal of Surgical Pathology, 2007. **31**(6): p. 882-8.

68.     Mosquera, J.M., et al., *Morphological features of TMPRSS2-ERG gene fusion prostate cancer.* Journal of Pathology, 2007. **212**(1): p. 91-101.

69.     Lakhani, S.R., et al., *The pathology of familial breast cancer: histological features of cancers in families not attributable to mutations in BRCA1 or BRCA2.* Clinical Cancer Research, 2000. **6**(3): p. 782-9.

70. Alexander, J., et al., *Histopathological identification of colon cancer with microsatellite instability.* American Journal of Pathology, 2001. **158**(2): p. 527-35.

71. Braeckman, J. and D. Michielsen, *Prognostic factors in prostate cancer.* Recent Results in Cancer Research, 2007. **175**: p. 25-32.

72. Bantis, A., et al., *Prognostic value of DNA analysis of prostate adenocarcinoma: correlation to clinicopathologic predictors.* Journal of Experimental & Clinical Cancer Research, 2005. **24**(2): p. 273-8.

73. Mazzucchelli, R., et al., *Vascular endothelial growth factor expression and capillary architecture in high-grade PIN and prostate cancer in untreated and androgen-ablated patients.* Prostate, 2000. **45**(1): p. 72-9.

74. Pelzer, A.E., *Words of wisdom. Re: under diagnosis and over diagnosis of prostate cancer.* Eur Urol, 2008. **54**(1): p. 234-5.

75. Afrin, L.B. and S.M. Ergul, *Medical therapy of prostate cancer: 1999.* Journal - South Carolina Medical Association, 2000. **96**(2): p. 77-84.

76. Mitchell, R.E. and S.S. Chang, *Current controversies in the treatment of high-risk prostate cancer.* Current Opinion in Urology, 2008. **18**(3): p. 263-8.

77. Stenman, U.H., et al., *Prostate-specific antigen.* Seminars in Cancer Biology, 1999. **9**(2): p. 83-93.

78. Hara, M., et al., *[Some physico-chemical characteristics of " -seminoprotein", an antigenic component specific for human seminal plasma. Forensic immunological study of body fluids and secretion. VII].* Nihon Hoigaku Zasshi - Japanese Journal of Legal Medicine, 1971. **25**(4): p. 322-4.

79. Koyanagi, Y., et al., *[Isolation of antigenic component specific for human seminal plasma " -seminoprotein ( -Sm)" by electrofocusing. Forensic immunological study of body fluids and secretions. 8].* Nihon Hoigaku Zasshi - Japanese Journal of Legal Medicine, 1972. **26**(2): p. 78-80.

80. Kuriyama, M., et al., *Use of human prostate-specific antigen in monitoring prostate cancer.* Cancer Research, 1981. **41**(10): p. 3874-6.

81. Catalona, W.J., et al., *Detection of organ-confined prostate cancer is increased through prostate-specific antigen-based screening.[see comment].* JAMA, 1993. **270**(8): p. 948-54.

82. Sardana, G., B. Dowell, and E.P. Diamandis, *Emerging biomarkers for the diagnosis and prognosis of prostate cancer.* Clin Chem, 2008. **54**(12): p. 1951-60.

83. Fradet, Y., et al., *uPM3, a new molecular urine test for the detection of prostate cancer.* Urology, 2004. **64**(2): p. 311-5; discussion 315-6.

84. Roth, T.J., et al., *B7-H3 ligand expression by prostate cancer: a novel marker of prognosis and potential target for therapy.* Cancer Res, 2007. **67**(16): p. 7893-900.

85. Evans, A.J., *Alpha-methylacyl CoA racemase (P504S): overview and potential uses in diagnostic pathology as applied to prostate needle biopsies.* J Clin Pathol, 2003. **56**(12): p. 892-7.

86. Ahram, M. and M.R. Emmert-Buck, *Approaches to proteomic analysis of human tumors.* Methods in Molecular Biology, 2003. **222**: p. 375-84.

87. van der Merwe, D.E., et al., *Mass spectrometry: uncovering the cancer proteome for diagnostics.* Adv Cancer Res, 2007. **96**: p. 23-50.

88.    Calvo, K.R., L.A. Liotta, and E.F. Petricoin, *Clinical proteomics: from biomarker discovery and cell signaling profiles to individualized personal therapy.* Biosci Rep, 2005. **25**(1-2): p. 107-25.

89.    Chung, C.H., et al., *Genomics and proteomics: emerging technologies in clinical cancer research.* Critical Reviews in Oncology-Hematology, 2007. **61**(1): p. 1-25.

90.    Rowen, L., G. Mahairas, and L. Hood, *Sequencing the human genome.* Science, 1997. **278**(5338): p. 605-7.

91.    Fenn, J.B., et al., *Electrospray ionization for mass spectrometry of large biomolecules.* Science, 1989. **246**(4926): p. 64-71.

92.    Hillenkamp, F. and M. Karas, *Mass spectrometry of peptides and proteins by matrix-assisted ultraviolet laser desorption/ionization.* Methods Enzymol, 1990. **193**: p. 280-95.

93.    Ashcroft, A.E., *Protein and peptide identification: the role of mass spectrometry in proteomics.* Nat Prod Rep, 2003. **20**(2): p. 202-15.

94.    Kolker, E., R. Higdon, and J.M. Hogan, *Protein identification and expression analysis using mass spectrometry.* Trends Microbiol, 2006. **14**(5): p. 229-35.

95.    Salzano, A.M. and M. Crescenzi, *Mass spectrometry for protein identification and the study of post translational modifications.* Ann Ist Super Sanita, 2005. **41**(4): p. 443-50.

96.    Sharon, M. and C.V. Robinson, *The Role of Mass Spectrometry in Structure Elucidation of Dynamic Protein Complexes.* Annu Rev Biochem, 2007.

97.    Karas, M. and F. Hillenkamp, *Laser desorption ionization of proteins with molecular masses exceeding 10,000 daltons.* Analytical Chemistry, 1988. **60**(20): p. 2299-301.

98.    Tanaka, K., Waki, H., Ido, Y., Akita, S., Yoshida, Y., Yoshida, T., *Protein and Polymer Analyses up to m/z 100 000 by Laser Ionization Time-of-Flight Mass Spectrometry.* Rapid Commun. Mass Spectrom. , 1988. **Vol.2** (No.8): p. 151–153.

99.    Ingelsson, E., et al., *Multimarker approach to evaluate the incidence of the metabolic syndrome and longitudinal changes in metabolic risk factors: the Framingham Offspring Study.* Circulation, 2007. **116**(9): p. 984-92.

100.   Lewis, J.K., Wei, Jing, Suizdak, Gary, *Matrix-assisted Laser Desorption/Ionization Mass Spectrometry in Peptide and Protein Analysis.* Encyclopedia of Analytical Chemistry, 2000. **R.A. Meyers (Ed.)**: p. pp. 5880–5894.

101.   Bahr, U., et al., *Delayed extraction time-of-flight MALDI mass spectrometry of proteins above 25,000 Da.* J Mass Spectrom, 1997. **32**(10): p. 1111-6.

102.   Roepstorff, P., *MALDI-TOF mass spectrometry in protein chemistry.* EXS, 2000. **88**: p. 81-97.

103.   Cohen, S.L. and B.T. Chait, *Influence of matrix solution conditions on the MALDI-MS analysis of peptides and proteins.* Analytical Chemistry, 1996. **68**(1): p. 31-7.

104.   Kussmann, M. and P. Roepstorff, *Sample preparation techniques for peptides and proteins analyzed by MALDI-MS.* Methods in Molecular Biology, 2000. **146**: p. 405-24.

105. Medzihradszky, K.F., et al., *The characteristics of peptide collision-induced dissociation using a high-performance MALDI-TOF/TOF tandem mass spectrometer.* Analytical Chemistry, 2000. **72**(3): p. 552-8.

106. Bienvenut, W.V., et al., *Matrix-assisted laser desorption/ionization-tandem mass spectrometry with high resolution and sensitivity for identification and characterization of proteins.* Proteomics, 2002. **2**(7): p. 868-76.

107. Keough, T., et al., *Tandem mass spectrometry methods for definitive protein identification in proteomics research.* Electrophoresis, 2000. **21**(11): p. 2252-65.

108. Suckau, D., et al., *A novel MALDI LIFT-TOF/TOF mass spectrometer for proteomics.* Anal Bioanal Chem, 2003. **376**(7): p. 952-65.

109. Kebarle, P., *A brief overview of the present status of the mechanisms involved in electrospray mass spectrometry.* Journal of Mass Spectrometry, 2000. **35**(7): p. 804-17.

110. Griffiths, W.J., et al., *Electrospray and tandem mass spectrometry in biochemistry.* Biochemical Journal, 2001. **355**(Pt 3): p. 545-61.

111. Canas, B., et al., *Mass spectrometry technologies for proteomics.* Briefings in Functional Genomics & Proteomics, 2006. **4**(4): p. 295-320.

112. Rodland, K.D., *Proteomics and cancer diagnosis: the potential of mass spectrometry.* Clinical Biochemistry, 2004. **37**(7): p. 579-83.

113. Adam, B.L., et al., *Serum protein fingerprinting coupled with a pattern-matching algorithm distinguishes prostate cancer from benign prostate hyperplasia and healthy men.* Cancer Res, 2002. **62**(13): p. 3609-14.

114. de Noo, M.E., et al., *Detection of colorectal cancer using MALDI-TOF serum protein profiling.* Eur J Cancer, 2006. **42**(8): p. 1068-76.

115. Howard, B.A., et al., *Identification and validation of a potential lung cancer serum biomarker detected by matrix-assisted laser desorption/ionization-time of flight spectra analysis.* Proteomics, 2003. **3**(9): p. 1720-4.

116. Petricoin, E.F., et al., *Use of proteomic patterns in serum to identify ovarian cancer.* Lancet, 2002. **359**(9306): p. 572-7.

117. Semmes, O.J., et al., *Discrete serum protein signatures discriminate between human retrovirus-associated hematologic and neurologic disease.* Leukemia, 2005. **19**(7): p. 1229-38.

118. Wadsworth, J.T., et al., *Serum protein profiles to identify head and neck cancer.* Clin Cancer Res, 2004. **10**(5): p. 1625-32.

119. Shen, D., et al., *Optimized prostate biopsy via a statistical atlas of cancer spatial distribution.* Med Image Anal, 2004. **8**(2): p. 139-50.

120. McDonald, W.H. and J.R. Yates, 3rd, *Shotgun proteomics and biomarker discovery.* Dis Markers, 2002. **18**(2): p. 99-105.

121. Aebersold, R. and M. Mann, *Mass spectrometry-based proteomics.* Nature, 2003. **422**(6928): p. 198-207.

122. Van den Bergh, G. and L. Arckens, *Fluorescent two-dimensional difference gel electrophoresis unveils the potential of gel-based proteomics.* Current Opinion in Biotechnology, 2004. **15**(1): p. 38-43.

123. Gygi, S.P., et al., *Evaluation of two-dimensional gel electrophoresis-based proteome analysis technology.* Proc Natl Acad Sci U S A, 2000. **97**(17): p. 9390-5.

124.  Klose, J. and U. Kobalz, *Two-dimensional electrophoresis of proteins: an updated protocol and implications for a functional analysis of the genome.* Electrophoresis, 1995. **16**(6): p. 1034-59.

125.  Kunz, G.M., Jr. and D.W. Chan, *The use of laser capture microscopy in proteomics research--a review.* Dis Markers, 2004. **20**(3): p. 155-60.

126.  Bonner, R.F., et al., *Laser capture microdissection: molecular analysis of tissue.* Science, 1997. **278**(5342): p. 1481,1483.

127.  Cazares, L.H., et al., *Normal, benign, preneoplastic, and malignant prostate cells have distinct protein expression profiles resolved by surface enhanced laser desorption/ionization mass spectrometry.* Clin Cancer Res, 2002. **8**(8): p. 2541-52.

128.  Espina, V., et al., *Use of proteomic analysis to monitor responses to biological therapies.* Expert Opin Biol Ther, 2004. **4**(1): p. 83-93.

129.  Xu, B.J., et al., *Direct analysis of laser capture microdissected cells by MALDI mass spectrometry.* J Am Soc Mass Spectrom, 2002. **13**(11): p. 1292-7.

130.  Emmert-Buck, M.R., et al., *An approach to proteomic analysis of human tumors.* Molecular Carcinogenesis, 2000. **27**(3): p. 158-65.

131.  Neverova, I. and J.E. Van Eyk, *Role of chromatographic techniques in proteomic analysis.* Journal of Chromatography B: Analytical Technologies in the Biomedical & Life Sciences, 2005. **815**(1-2): p. 51-63.

132.  Wall, D.B., et al., *Isoelectric focusing nonporous RP HPLC: a two-dimensional liquid-phase separation method for mapping of cellular proteins with identification using MALDI-TOF mass spectrometry.* Analytical Chemistry, 2000. **72**(6): p. 1099-111.

133.  Wolters, D.A., M.P. Washburn, and J.R. Yates, 3rd, *An automated multidimensional protein identification technology for shotgun proteomics.* Anal Chem, 2001. **73**(23): p. 5683-90.

134.  Tomlinson, A.J., et al., *Global proteome analysis of a human gastric carcinoma.* Electrophoresis, 2002. **23**(18): p. 3233-40.

135.  Zhu, H. and M. Snyder, *"Omic" approaches for unraveling signaling networks.* Curr Opin Cell Biol, 2002. **14**(2): p. 173-9.

136.  Templin, M.F., et al., *Protein microarrays: promising tools for proteomic research.* Proteomics, 2003. **3**(11): p. 2155-66.

137.  Haab, B.B., *Methods and applications of antibody microarrays in cancer research.* Proteomics, 2003. **3**(11): p. 2116-22.

138.  Paweletz, C.P., et al., *Reverse phase protein microarrays which capture disease progression show activation of pro-survival pathways at the cancer invasion front.* Oncogene, 2001. **20**(16): p. 1981-9.

139.  Diaz, J.I., et al., *Selective capture of prostatic basal cells and secretory epithelial cells for proteomic and genomic analysis.* Urol Oncol, 2004. **22**(4): p. 329-36.

140.  Guo, J., et al., *Direct analysis of laser capture microdissected endometrial carcinoma and epithelium by matrix-assisted laser desorption/ionization mass spectrometry.* Rapid Commun Mass Spectrom, 2005. **19**(19): p. 2762-6.

141.  Todd, P.J., et al., *Organic ion imaging of biological tissue with secondary ion mass spectrometry and matrix-assisted laser desorption/ionization.* J Mass Spectrom, 2001. **36**(4): p. 355-69.

142. Chaurand, P. and R.M. Caprioli, *Direct profiling and imaging of peptides and proteins from mammalian cells and tissue sections by mass spectrometry.* Electrophoresis, 2002. **23**(18): p. 3125-35.

143. Chaurand, P., M. Stoeckli, and R.M. Caprioli, *Direct profiling of proteins in biological tissue sections by MALDI mass spectrometry.* Anal Chem, 1999. **71**(23): p. 5263-70.

144. Caldwell, R.L. and R.M. Caprioli, *Tissue profiling by mass spectrometry: a review of methodology and applications.* Mol Cell Proteomics, 2005. **4**(4): p. 394-401.

145. Yanagisawa, K., et al., *Proteomic patterns of tumour subsets in non-small-cell lung cancer.* Lancet, 2003. **362**(9382): p. 433-9.

146. Cornett, D.S., et al., *A novel histology-directed strategy for MALDI-MS tissue profiling that improves throughput and cellular specificity in human breast cancer.* Molecular & Cellular Proteomics, 2006. **5**(10): p. 1975-83.

147. Reyzer, M.L., et al., *Early changes in protein expression detected by mass spectrometry predict tumor response to molecular therapeutics.* Cancer Research, 2004. **64**(24): p. 9093-100.

148. Schwartz, S.A., et al., *Proteomic-based prognosis of brain tumor patients using direct-tissue matrix-assisted laser desorption ionization mass spectrometry.* Cancer Res, 2005. **65**(17): p. 7674-81.

149. Lemaire, R., et al., *Direct Analysis and MALDI Imaging of Formalin-Fixed, Paraffin-Embedded Tissue Sections.* J Proteome Res, 2007. **6**(4): p. 1295-1305.

150. Schwamborn, K., et al., *Identifying prostate carcinoma by MALDI-Imaging.* International Journal of Molecular Medicine, 2007. **20**(2): p. 155-9.

151. Shimma, S., et al., *MALDI-based imaging mass spectrometry revealed abnormal distribution of phospholipids in colon cancer liver metastasis.* J Chromatogr B Analyt Technol Biomed Life Sci, 2007.

152. Hsieh, Y., J. Chen, and W.A. Korfmacher, *Mapping pharmaceuticals in tissues using MALDI imaging mass spectrometry.* J Pharmacol Toxicol Methods, 2007. **55**(2): p. 193-200.

153. Reyzer, M.L. and R.M. Caprioli, *MALDI-MS-based imaging of small molecules and proteins in tissues.* Curr Opin Chem Biol, 2007. **11**(1): p. 29-35.

154. Hsieh, Y., et al., *Matrix-assisted laser desorption/ionization imaging mass spectrometry for direct measurement of clozapine in rat brain tissue.* Rapid Commun Mass Spectrom, 2006. **20**(6): p. 965-72.

155. Groseclose, M.R., et al., *Identification of proteins directly from tissue: in situ tryptic digestions coupled with imaging mass spectrometry.* J Mass Spectrom, 2007. **42**(2): p. 254-62.

156. Skrzydlewska, E., et al., *Proteolytic-antiproteolytic balance and its regulation in carcinogenesis.* World Journal of Gastroenterology, 2005. **11**(9): p. 1251-66.

157. Taban, I.M., et al., *Imaging of peptides in the rat brain using MALDI-FTICR mass spectrometry.* J Am Soc Mass Spectrom, 2007. **18**(1): p. 145-51.

158. Cornett, D.S., S.L. Frappier, and R.M. Caprioli, *MALDI-FTICR imaging mass spectrometry of drugs and metabolites in tissue.* Analytical Chemistry, 2008. **80**(14): p. 5648-53.

159. Gupta, D. and L.J. Layfield, *Prevalence of inter-institutional anatomic pathology slide review: a survey of current practice.* Am J Surg Pathol, 2000. **24**(2): p. 280-4.

160. Andrion, A., et al., *Malignant mesothelioma of the pleura: interobserver variability.* J Clin Pathol, 1995. **48**(9): p. 856-60.

161. Ismail, S.M., et al., *Observer variation in histopathological diagnosis and grading of cervical intraepithelial neoplasia.* Bmj, 1989. **298**(6675): p. 707-10.

162. Tabor, M.P., et al., *Persistence of genetically altered fields in head and neck cancer patients: biological and clinical implications.* Clin Cancer Res, 2001. **7**(6): p. 1523-32.

163. Partridge, M., et al., *Detection of minimal residual cancer to investigate why oral tumors recur despite seemingly adequate treatment.* Clin Cancer Res, 2000. **6**(7): p. 2718-25.

164. Braakhuis, B.J., et al., *A genetic explanation of Slaughter's concept of field cancerization: evidence and clinical implications.* Cancer Res, 2003. **63**(8): p. 1727-30.

165. Dakubo, G.D., et al., *Clinical implications and utility of field cancerization.* Cancer Cell Int, 2007. **7**: p. 2.

166. Lemaire, R., et al., *Specific MALDI imaging and profiling for biomarker hunting and validation: fragment of the 11S proteasome activator complex, Reg alpha fragment, is a new potential ovary cancer biomarker.* Journal of Proteome Research, 2007. **6**(11): p. 4127-34.

167. Chaurand, P., et al., *Monitoring mouse prostate development by profiling and imaging mass spectrometry.* Molecular & Cellular Proteomics, 2008. **7**(2): p. 411-23.

168. Ronci, M., et al., *Protein unlocking procedures of formalin-fixed paraffin-embedded tissues: application to MALDI-TOF imaging MS investigations.* Proteomics, 2008. **8**(18): p. 3702-14.

169. Morales, A.R., et al., *Experience with an automated microwave-assisted rapid tissue processing method: validation of histologic quality and impact on the timeliness of diagnostic surgical pathology.* Am J Clin Pathol, 2004. **121**(4): p. 528-36.

170. Vincek, V., et al., *A tissue fixative that protects macromolecules (DNA, RNA, and protein) and histomorphology in clinical samples.* Lab Invest, 2003. **83**(10): p. 1427-35.

171. Nadji, M., et al., *Immunohistochemistry of tissue prepared by a molecular-friendly fixation and processing system.* Appl Immunohistochem Mol Morphol, 2005. **13**(3): p. 277-82.

172. Thompson, J.H. and W.R. Richter, *Hemotoxylin-eosin staining adapted to automatic tissue processing.* Stain Technol, 1960. **35**: p. 145-8.

173. Carson, F., *Histotechnology: A Self-Instructional Text.* ASCP Press, 1997. **2nd Edition Chicago**.

174. Morales, A.R., et al., *Continuous-specimen-flow, high-throughput, 1-hour tissue processing. A system for rapid diagnostic tissue preparation.* Arch Pathol Lab Med, 2002. **126**(5): p. 583-90.

175. Amann, J.M., et al., *Selective profiling of proteins in lung cancer cells from fine-needle aspirates by matrix-assisted laser desorption ionization time-of-flight mass spectrometry.* Clinical Cancer Research, 2006. **12**(17): p. 5142-50.

176. Schneider, J.J., et al., *Human defensins.* Journal of Molecular Medicine, 2005. **83**(8): p. 587-95.

177. Patterson, S.D., *Proteomics: beginning to realize its promise?* Arthritis Rheum, 2004. **50**(12): p. 3741-4.

178. Wright, M.E., D.K. Han, and R. Aebersold, *Mass spectrometry-based expression profiling of clinical prostate cancer.* Mol Cell Proteomics, 2005. **4**(4): p. 545-54.

179. Guerrera, I.C. and O. Kleiner, *Application of mass spectrometry in proteomics.* Biosci Rep, 2005. **25**(1-2): p. 71-93.

180. Westmacott, G., et al., *Investigating ion-surface collisions with a niobium superconducting tunnel junction detector in a time-of-flight mass spectrometer.* Rapid Commun Mass Spectrom, 2000. **14**(7): p. 600-7.

181. Nair, R.R., J. Solway, and D.D. Boyd, *Expression cloning identifies transgelin (SM22) as a novel repressor of 92-kDa type IV collagenase (MMP-9) expression.* J Biol Chem, 2006. **281**(36): p. 26424-36.

182. Yu, H., et al., *Transgelin is a direct target of TGF-beta/Smad3-dependent epithelial cell migration in lung fibrosis.* Faseb J, 2008. **22**(6): p. 1778-89.

183. Lin, D.C., et al., *Identification and molecular characterization of two closely related G protein-coupled receptors activated by prokineticins/endocrine gland vascular endothelial growth factor.* J Biol Chem, 2002. **277**(22): p. 19276-80.

184. Zhou, Q.Y. and R. Meidan, *Biological function of prokineticins.* Results Probl Cell Differ, 2008. **46**: p. 181-99.

185. Fanger, G.R., N.L. Johnson, and G.L. Johnson, *MEK kinases are regulated by EGF and selectively interact with Rac/Cdc42.* EMBO Journal, 1997. **16**(16): p. 4961-72.

186. Raman, M., W. Chen, and M.H. Cobb, *Differential regulation and properties of MAPKs.* Oncogene, 2007. **26**(22): p. 3100-12.

187. Cuevas, B.D., A.N. Abell, and G.L. Johnson, *Role of mitogen-activated protein kinase kinase kinases in signal integration.* Oncogene, 2007. **26**(22): p. 3159-71.

188. Avruch, J., *MAP kinase pathways: the first twenty years.* Biochimica et Biophysica Acta, 2007. **1773**(8): p. 1150-60.

189. Winter-Vann, A.M. and G.L. Johnson, *Integrated activation of MAP3Ks balances cell fate in response to stress.* Journal of Cellular Biochemistry, 2007. **102**(4): p. 848-58.

190. Guo, Z., et al., *Disruption of Mekk2 in mice reveals an unexpected role for MEKK2 in modulating T-cell receptor signal transduction.* Molecular & Cellular Biology, 2002. **22**(16): p. 5761-8.

191. Schaefer, B.C., et al., *Live cell fluorescence imaging of T cell MEKK2: redistribution and activation in response to antigen stimulation of the T cell receptor.* Immunity, 1999. **11**(4): p. 411-21.

192. Su, B., et al., *MEKK2 is required for T-cell receptor signals in JNK activation and interleukin-2 gene expression.* Journal of Biological Chemistry, 2001. **276**(18): p. 14784-90.

193. Kesavan, K., et al., *MEKK2 regulates the coordinate activation of ERK5 and JNK in response to FGF-2 in fibroblasts.* J Cell Physiol, 2004. **199**(1): p. 140-8.

194. Sun, W., et al., *MEK kinase 2 and the adaptor protein Lad regulate extracellular signal-regulated kinase 5 activation by epidermal growth factor via Src.* Molecular & Cellular Biology, 2003. **23**(7): p. 2298-308.

195. Hammaker, D.R., et al., *Regulation of c-Jun N-terminal kinase by MEKK-2 and mitogen-activated protein kinase kinase kinases in rheumatoid arthritis.* Journal of Immunology, 2004. **172**(3): p. 1612-8.

196. Hammaker, D.R., et al., *Regulation of the JNK pathway by TGF-beta activated kinase 1 in rheumatoid arthritis synoviocytes.* Arthritis Research & Therapy, 2007. **9**(3): p. R57.

197. Chayama, K., et al., *Role of MEKK2-MEK5 in the regulation of TNF-alpha gene expression and MEKK2-MKK7 in the activation of c-Jun N-terminal kinase in mast cells.* Proceedings of the National Academy of Sciences of the United States of America, 2001. **98**(8): p. 4599-604.

198. Blank, J.L., et al., *Molecular cloning of mitogen-activated protein/ERK kinase kinases (MEKK) 2 and 3. Regulation of sequential phosphorylation pathways involving mitogen-activated protein kinase and c-Jun kinase.* Journal of Biological Chemistry, 1996. **271**(10): p. 5361-8.

199. Nakamura, K. and G.L. Johnson, *Noncanonical function of MEKK2 and MEK5 PB1 domains for coordinated extracellular signal-regulated kinase 5 and c-Jun N-terminal kinase signaling.* Molecular & Cellular Biology, 2007. **27**(12): p. 4566-77.

200. Nakamura, K., et al., *PB1 domain-dependent signaling complex is required for extracellular signal-regulated kinase 5 activation.* Molecular & Cellular Biology, 2006. **26**(6): p. 2065-79.

201. Uhlik, M.T., et al., *Wiring diagrams of MAPK regulation by MEKK1, 2, and 3.* Biochemistry & Cell Biology, 2004. **82**(6): p. 658-63.

202. Moscat, J., et al., *Cell signaling and function organized by PB1 domain interactions.* Molecular Cell, 2006. **23**(5): p. 631-40.

203. Nakamura, K. and G.L. Johnson, *PB1 domains of MEKK2 and MEKK3 interact with the MEK5 PB1 domain for activation of the ERK5 pathway.* Journal of Biological Chemistry, 2003. **278**(39): p. 36989-92.

204. Lamark, T., et al., *Interaction codes within the family of mammalian Phox and Bem1p domain-containing proteins.* Journal of Biological Chemistry, 2003. **278**(36): p. 34568-81.

205. Wang, X. and C. Tournier, *Regulation of cellular functions by the ERK5 signalling pathway.* Cell Signal, 2006. **18**(6): p. 753-60.

206. Mehta, P.B., et al., *MEK5 overexpression is associated with metastatic prostate cancer, and stimulates proliferation, MMP-9 expression and invasion.* Oncogene, 2003. **22**(9): p. 1381-9.

207. McCracken, S.R., et al., *Aberrant expression of extracellular signal-regulated kinase 5 in human prostate cancer.* Oncogene, 2008. **27**(21): p. 2978-88.

208. Raviv, Z., E. Kalie, and R. Seger, *MEK5 and ERK5 are localized in the nuclei of resting as well as stimulated cells, while MEKK2 translocates from the cytosol to*

*the nucleus upon stimulation.* Journal of Cell Science, 2004. **117**(Pt 9): p. 1773-84.

209. Gortz, B., et al., *Tumour necrosis factor activates the mitogen-activated protein kinases p38alpha and ERK in the synovial membrane in vivo.[see comment].* Arthritis Research & Therapy, 2005. **7**(5): p. R1140-7.

210. Karin, M., *The IkappaB kinase - a bridge between inflammation and cancer.* Cell Research, 2008. **18**(3): p. 334-42.

211. Garaude, J., et al., *ERK5 activates NF-kappaB in leukemic T cells and is essential for their growth in vivo.* J Immunol, 2006. **177**(11): p. 7607-17.

212. Balkwill, F. and A. Mantovani, *Inflammation and cancer: back to Virchow? [see comment].* Lancet, 2001. **357**(9255): p. 539-45.

213. Maeda, S. and M. Omata, *Inflammation and cancer: role of nuclear factor-kappaB activation.* Cancer Science, 2008. **99**(5): p. 836-42.

214. Woenckhaus, J. and I. Fenic, *Proliferative inflammatory atrophy: a background lesion of prostate cancer?* Andrologia, 2008. **40**(2): p. 134-7.

215. Condon, M.S., *The role of the stromal microenvironment in prostate cancer.* Seminars in Cancer Biology, 2005. **15**(2): p. 132-7.

216. Ben-Baruch, A., *Inflammation-associated immune suppression in cancer: the roles played by cytokines, chemokines and additional mediators.* Seminars in Cancer Biology, 2006. **16**(1): p. 38-52.

217. Luster, A.D., R. Alon, and U.H. von Andrian, *Immune cell migration in inflammation: present and future therapeutic targets.* Nature Immunology, 2005. **6**(12): p. 1182-90.

218. Mantovani, A., et al., *Macrophage polarization: tumor-associated macrophages as a paradigm for polarized M2 mononuclear phagocytes.[see comment].* Trends in Immunology, 2002. **23**(11): p. 549-55.

219. de Visser, K.E., A. Eichten, and L.M. Coussens, *Paradoxical roles of the immune system during cancer development.* Nature Reviews. Cancer, 2006. **6**(1): p. 24-37.

220. Hadden, J.W., *Immunodeficiency and cancer: prospects for correction.* International Immunopharmacology, 2003. **3**(8): p. 1061-71.

221. Assinder, S.J., J.A. Stanton, and P.D. Prasad, *Transgelin: An actin-binding protein and tumour suppressor.* Int J Biochem Cell Biol, 2008.

222. Shields, J.M., K. Rogers-Graham, and C.J. Der, *Loss of transgelin in breast and colon tumors and in RIE-1 cells by Ras deregulation of gene expression through Raf-independent pathways.* J Biol Chem, 2002. **277**(12): p. 9790-9.

223. Yang, Z., et al., *Transgelin functions as a suppressor via inhibition of ARA54-enhanced androgen receptor transactivation and prostate cancer cell growth.* Mol Endocrinol, 2007. **21**(2): p. 343-58.

224. LeCouter, J. and N. Ferrara, *EG-VEGF and Bv8. a novel family of tissue-selective mediators of angiogenesis, endothelial phenotype, and function.* Trends Cardiovasc Med, 2003. **13**(7): p. 276-82.

225. Negri, L., et al., *Bv8/Prokineticin proteins and their receptors.* Life Sci, 2007. **81**(14): p. 1103-16.

226. LeCouter, J., et al., *Bv8 and endocrine gland-derived vascular endothelial growth factor stimulate hematopoiesis and hematopoietic cell mobilization.* Proc Natl Acad Sci U S A, 2004. **101**(48): p. 16813-8.

227. Pasquali, D., et al., *The endocrine-gland-derived vascular endothelial growth factor (EG-VEGF)/prokineticin 1 and 2 and receptor expression in human prostate: Up-regulation of EG-VEGF/prokineticin 1 with malignancy.* Endocrinology, 2006. **147**(9): p. 4245-51.

228. Bok, R.A., et al., *Patterns of protease production during prostate cancer progression: proteomic evidence for cascades in a transgenic model.* Prostate Cancer & Prostatic Diseases, 2003. **6**(4): p. 272-80.

229. Clements, J.A., et al., *The tissue kallikrein family of serine proteases: functional roles in human disease and potential as clinical biomarkers.* Crit Rev Clin Lab Sci, 2004. **41**(3): p. 265-312.

230. Yamashita, M., et al., *Ubiquitin ligase Smurf1 controls osteoblast activity and bone homeostasis by targeting MEKK2 for degradation.[see comment].* Cell, 2005. **121**(1): p. 101-13.

231. Winsauer, G., et al., *XIAP regulates bi-phasic NF-kappaB induction involving physical interaction and ubiquitination of MEKK2.* Cell Signal, 2008. **20**(11): p. 2107-12.

232. Benowitz, S., *Biomarker boom slowed by validation concerns.* Journal of the National Cancer Institute, 2004. **96**(18): p. 1356-7.

233. Hartwell, L., et al., *Cancer biomarkers: a systems approach.* Nature Biotechnology, 2006. **24**(8): p. 905-8.

234. Pepe, M.S., et al., *Phases of biomarker development for early detection of cancer.* Journal of the National Cancer Institute, 2001. **93**(14): p. 1054-61.

235. Good, D.M., et al., *Body Fluid Proteomics for Biomarker Discovery: Lessons from the Past Hold the Key to Success in the Future.* J Proteome Res, 2007.

236. Hedenfalk, I., et al., *Gene-expression profiles in hereditary breast cancer.[see comment].* New England Journal of Medicine, 2001. **344**(8): p. 539-48.

237. Storey, J.D. and R. Tibshirani, *Statistical significance for genomewide studies.* Proceedings of the National Academy of Sciences of the United States of America, 2003. **100**(16): p. 9440-5.

238. deVera, I.E., J.E. Katz, and D.B. Agus, *Clinical proteomics: the promises and challenges of mass spectrometry-based biomarker discovery.* Clinical Advances in Hematology & Oncology, 2006. **4**(7): p. 541-9.

239. Hoque, A., et al., *Quantitative nuclear morphometry by image analysis for prediction of recurrence of ductal carcinoma in situ of the breast.* Cancer Epidemiology, Biomarkers & Prevention, 2001. **10**(3): p. 249-59.

240. Matthiesen, R., *Methods, algorithms and tools in computational proteomics: a practical point of view.* Proteomics, 2007. **7**(16): p. 2815-32.

241. Kao, J., et al., *Individual prostate biopsy core embedding facilitates maximal tissue representation.* Journal of Urology, 2002. **168**(2): p. 496-9.

242. Chan, T.Y. and J.I. Epstein, *Patient and urologist driven second opinion of prostate needle biopsies.* Journal of Urology, 2005. **174**(4 Pt 1): p. 1390-4; discussion 1394; author reply 1394.

243. Nguyen, P.L., et al., *The impact of pathology review on treatment recommendations for patients with adenocarcinoma of the prostate.* Urologic Oncology, 2004. **22**(4): p. 295-9.

244. Fukuhara, S., et al., *Signaling from G protein-coupled receptors to ERK5/Big MAPK 1 involves Galpha q and Galpha 12/13 families of heterotrimeric G proteins. Evidence for the existence of a novel Ras AND Rho-independent pathway.* J Biol Chem, 2000. **275**(28): p. 21730-6.

245. Gioeli, D., et al., *Stress kinase signaling regulates androgen receptor phosphorylation, transcription, and localization.* Molecular Endocrinology, 2006. **20**(3): p. 503-15.

246. Thiery, G., et al., *Multiplex target protein imaging in tissue sections by mass spectrometry--TAMSIM.* Rapid Commun Mass Spectrom, 2007. **21**(6): p. 823-9.

247. Lemaire, R., et al., *Tag-mass: specific molecular imaging of transcriptome and proteome by mass spectrometry based on photocleavable tag.* Journal of Proteome Research, 2007. **6**(6): p. 2057-67.

248. Thiery, G., et al., *Improvements of TArgeted multiplex mass spectrometry IMaging.* Proteomics, 2008. **8**(18): p. 3725-34.

249. Ludwig, M., et al., *Comparison of expressed prostatic secretions with urine after prostatic massage--a means to diagnose chronic prostatitis/inflammatory chronic pelvic pain syndrome.* Urology, 2000. **55**(2): p. 175-7.

250. Sebolt-Leopold, J.S., *Development of anticancer drugs targeting the MAP kinase pathway.* Oncogene, 2000. **19**(56): p. 6594-9.

# VITA

## LISA HARRIS CAZARES

Eastern Virginia Medical School

Department of Microbiology and Molecular Cell Biology

700 W. Olney Rd.

Norfolk, VA 23507

Old Dominion University

Hampton Boulevard

Norfolk, VA 23529

## Education

### Bachelor of Science in Microbiology

University of South Florida Tampa, FL (1982-1986)

## Publications

**Cazares LH**, Diaz JI, Drake RR, Semmes OJ.
MALDI/SELDI protein profiling of serum for the identification of cancer biomarkers.
Methods Mol Biol. 2008;428:125-40.

Drake RR, **Cazares LH** and Semmes OJ. (2007) Mining the Low Molecular Weight Proteome of Blood. Proteomics Clinical Applications 1(8):758-768..

**Cazares, LH**, Adam, BL, Ward, MD, Nasim, S., Schellhammer, PF., Semmes, OJ, Wright, Jr., G.L. Normal, benign, pre-neoplastic, and malignant prostate cells have distinct protein expression profiles resolved by SELDI mass spectrometry. Clin. Cancer Res. 8:2541-2552, 2002